Alma Mater Studiorum – Università di Bologna

DOTTORATO DI RICERCA IN

Scienze e Tecnologie Agrarie, Ambientali e Alimentari

Ciclo XXXII

Settore Concorsuale: 07/B1

Settore Scientifico Disciplinare: AGR/02

Modelling new sustainable cropping systems for advanced biofuel production

Presentata da: Andrea Parenti

Coordinatore Dottorato

Prof. Massimiliano Petracci

Supervisore

Prof. Andrea Monti

Co-Supervisore

Dr. Walter Zegada-Lizarazu

Esame finale anno 2020

Andrea Parenti

Modelling new sustainable cropping systems for advanced biofuel production.

PhD. Thesis in Agricultural, Environmental and Food science and Technology. Cycle: XXXII, University of Bologna.

Thesis supervisor: Prof. Andrea Monti - Department of Agricultural and Food Sciences (DISTAL), University of Bologna, Viale G. Fanin, 44, 40127 Bologna, ITALY.

Thesis Co-Supervisor: Dr. Walter Zegada-Lizarazu - Department of Agricultural and Food Sciences (DISTAL), University of Bologna, Viale G. Fanin, 44, 40127 Bologna, ITALY.

Research collaboration: Fabrizio Ginaldi, Giovanni Cappelli, Simone Bregaglio – Council for Agricultural Research and Economics (CREA), Research Centre for Agriculture and Environment (AA) – Via di Corticella 133, 40128 Bologna, ITALY.

Contents

List of Acronyms and Abbreviations

ADP	Asymptotic deceleration point
AGB	aboveground biomass
AGR	Absolute growth rate
ASEASN	Southeast Asian Nations
BECOOL	Brazil-EU Cooperation for Development of Advanced Lignocellulosic Biofuels
BEP	Breakeven point
BioMA	Biophysical Model Application platform
BN	Branches number
BNF	Biological nitrogen fixation
CRM	Coefficient of residual mass
DOY	Day of the year
EEA	European Environmental Agency
EF	Modelling efficiency
EU	European Union
FAO	Food and Agriculture Organization
GDD	Growing degree days
GHG	Greenhouse gases
GJ	Gigajoule
HT	Harvest time
ICCT	International Council of Clean Transportation
ID	Experimental number
IEA	International Energy Agency
iLUC	Indirect Land Use Change
IP	Inflection point
IQD	Interquartile distance
KGT	Köppen-Giger taxonomy
LAI	Leaf Area Index
LER	Land Equivalent Ratio
LL	Leaves lenght
LN	Leaves number
LW	Leaves width
MAP	Maximum acceleration point
MDP	Maximum deceleration point
Mha	Million hectares
PAR	Photosynthetic active radiation
PD	Plant density
PH	Phenology
RoW	Rest of the World
SD	Sowing density
SDK	Software Development Kit
SDS	Sustainable Development Scenario
ST	Sowing time
TDM	Total dry matter

Ringraziamenti

Desidero ringraziare in primis il prof. Andrea Monti per avermi dato l'opportunità di intraprendere il percorso di dottorato e nel contempo anche tutto il fantastico team di ricerca: Walter Zegada-Lizarazu, Federica Zanetti, Marco Acciai, Arianna Borghesi, Barbara Alberghini, Angela Vecchi e Ali Al-Baghdadi del presente e del passato con Giuseppe Di Girolamo, Carla Lambertini, Daria Righini, Andrea Nocentini, Jacqueline Almeyda Ramirez. Non dimentico inoltre il supporto morale e la condivisione di tanti momenti spensierati con tutti i ragazzi/e AGR/02 e non: Lorenzo Barbanti, Roberta Calone, Maria Teresa Senatore, Abid Sheraz, Lorenzo Negri, Rocco Sferrazza, Giuseppe Condorelli, Marco Vignudelli, Ghaith Ben Hammouda, Marco Bortolotti, Elliot Pascoletti e Vincenzo La Froscia; le simpatiche ragazze dell'amministrazione, in ordine sparso: Luisella Sistu, Mariangela Canè, Cecilia Bellettato, Simonetta Paolucci, Loredana, Vito Brancati. I ragazzi dell'AUB che mi hanno sopportato per tre lunghissime estati: Stefano Vecchi, Angelo Ferrari, Debora Trebbi, Renzo Gobbo, Claudio. I mitici ricercatori del CREA Bologna: Simone Bregaglio, Giovanni Cappelli e Fabrizio Ginaldi. Tutti i partner del progetto BECOOL e in particolare: Marco Buffi, Simone Bergonzoli e Jacopo Fanti. La prof.ssa Marisol Berti per avermi ospitato alla North Dakota State University e ai suoi collaboratori: Sergio Cabello, Alan Peterson, Amy Greenberg, Kennneth Izioma Mozea, Alex Wittenberg e Andrea Cecchin per avermi fatto sentire in famiglia. Infine gli amici di una vita: Elisabetta Iacopini, Mattia Lanzarini, Manuel Ventura, Alberto Olimpi, Pier Federico Galasso, Andrea Zannoni, Davide Capucci, Luca Bassani, Giacomo Tini, Francesco Camassa, Marco Brigoli, Marco Guerrini, Luca Fava, Luca Aureli, Claudio Baroni, Carolina Guardabascio, Nicola Fenni.

Il socio in affari e amico Marcello Campo e Alessia Filippini & famiglia per averci aiutato a perseguire un sogno. I mitici Valerio Zucchini e Augusto Cibotto per averci fatto capire che non si molla mai. Quelle vecchie volpi del gruppo agronomi bolognesi: Gianfranco Lionel Lettieri, Andrea Camassa, Nicola Scacchetti e Riccardo Zazzetti.

La famiglia intera per avermi insegnato, dandomi l'esempio giorno per giorno, che con il lavoro duro e l'impegno si possono tagliare traguardi importanti.

Abstract

Through the re-use of empirical functions and new model development, this study aims at contributing to the development of advanced biofuels in Europe. Four lignocellulosic crops were selected and tested in stand-alone (sunn hemp – *Crotalaria juncea* L.) and rotation system (sunn hemp, biomass sorghum - *Sorghum bicolor* x *Sorghum sudangrass*, kenaf - *Hibiscus cannabinus* L. and industrial hemp - *Cannabis sativa* L.) in different European environments. The first Chapter deals with a new model development (SunnGro) to reproduce sunn hemp, an interesting summer crop for advanced biofuels in Europe; in the second Chapter, the same model was used to simulate 20-year sunn hemp productivity across Europe. The SunnGro model reproduces sunn hemp development and growth, while providing a detailed description of leaf/branch size heterogeneity and its evolution during the vegetative season, depending on thermal time accumulation (GDD), sowing time (ST) and density (SD). The model was calibrated and evaluated using 20 sunn hemp field datasets collected in Greece, Spain and Italy. Interesting correlations were found between simulated and measured values of branch and leaf number ($0.80<R^2<0.92$) and biomass accumulation ($0.67<R^2<0.82$). Hence, SunnGro can be a valuable tool for estimating the potentialities of sunn hemp, either as main or intercropping, as feedstock for advanced biofuels across Europe.

The third Chapter is dedicated to the in-season growth simulation of first-of-a-kind food/energy crop rotations aimed at providing lignocellulosic feedstock for advanced biofuels without increasing land pressure. The rotations with biomass sorghum, industrial hemp and sunn hemp resulted in the highest biomass yields, whereas kenaf was less productive.

The presented models were developed to provide user-friendly tools to estimate the potentialities of the selected lignocellulosic crops across Europe. Even though these models need further ameliorations and extensions, to now, they represent reliable tools for preliminary assessments.

General introduction

The European context

Europe aims at leading the global clean energy transition binding the renewable energy target for the EU for 2030 to 32%, with possible upward revision by 2023 (ICCT, 2018). The decarbonizing scenario is lifting this gauntlet to 75% to 2050 for the renewable energy sources in gross final energy consumption (EC, 2011). In this framework, the advanced biofuels will be double counted in the share of the renewable energy consumed in road and rail transport with a minimum of 3.5% by 2030 (ICCT, 2018). The advanced biofuels are derived through biochemical or thermochemical processes of renewable biomass (Balat, 2007) not eligible for food/feed consumption as agricultural and forestry by-products (e.g. straw, grape marcs, wine lees, bagasse, biomass fraction from agro-industrial waste, tree pruning, biomass from understory) in order to avoid competition with food/feed products (Directive EU, 2015/1513). In this context, the European member states will have to dramatically increase the current production of advanced biofuels from agricultural and forestry by-products from 500 to 10,000 thousand Mg of oil equivalent in ten years' time, requiring the setting up of about a hundred cellulosic bioethanol plants with an annual production capacity of 200 million litres (Phillips et al., 2018). Such ambitious target requires a massive supply-chain development effort starting from the agricultural sector, going through logistic and ending at the processing bioethanol plants and fuel distribution (Oehmichen et al., 2018). The global investments on biofuels embrace 65 countries, which have established blending mandates or targets to increase their production capacity with United States, Brazil and Europe accounting for the lion's share (Figure 1).

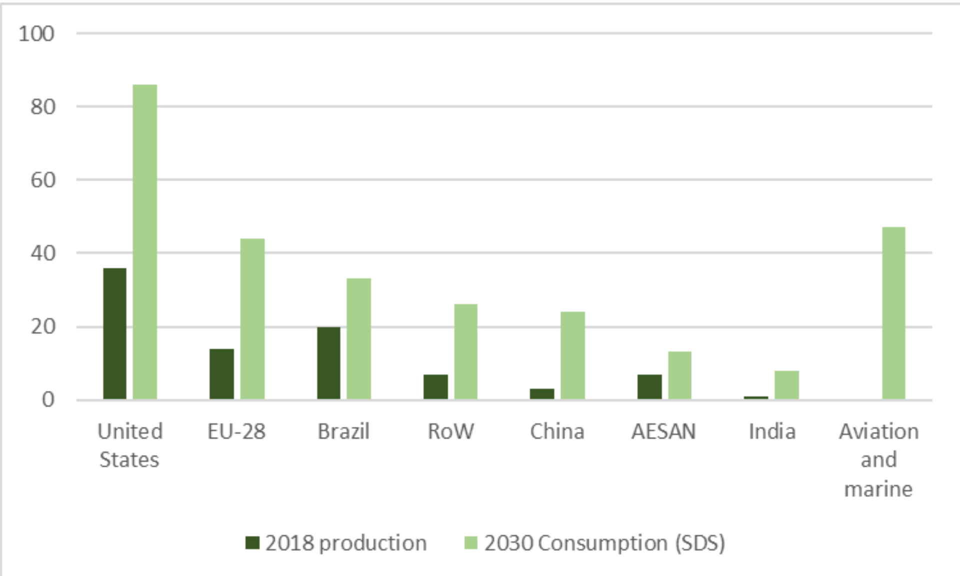

Figure 1. Biofuels alignment with the Sustainable Development Scenario (SDS) for 2030. RoW stands for Rest of the world and ASEAN for Southeast Asian nations (source IEA, 2019).

"A huge mobilization of biomass resources can be expected even in the short term. The obvious question does, however, arise as to how and where feedstock demand can be satisfied" (BECOOL project, 2017)**.** In order to do that, several actions were investigated by IRENA (2016) for maximizing the bioenergy production "*without competing with food production or causing land use change*" (i.e. indirect Land Use Change, iLUC). The iLUC is the shift of an area that might have a high carbon stock (e.g. forest, wetland) to food production due to a former change from food/feed to bioenergy happening in another area. In this scenario the overall GHG emissions increase (Gawel and Ludwig, 2011). This phenomenon occurs to keep the food production constant in the framework of the global market.

The majority of feedstock used to produce advanced biofuels is currently derived from wood and cereals residues. Nonetheless, even with an efficient logistic management, crop residues can hardly meet the demand for biomass of an advanced biofuel plants; their availability and price are, in fact, highly influenced by climatic conditions and competing markets, including the animal feed. Potential biofuels investors will be cautious where there is uncertain biomass availability at no fixed prices; therefore, in addition to crop residues, the introduction of dedicated lignocellulosic crops, annual and perennials, is highly recommended to increase the security of feedstock supply. Avoiding the competition with food crops, paves the way for the recovery of abandoned marginal land, even though these areas are considered to be inappropriate in meeting the European goals (Allen et al., 2014; Khawaja and Janssen, 2014). The Final recast of Renewable Energy Directive for 2021-2030 (ICCT, 2018) in ANNEX IXa encompasses non-food cellulosic material as eligible for biofuel conversion. These non-food cellulosic material is defined in the Directive 2018/2001 of European Parliament and of the Council (2018) as: "*feedstock mainly composed of cellulose and hemicellulose, and having a lower lignin content than ligno-cellulosic material, including food and feed crop residues, such as straw, stover, husks and shells; grassy energy crops with a low starch content, such as ryegrass, switchgrass, miscanthus, giant cane; cover crops before and after main crops; ley crops; industrial residues, including from food and feed crops after vegetal oils, sugars, starches and protein have been extracted; and material from biowaste, where ley and cover crops are understood to be temporary, short-term sown pastures comprising grass-legume mixture with a low starch content to obtain fodder for livestock and improve soil fertility for obtaining higher yields of arable main crops*".

An innovative idea developed in some European founded project (4FCROPS project, Alexopoulou et al., 2010; BECOOL project, Christou et al., 2018) for meeting the advanced biofuel caps relies in the intensification of the land use without threatening food security, neither reducing food land; otherwise introducing new genetically tailored annual high fibre yielding crops in the long gaps spared from traditional agriculture. The land intensification through sequentially raising and harvesting a second crop in a single growing season is called ‘double cropping’. The sum of the fractions of the yields of a double crop system divided by the yield of the former sole crop system produced on an equal area is the Land Equivalent Ratio (LER, Verheye, 2006). Hence, the LER shows the relative area under the sole crop system that would be needed to achieve double crop yields under the same set of production conditions (Willey, 1979a).

Besides the possibility of introducing dedicated industrial crop for advanced biofuel purposes represents a viable solution to approach the European target. The introduction of new dedicated lignocellulosic crop into the agricultural context requires prompt solutions that need to be scientifically tested and validated to test the feasibility, the potential yields and the best managements of the new systems. Moreover, transferring knowledge from experiments to industries investments requires accurate business planning and many years trials. In addition to the market demands for advanced biofuels, stakeholders need reliable data on the feedstock supply chain for a rationale decision-making process. Speeding up the data gathering on agronomic cultivation test carried out across different conditions is possible using dedicated modelling tools in order to predict the outcome of alternatives systems in the domains of agriculture and environment. Biophysical models are designed in a software framework and implemented for developing, parametrizing and running modelling solutions (Porter and Semenov, 2005). Whether correctly parametrized and validated, these models can extend their range of use to new environments, enabling quick provisions to the selected systems. One of these modelling platforms, specifically developed by European Commission Joint Research Centre in 2008 is the Biophysical Model Application (BioMA, Stöckle et al., 2014).

BioMA platform

In the last decade, process-based crop simulation models were increasingly used as supporting tools for in-season agricultural management, as well as to forecast crop yield at regional to global level. Moreover, they are considered as the reference tools to predict the future evolution of agricultural systems in the medium-long term, being capable to forecast crop yield across different environments. Biophysical Model Application (BioMA, Stöckle et al., 2014), was specifically designed and developed by European Commission Joint Research Centre (JRC) in 2008. It is an application for analysing, parameterizing and running modelling solutions based on biophysical models against a database which includes spatially explicit units (Donatelli et al., 2012) in the domains of agriculture and environment. BioMA is extendable autonomously by any users adding, modifying modelling solutions or making use of components already used by the application. The component-based structure allows BioMA to implement diverse modelling solutions targeted to specific modelling goals, together with sensitivity analysis and optimizer functions. The purpose of this framework is to rapidly bridge from prototypes to operational applications, enabling running and comparing different modelling solutions. A key aspect of the framework is the transparency which allows for quality evaluation outputs in the various steps of the modelling workflow. The framework is based on independent components, both for the modelling solutions and the graphical user interfaces. The goal is not only to provide a framework for model development and operational use also, and of no lesser importance, to provide a loose collection of re-usable objects either stand alone or in different frameworks. The software is developed using Microsoft C# language in the .NET framework. What is shortly called the BioMA platform is, in fact, a set of software layers with bottom-up dependencies. Each layer has its own tools, features and requirements. A first version of BioMA forecasted with great accuracy the rice yield in 27 European countries (Donatelli et al., 2012).

Given the rising importance of advanced biofuel crops worldwide, the application of simulation models to compare the performances of cropping systems in different environments and under alternative management represents a viable solution to support the development of targeted agricultural policies, as well as to help farmers in their management choices. Agricultural system models play increasingly important roles in the development of sustainable land management across diverse agro-ecological and socioeconomic conditions because field and farm experiments require large amounts of resources and may still not provide sufficient information in space and time to identify appropriate and effective management practices (Teng and Penning de Vries, 1992).

At this point some questions arise: what is the state of the art of the conventional cropping systems? Is there any chance for a more intensive sustainable management of the land?

Crop rotations

Conventional agricultural systems

Monoculture, crop rotations and intercropping are three historical agricultural practices aiming at feeding the world. All of them leads to advantages and disadvantages in the medium/long term. In particular, crop rotation has been used since long time, as far as traces of it date back to 3000 years ago (MacRae and Mehuys, 1985) in the Middle East, nonetheless in the Bible, God instructs the Israelites to practice a Sabbath of the land, leaving the land fallow once every seven years. The progress in the development of synthetic fertilizers and pesticides after the Second World War raised the feeling that crop rotation could be abandoned in favour of less complex systems such as monoculture (Benson 1985; Schrader et al., 1966). This belief was short-lived since the benefits of crop rotation effect (still unknown) on yields (> 10 – 25 %, Zeng et al., 2016) was not achievable through increased agronomical input, that, besides, brought a series of environmental problems, including air pollution, degraded water quality and increased greenhouse gas emissions (Giller et al., 1997; Karlen et al., 1994; Malézieux et al., 2009; Tilman et al., 2002; Zegada and Monti, 2011). On the other hand, the effects of crop rotations paired with a reduced soil tillage is beneficial in terms of: soil fertility, soil organic matter, soil structure, soil erosion, soil microbial communities, pests, allelopathy (Bullock, 1992) and furthermore bring environmental benefits such as crop diversification (Liebman and Dyck, 1993), system resilience and robustness (Li et al., 2019). In order to maximize the performances of the whole cropping system, the rotation should be carefully planned and tailored following the site-specific pedo-climatic conditions (Gebremedhin and Schwab, 1998).

At least two thirds of the 100 Mha arable land in EU-28 is dominated by conventional crops rotations, with a share of 60% of cereals (Barel et al., 2017; Eurostat, 2018). Conventional agriculture deals with long gaps within crop rotations: winter crops (wheat or rapeseed) are normally sown in autumn and harvested at the beginning of summer, whereas spring crops (sunflower, sorghum and maize) cycle go from spring to autumn. The maize based cropping systems are by far the most common in the southern and western regions of Europe. In the Ebro valley in Spain and in the Po valley in central Italy the grain/silage maize-fallow-winter wheat rotation acreage reached 100,000 and 700,000 ha in 2011, respectively (Vasileiadis et al., 2011). Hence, fallowing still represents an important practice in southern Europe, useful in reducing soil nutrient depletion, pests incidence (Connor et al., 2011) and increasing soil water retention (French, 1978); on the other hand it reduces the farmer income, increase the soil erosion (Biederbeck and Bouman, 1994) detrimental for soil fertility.

The replacement of fallowing with cash crops on fertile arable lands could lead to a soil organic matter depletion (Karlen et al., 1994) in a direct proportion to soil tillage intensity: conventional tillage > reduced tillage > no tillage (Havlin et al., 1990). However, the productivity is not entailed in the short and medium term (Chatskikh and Olesen, 2007) but rather it is enhanced for the subsequent crop by a better root penetration through the soil layers. Therefore, the replacement of a fallow/pasture to crop production will provoke a downward trend in the soil organic matter content raising concerns about the sustainability of the system. Otherwise, according to Larson et al. (2010), the soil organic matter drop can be stopped to a new equilibrium point leaving on soil at least 5 Mg ha^{-1} y^{-1} of residues. In line with that Johnson et al. (2014) assessed a 6 Mg ha^{-1} y^{-1} of residues, whereas (Muth et al., 2012) in a spatially comprehensive assessment of sustainable agricultural residue removal potential across the USA for bioenergy production found out that 2.3 Mg ha^{-1} y^{-1} is the average crop residue removal threshold to leave on the soil for a soil organic carbon sustainable management.

Careful agronomical practices in a LER intensification scenario minimizing the deterioration of the environment are, therefore, feasible. In order to assess the case-specific crop rotation sustainability and productivity, the customized agronomic model represent an effective tool to extend a given crop scheme solution that might be feasible in a certain area to other sites, in order to predict its productive traits and highlights possible constraints. Furthermore, the advantage of modelling relies in the time and money-saving compared to lengthy multi-year, multi-site field crop rotations (Teng and Penning de Vries, 1992). Then, to i) fulfil the mentioned European targets in terms of advanced biofuel, ii) test near-to-practice solution to increase the biomass mobilization, iii) avoid competition with food crops, iv) test alternative crop management according to different pedo-climatic conditions v) save resources reducing field and farm experiences, a possible solution might be to apply a modelling approach to the design of new cropping systems alongside conventional rotations. Integrating fast growing, short cycle, high yielding and low input crop in order to enhance the multifunctionality of agriculture, can help to meet the European bioenergy targets, increase farmers' income, increase biodiversity and thrive the economy of rural areas.

In this light, new questions arise: Is it feasible introducing energy crop within food/feed crop schemes? How much biomass could be yielded? What is the effect of these new crop on the succeeding ones?

Integrated food-energy crop rotations

The issue of mobilizing high amounts of eligible feedstocks for energy production is addressing modern agriculture. According to the ICCT report (2014) that assessed a 16% contribution to the road transport fuel needed in 2030, traditional food crop residues offer inadequate amount of available feedstocks to bioenergy. The main constraints are related to the annual biomass availability (Table 1), its nature and price, together with a difficult logistic harmonization due to the year-to-year variability (Scarlat et al., 2010). Overcoming the food crop residues flaws might be possible through their integration with dedicated cellulosic crops with genetic traits tailored for maximizing the biomass production, increasing the system overall cellulosic potential.

Table 1. Biomass availability from food crop for a sustainable bioenergy production in EU-28. Grain yield (Schils et al., 2018), biomass production calculated with the residue to product ratio (Scarlat et al., 2019), sustainable removal rates (Scarlat et al., 2010).

Crop	Grain yield* (Mg ha^{-1})	Biomass production (Mg ha^{-1})	Sustainable removal rates (%)	Biomass availability (Mg ha^{-1})
Maize	3.5-10	3-8	25-82	0.8-6.6
Wheat	2.5-7.4	3-7	15-60	0.5-4.2
Barley	2.2-6.3	2-6	15-60	0.3-3.6

*range between the 10th and 90th percentile of the observed yields by country in EU-28.

The goal of the integrated food-energy crop rotations is to meet the European target without reducing food land. In the northern and southern Mediterranean climates of Europe many agronomical experiments and projects have been carried out across the last 20 years testing annual summer, multipurpose, high yielding and fast growing crops with good potential for advanced biofuel (Zegada-Lizarazu and Monti, 2011) such as industrial hemp (*Cannabis sativa*) (CROPGEN project, 2004), kenaf (*Hibiscus cannabinus*) (BIOKENAF project, Alexopoulou et al., 2004), sweet sorghum (*Sorghum sp.*) (SWEETFUEL project, Zegada and Monti 2012; FUTUROL project, Dureuil, 2008; 4FCROPS project, Alexopoulou et al., 2010) and, in a lesser extent sunn hemp (*Crotalaria juncea* L.) (BECOOL project, 2017). The mentioned dedicated lignocellulosic crops have the chance to produce large amounts of lignocellulosic biomass (Amaducci et al., 2000; Danalatos et al., 2010; Rooney et al., 2007; Struik et al., 2000) in a short growing period preceding a winter cereal. Thus, these crops could be double cropped (Figure 2) replacing the fallows of the conventional food rotation. In addition, a biomass crop is flexible in the crop rotation framework, since the harvest time is not bound to a certain phenological phase, besides the interest relies simply in biomass maximization and not in mature seeds. This is a relevant point allowing farmers to avoid late soil bed preparation risks for the subsequent crop and a prompter decision-making.

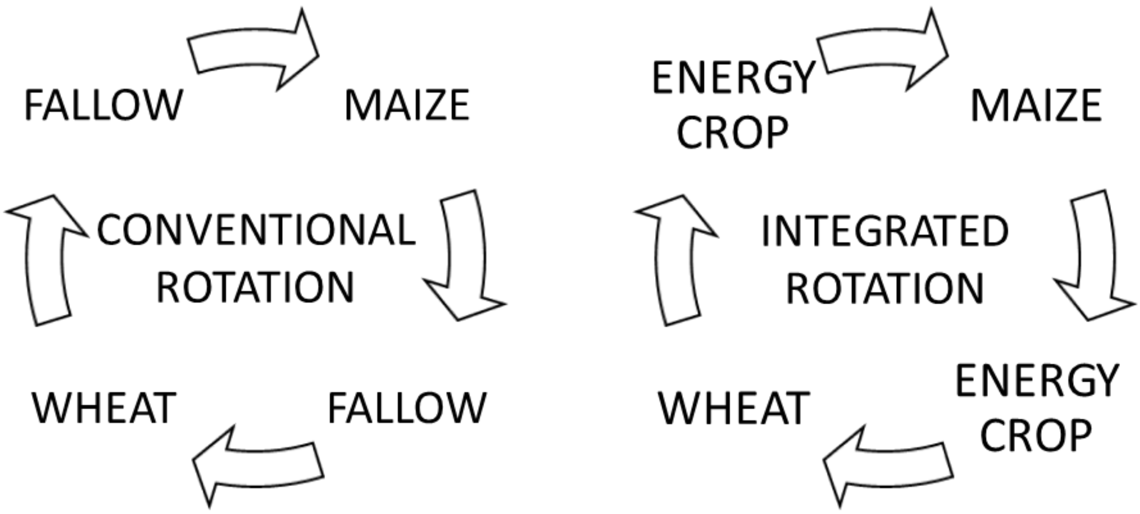

Figure 2. Conventional crop rotation with maize in the first year followed by a long gap (>12 months) before wheat sowing, then another gap (>7 months) for an overall of three crops in four year. On the right a food/energy integrated rotation with the fallow replaced by energy crops, for an overall of five crops in four-years rotation.

At this point, some questions arise before new cropping systems can take off. It is, indeed, important to gather data on the amount of biomass potentially available in the intensive agricultural areas of Europe, on the effective quality of the feedstocks, on the harvesting technology, logistic, transportation and treatment (BECOOL project, 2017). For instance, it is self-explanatory that in case of unsatisfactory yields the investment in the bioenergy value chain would be quenched. A conservative biomass production for a dedicated crop should, at least, be higher than the food crop residues to bioenergy, which for a maize on fertile lands in Europe can reach up to 10 Mg ha^{-1} (Scarlat et al., 2010). Within the aforementioned lignocellulosic crops able to yield in about 90 days more than 10 Mg ha^{-1} in southern Europe environments one of them is recently raising interest as a result of its unique characteristics. Sunn hemp is a tropical legume crop with great potential in the temperate environments of Europe (Parenti et al., 2019) able to combine high biomass production in a short growing season (Balkcom and Reeves, 2005; Mansoer et al., 1997; Rotar and Joy, 1983; Schomberg et al., 2007), resilient to pedo-climatic stress (Kamireddy et al., 2013), low input requirements (Rotar and Joy, 1983) and increase nitrogen into the soil for the subsequent crop through biologically nitrogen fixation (Ashworth et a., 2015; Mappaona et al., 1995). As far as the agricultural sector contributes to the 10% of the total EU-28 GHG emissions (EEA, 2015), sunn hemp seems to be able to provide a win-win strategy aimed at producing adequate feedstock availability with a minimum input requirement.

Sunn hemp, a tropical legume as a potential advanced biofuel feedstock in rotation with food crops

Among leguminous crops, the tropical sunn hemp is carving out a niche even in temperate environments with warm summer for its interesting characteristics. In sunn hemp native areal it is traditionally grown for fiber (Bhardwaj et al., 2005; Montgomery, 1954; Tripathi et al., 2013), albeit is widely used in the subtropical areas as green manure (Cherr et al., 2006; Mosjidis et al., 2013), soil amendment, cover crop and in intercropping (Bybee-Finley et al., 2016; Mansoer et al., 1997). Sunn hemp started to be known in Europe only recently where it has been studied for the weed suppression properties (Mosjidis and Wehtje, 2011), resistance to nematodes (Wang et al., 2002) and more recently as an advanced biofuel feedstock (Paul and Chakraborty, 2018) thanks to its fast growth, high cellulose and hemicellulose stems accumulation in a short growing season (Balkcom and Reeves, 2005; Schomberg et al., 2007). In case of successful nodulation, sunn hemp can biologically fix nitrogen (BNF), contributing to a net soil nitrogen gain ranging from 35 kg ha^{-1} in a temperate climate to 132 kg ha^{-1} in a tropical intercrop system (Ashworth et al., 2015). Hence, a winter cereal following sunn hemp could inherit additional nitrogen and a lower weed pressure due to the sunn hemp phytotoxic compounds and ground cover. Moreover, the whole cropping system might improve water infiltration, organic matter accumulation that reduce the soil bulk density and boost the formation/cementification of the aggregates across the soil layers due to the different root biomass production and structure characteristics (Robson et al., 2002; Sumner, 1982). The data on sunn hemp potential yield and its effect in a rotational system in the temperate environment of Europe are lacking. Nevertheless, some promising results outcome from an experiment in northern Italy (Parenti et al., 2018) in which sunn hemp double cropped with winter wheat under no tillage condition improved the emergence rate, the canopy cover and plant height; moreover reducing the soil preparation cost by four times compared to a conventional tillage. Sunn hemp does not require nitrogen input on average soil nutritional status compared to other moderately nitrogen-demanding lignocellulosic crop such as biomass sorghum (Heitman et al., 2018), industrial hemp (Papastylianou et al., 2018; Zatta et al., 2012) and kenaf (Bangoo et al., 1986; Webber et al., 1996). The mechanization seems to be straightforward compared to the challenging field drying phase hampering biomass sorghum harvest (Colauzzi et al., 2018; Pari et al., 2015) and the need of dedicated machinery for industrial hemp (Zatta et al., 2012). In this light, saving GHG emissions from input reduction and lowering the cultivation cost are strengthening the interest on sunn hemp. Otherwise, designing new advanced biofuel value chain fed by annual summer double crop and food crop residues needs to be deeply investigated to assess the feasibility of the logistics and transformation plants scale.

The objectives of the following Chapters are to create and re-use specific crop simulation model targeting four highly promising lignocellulosic crops for advanced biofuel (sunn hemp, biomass sorghum, kenaf and industrial hemp) in stand-alone and rotation system. The focus is to find tools able to forecast the yields and the best harvest moment of such crops to support both private and public stakeholders of agricultural sector in shifting from conventional to integrated food/energy cropping systems. The road to the implementation of crop model to the whole rotation simulation is paved in the following Chapters. Thus, some crop specific Logistic models were exploited, and a preliminary evaluation of the cropping system food/biomass potential is provided.

CHAPTER 1
SunnGro*: a new model to reproduce the morphologic traits, canopy architecture and biomass yield of sunn hemp

1.1 Introduction

Sunn hemp (*Crotalaria juncea* L.) is a C3 tropical legume crop (Kamireddy et al., 2013) suitable to a wide range of soils (Ashworth et al., 2015; Mappaona et al., 1995) and resistant to root-knot and soybean cyst nematodes (Wang et al., 2002), due to the presence of monocrotaline (i.e. a pyrrolizidine alkaloid with nematicide effect) in crop seed, leaves and stems (Valenzuela et al., 2002). Canopy architecture is strongly affected by the emergence rate, plant density and apical dominance, which in turns regulate leaves/branches size heterogeneity and number, thus influencing the final quantity and quality of the biomass at harvest (Abdul-baki et al., 2001; Cho et al., 2015). Sunn hemp is popular in tropical areas as soil improver and source of bast fiber and green manure (Cook and White, 1996; Rotar and Joy, 1983); recent studies demonstrated that it was able to yield up to 10 Mg ha^{-1} in 90-120 days also in more humid subtropical and temperate environments (Balkcom and Reeves, 2005; Mansoer et al., 1997; Rotar and Joy, 1983; Schomberg et al., 2007) that make this crop an interesting source for the production of advanced biofuels (Paul and Chakraborty, 2018). Cantrell et al., (2010) in his experiment conducted in South Carolina assessed a sunn hemp biomass yield of about 11 Mg ha^{-1} that via thermochemical conversion produced an energy yield of 204 GJ ha^{-1}. Biophysical models can be used to estimate the potentials of sunn hemp in Europe as main or secondary crop (Porter and Semenov, 2005). There are several generic (e.g. CROP-GRO, Boote et al., 2002; APSIM-Legume, Robertson et al., 2002; STICS, Falconnier et al., 2019) and specific models (Sinclair, 1986; Sinclair et al., 1987; Soltani et al., 1999) designed to simulate the development and growth of diverse legume species (e.g. common bean, peanut, soybean, cowpea, black gram, chickpea), however, a specific model for sunn hemp has not been yet provided. The few available modelling studies were performed using a generic simulator originally developed for cereals adapted via parameterization (e.g., EPIC, Le et al., 2018), or using empirical relationships between productive/biometric traits (e.g. total dry matter, plant height, stem diameters) and time after sowing (Bem et al., 2017a,b). In this context, both approaches have limitations: indeed forcing a generic model to fit crop growth dynamics without considering algorithms specific for sunn hemp-peculiar traits (e.g. complex canopy architecture and

***Software availability**
BioMA component name: UniboCrea.SunnGro.
Developers: Fabrizio Ginaldi, Giovanni Cappelli, Andrea Parenti.
Availability and online documentation: UniboCrea.SunnGro is available as Software Development Kit (SDK) on http://www.biomamodelling.org/Components/Components.aspx?node=30057. The SDK contains a help file with the documentation of algorithms and models, and a sample application illustrating how to use the component. UniboCrea.SunnGro is released as C# libraries compiled for the NET 4.5 platform.

heterogeneity), and/or using empirical models without any relation with the underlying process, strongly reduce the applicability of existing models outside the conditions for which they are calibrated.

The aim of the present study is the adaptation of a process-based simulation model to sunn hemp and the evaluation of its capability in reproducing measured crop biometric data collected under alternative plant density and harvest times in three European sites.

1.2 Material and methods

This study articulates in a three-step workflow (Figure 1.1), envisaging the development and evaluation of a new model specific for sunn hemp in different European environments.

	Activity	**Objective**	**Method**
Step A	Adaptation of the Arungro model to simulate sunn hemp	Release of a new model able to reproduce the evolution of sunn hemp canopy architecture during vegetative season	Model modification and simplification
Step B	Single-site calibration of the sunn hemp model using field observations	Demonstrate the capability of the model to reproduce the year-to-year variability in crop canopy expansion, leaf area index evolution and biomass accumulation under different management (sowing time and density) in Northern Italy	Multi-start downhill simplex method
Step C	Multi-site evaluation of the sunn hemp model using field observations	Demonstrate the capability of the model to simulate the year-to-year yield variability in Mediterranean environments (Greece, Italy, Spain) under alternative crop management	Multi-metric evaluation of model performances

Figure 1.1 Activities performed in the present study, with specific objectives and methodology.

The Arungro model (Stella et al., 2015) was used as the basis for the development of a new sunn hemp process-based model, SunnGro (*step A*, section 1.2.3). Arungro was chosen since it provides a more detailed representation of canopy structure and of its dynamics over vegetative growth, compared to mono- and multi-layer crop models. Unlike Arungro, SunnGro assumes that primary and secondary branches are representative of the whole stem population, and replaces the original approaches for handling stem population, leaf number and size evolution with species-specific algorithms. The simulation of photosynthetic process, biomass accumulation and partitioning of assimilates have been borrowed from the seminal model, although the number of model parameters was reduced.

A stepwise automatic calibration of the model was then carried out using multi-year experimental data collected under different sowing time and density in northern Italy (2016-2018), aimed at reproducing the dynamics of branch and leaf number, leaf area index (LAI, $m^2\ m^{-2}$) and aboveground biomass (AGB, Mg ha^{-1}) (*Step B*, section 1.2.4).

This activity laid the basis for a multi-site model validation (*step C*, section 1.2.4), in which the set of calibrated model parameters was applied to reproduce AGB measurements from independent field trials carried out in different Mediterranean countries (Greece, Italy, Spain).

1.2.1 Experimental sites and agronomic details

A registered sunn hemp variety 'Ecofix' was tested across three locations: i) Cadriano, Italy (44° 33' N, 32 m a.s.l.), ii) Guadajira, Spain (38° 51' N, 222 m a.s.l) and iii) Aliartos, Greece (38° 22′ N, 114 m a.s.l.) in the North and South Mediterranean areas (Metzger et al., 2005) in the period 2016-2018 (Figure 1.2, Table 1.1) in irrigated systems.

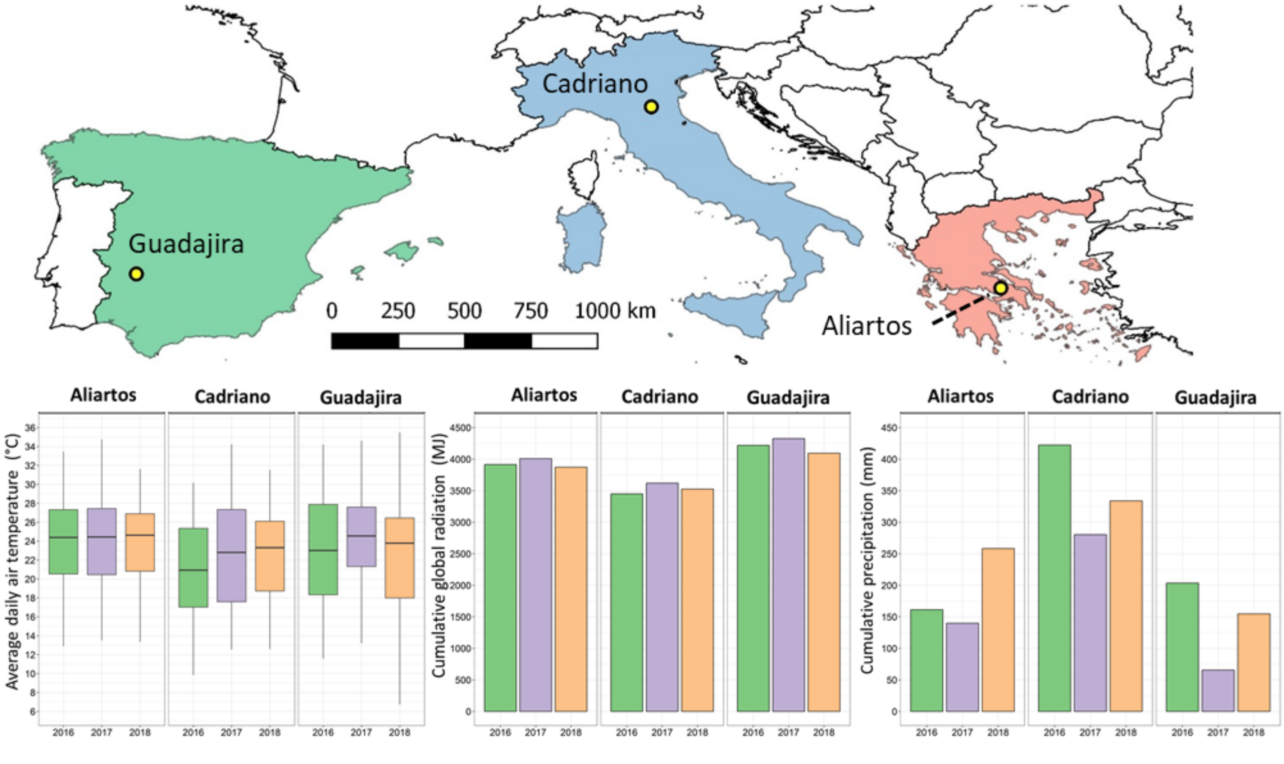

Figure 1.2 Experimental sites (yellow circles) and related climate variability during sunn hemp growing season (May-October) in the period 2016-2018.

Thirteen data points were collected at the experimental farm of the Bologna University in Cadriano (44° 33' lat N, 11° 21' E, 32 m a.s.l.) in a loam silty soil, neutral (pH 6.6-7.3), rich in K_2O (~159 mg kg^{-1}), with average N, P_2O_5 and organic matter contents of about 1.1 g kg^{-1}, 69 mg kg^{-1} and 1.3%, respectively. In 2017 and 2018 experiments, the design was a randomized complete block (n=4), whereas in 2016 an exploratory trial without replicates was conducted. Two harrowing and one glyphosate (4 L ha^{-1}) treatments were performed to achieve a weed-free and firm seedbed preparation; then sunn hemp was sown with a pneumatic planter alongside a granular soil sterilant application lambda-cyhalothrin based. The sowing density (SD) was 4.4 cm on the row, with three row spacings: 22.5 cm (high SD), 45 cm (medium SD) and 70 cm (low SD). The plots were kept weed-free by mechanical weeding when plants height reached around 30 cm. Fertilization was not applied due to the soil nutritional status (Appendix A, Table A.1 in supplementary material), which was sufficient to meet the crop N-requirements as demonstrated by Parenti et al. (2019), in a dedicated study conducted on the same crop, field and period. Sprinkler irrigation was performed in 2017, with a volume of 200 mm at 7-day interval until two months after sowing, due to the drought conditions (+2 °C of air temperature and -129 mm of precipitation compared to the mean values of the period 2016–2018) occurred in the first two months after sowing. The abundant cumulative precipitation (mean of all the experiments=345 ± 71.7 mm, Figure 1.2) and the high soil water retention capacity prevented supplemental irrigations during the 2016 and 2018 growing seasons.

Additional field trials were carried out in Guadajira, a region of Extremadura (Spain, 38° 51' lat. N, 6° 40' W, 222 m a.s.l) following the same experimental design as Cadriano. The soil in Guadajira was slightly acidic (pH 6.2) and loam, with a N-P-K content of 0.7 g kg^{-1}, 14 and 54.7 mg kg^{-1}, respectively; the organic matter content was about 0.8% (Appendix A, Table A.2 in supplementary material). The seedbed was arranged using a disk plough, a cultivator tiller and a rotary harrow, by incorporating 32 kg ha^{-1} of N, 60 kg ha^{-1} of P_2O_5 and 60 kg ha^{-1} of K_2O. Two consecutive treatments of glyphosate (2 L ha^{-1}) and Stomp (pendimenthalin 3 L ha^{-1}) were applied with a boom sprayer in pre-sowing. Sunn hemp was drill-seeded at a density of 52 seeds m^{-2}. Experiment 14 (ID 14 in Table 1.1) was affected by pests (*Agriotes* spp. and *Spodoptera* spp.) at the very beginning of the growing season, thus requiring an additional application of Chlorpyrifos-Methyl 22.4% (m/v). No damage was observed on ID 15. Sunn hemp was drip-irrigated every three days, with an average amount of 384 mm.

Five samplings were performed in Aliartos (38° 22′ lat. N, 23° 10′ E, 114 m a.s.l.) in a randomized complete block design (n=4) in the period 2016-2018. The soil was moderately alkaline (pH 7.9-8.4) and sandy loam (Appendix A, Table A.3 in supplementary material). The seedbed was prepared with a disc plough and a rotary harrow, incorporating 33 kg ha^{-1} of N, 45 kg ha^{-1} of P_2O_5 and 45 kg ha^{-1} of

K_2O fertilizer. Weed control was performed in pre-sowing using glyphosate at a concentration of 4 L ha^{-1} and in post-emergence by hand hoeing. Sowing was carried out manually, at 50 cm row spacing and three densities on the row, i.e. 5, 10 and 15 cm. A total amount of 323 mm of irrigation water was applied via drip irrigation during each growing season. Irrigation in Spanish and Greek experimental sites aimed at avoiding crop water stress, given the low precipitation in the period May-October (average cumulative precipitation of 141 mm in Guadajira and 186 mm in Aliartos in 2016-2018 compared to 345 mm of Cadriano; Figure 1.2).

Daily air temperature (°C), precipitation (mm), radiation (MJ m^{-2} d^{-1}) and wind speed (m s^{-1}) referred to the three experimental sites were downloaded by the Prediction of Worldwide Energy Resources (POWER) at the NASA Langley Research Centre (Stackhouse, 2006), at a spatial resolution of 0.5° latitude by 0.5° longitude.

1.2.2 Methodology of field samplings

The field samplings provided the reference data used for model calibration and evaluation (Table 1.1). The sowing dates were classified as early (May) and late (June, after wheat harvesting). Likewise, the harvest time was classified as early (i.e. August), medium (September) and late (October).

Phenological observations were collected at 50% emergence and 50% flowering stage. Plant density (PD, plants m^{-2}), and AGB were measured twice, in post-emergence and at harvest, respectively. AGB was assessed by sampling plants in a random 6 m^2 area of the plot, and then oven-drying the fresh mass at 105°C until constant weight. Additional biometric parameters were monthly monitored in the 2017 and 2018 Italian experiments in a random plot area of 1 m^{-2}, including leaf (LN, number m^{-2}) and branch (BN, number m^{-2}) number, LAI (m^2 m^{-2}), and leaf width (LW, cm) and length (LL, cm). LN and BN of each plant in the sample was counted, separately for primary and secondary stems. In experiments ID 9, 10 LW and LL were measured at each sampling date on 20 expanding and 20 fully expanded leaves. LAI was determined by destructive method using a LI-COR LI 3100C area meter.

Table 1.1 Datasets from Cadriano (C, Italy), Guadajira (G, Spain) and Aliartos (A, Greece) used for model calibration (C) and evaluation (E): phenology (PH), leaf number (LN, leaves per plant), leaf length (LL, mm), leaf width (LW, mm), branch number (BN, branches per plant), plant density (PD, plants m^{-2}), aboveground biomass (AGB, Mg ha^{-1}). Sowing d=sowing density; Tavg=average daily temperature during crop cycle; Reps n.=replications number; Rain=cumulative precipitation during crop cycle; Irr.=irrigation water.

ID	Site	Year	Sowing date	Harvest time	Sowing d (seed m^{-2})	Reps n.	Plot area	Measured variables	Use	Tavg (°C)	Rain (mm)	Irr. (mm)
1	C	2016	18/05	1/08	52	1	64	PH, LN,	C	23.1	156	
2				23/08	104	1	64	BN, PD,	C	23.5	196	
3					52	1	64	AGB	C			
4					33	1	70		C			
5				20/09	104	1	64		E	23.7	245	
6					52	1	64		E			
7					33	1	70		E			
8			22/06	25/10	52	1	64		E	22.9	220	
9	C	2017	26/06	10/10	52	4	135	PH, LN,	C	24.2	182	174
10			5/07	26/10	52	4	231	LL, LW, BN, PD, AGB, LAI	C	24.1	167	201
11	C	2018	8/05	27/09	52	4	41	PH, LN,	C	24.0	231	
12			25/05	9/10	52	4	231	BN, PD,	C	24.2	221	16
13			2/07		52	4	231	AGB, LAI	C	24.5	161	
14	G	2018	1/06	8/10	52	4	120	AGB	E	24.2	67	421
15	G		17/07	11/10	52	4	120		E	26.3	24	347
16	A	2017	21/05	27/10	13	3	13	PH, PD, AGB	E	24.7	125	415
17					20	3	13		E			
18					40	3	13		E			
19			20/06		20	4	98		E	25.3	48	344
20	A	2018	16/06	1/10	20	4	98	PH, PD, AGB	E	25.7	219	209

1.2.3 Adaptation of the Arungro model to simulate sunn hemp

The Arungro model, specifically designed for giant reed (*Arundo donax* L.), was adapted to simulate sunn hemp to give a new simulation model, SunnGro. Arungro simulates gross photosynthesis and respiration costs to estimate net carbon fixation, depending on radiation interception and crop transpiration. The original model provides a detailed description of LAI dynamics at shoot and plant levels, considering leaf width/length heterogeneity on a single tiller and among tiller cohorts. The evolution of tiller number is simulated based on thermal time, with emission of new stems regulated by rhizome biomass during sprouting. While the algorithmic description of Arungro is provided in the original paper (Stella et al., 2015), the graphic representation of the processes implemented in SunnGro is shown in Figure 1.3, which highlights the modifications with respect to the original model.

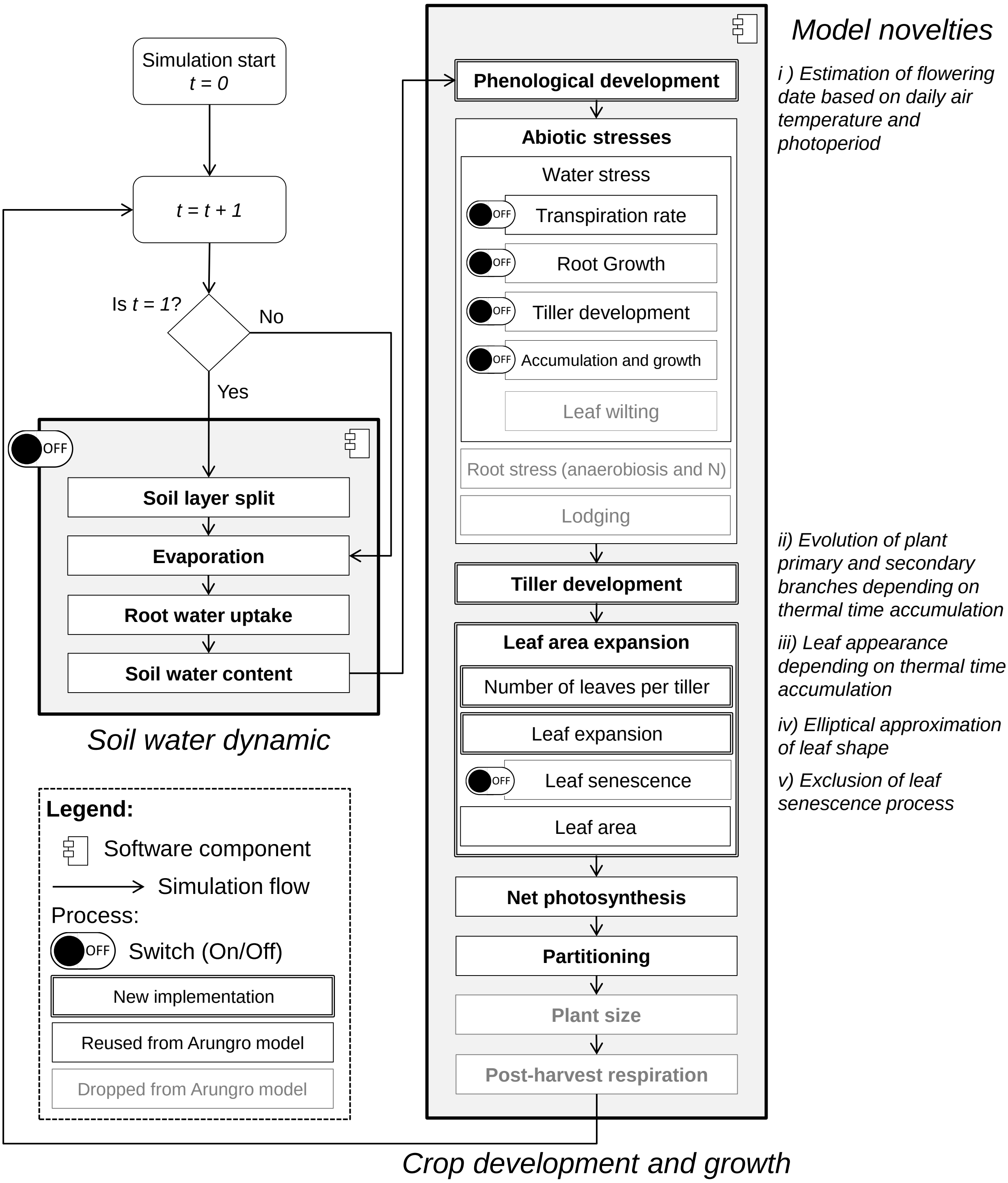

Figure 1.3 Schematic representation of the main processes simulated by SunnGro. The simulation flow traces the execution order of sub-processes in a time step. Main processes are highlighted in bold, whereas sub-processes are reported in regular font style. Double line boxes highlight changes with respect to the original model. Boxes with light grey border indicates processes that have been removed from the seminal implementation.

The SunnGro model was implemented in the BioMA framework (Donatelli et al., 2014), which consists of platform-independent and re-usable components, allowing for a modular representation of the agricultural systems. The main modifications in SunnGro concerned i) the estimation of flowering date, through a linear, upper-limited, response to daily temperature after emergence, optionally corrected for photoperiod (Stöckle et al., 2003): the parameters driving phenological development are the thermal time needed to reach flowering, the cardinal temperatures for development (i.e. base and cutoff temperature), and the day length for insensitivity and to inhibit flowering; ii) the simulation of the evolution of primary and secondary branches of sunn hemp, instead of considering the tiller population as in Arungro (Equation 1); iii) the formalization of a specific function to estimate the number of leaves per plant (Equation 2); iv) the consideration of the elliptical shape of sunn hemp leaves, which were triangular in Arungro, in order to compute the leaf area; v) the impact of leaf senescence on LAI dynamic and on the daily rate of gross photosynthesis was switched off (in non-tropical environments the shortness of the warm season does not allow sunn hemp leaves to senescence and prevents seed formation; Mansoer et al., 1997). BN (branch plant^{-1}; Equation 1) and LN (leaf plant^{-1}; Equation 2) were dynamically simulated according to Bem et al. (2017a), using three-parameter Logistic function based on the thermal time ($\sum_{em}^{pbp} TT_i$, °C day^{-1}) daily accumulated from emergence (em) to peak of branch population (pbp).

$$BN = 1 + \frac{SBN_{\max}}{1 + e^{\left(-b_{SB} - k_{SB}\sum_{em}^{pbp} TT_i\right)}}$$

[1]

Where SBN_{max} (number plant^{-1}) is the maximum number of secondary branches per plant; b_{SB} and k_{SB} (unitless) represent empirical coefficients modulating the steepness of BN accumulation and related to the site and to the rate of maturity/precociousness of the cultivar, respectively.

$$LN = 1 + \frac{LN_{avg}}{1 + e^{\left(-b_L - k_L\sum_{em}^{pbp} TT_i\right)}}$$

[2]

Where LN_{avg} (number plant^{-1}) is the average number of leaves per branch; b_L and k_L (unites) represent empirical coefficients modulating the steepness of LN accumulation and related to the site and to the rate of maturity/precociousness of the cultivar, respectively.

All the functions specific for giant reed and sugar cane of Arungro were removed from SunnGro (i.e. lodging effect on light interception, stress days affecting green leaves, anaerobic stress on root development). The algorithms accounting for the impact of water stress on root and branch development and on plant assimilation and growth were switched off until experimental datasets collected under contrasting pluviometric and irrigation regimes will be available.

1.2.4 Model calibration and evaluation

All the simulations performed in model calibration and evaluation were carried out under non-limiting conditions for water, nutrients, pests and weeds, thus considering only temperature and radiation as limiting factors (i.e., potential level, van Ittersum and Rabbinge, 1997).

SunnGro was calibrated using the data collected at Cadriano in 2016-2018 experiments (IDs 1-4 and 9-13 in Table 1.1). The phenological development was set by manually tuning the thermal time needed to reach flowering according to field observations. Then, the parameters connected to BN, LN, leaf expansion and photosynthesis were varied within the biophysical ranges reported in literature and available from experimental data to increase model accuracy (Appendix C, Tables C1 of the supplementary materials). The multi-start downhill simplex (Acutis and Confalonieri, 2006; Nelder and Mead, 1965) was used as optimization algorithm, which generates a simplex, a geometrical figure with N+1 vertexes, with N as the parameter number under calibration. The average root mean square error (RMSE, minimum and optimum=0; maximum=+∞, it quantifies the average difference between simulated and measured data in the unit of the analysed variable; values lower than half of the standard deviation of the measurements reveal good results, Moriasi et al., 2007) was chosen as objective function and evaluated after each simulation run. The automatic optimization ended when the difference of RMSE between consecutive simulations felt below a tolerance range; 20 simplexes, 100 iterations and a tolerance of 0.01% were set as operational settings.

A multi-site evaluation was carried out to test the accuracy of SunnGro across experimental sites. The parameter set derived from model calibration was used and SunnGro performances were tested using the AGB measurements from field trials carried out in Cadriano (IDs 5-8), Guadajira (IDs 14-15) and Aliartos (IDs 16-20) in the period 2017-2018 as reference variables.

The model performances in calibration and validation were quantified with standard metrics in crop modelling studies, i.e., RMSE, relative root mean square error (RRMSE, minimum and optimum=0%; maximum=+∞, Jørgensen et al., 1986; performances can be rated as very accurate when lower than 10% of the mean, good when between 10 and 20%, acceptable if between 20 and 35 % and poor if higher than 35%, Jamieson et al., 1991; Domeneghetti et al., 2018), coefficient of residual mass (CRM, minimum=-∞, maximum=+ ∞, optimum=0, unitless, Loague and Green 1991; if positive indicates model underestimation and *vice versa*), the modelling efficiency (EF, minimum=-∞, optimum and maximum=1, unitless, Nash and Sutcliffe, 1970; if positive, the model is a better predictor than the mean of measured values and results can be considered acceptable, Moriasi et al., 2007), the coefficient of determination (R^2, minimum=0, optimum and maximum=1), and Pearson's correlation coefficient (*r*, minimum=-1, maximum=+1; extremes reveal a perfect negative or positive linear relationship; if *r* is equal to 0, no linear relationship occurs, unitless; in absolute value, correlations can be considered weak when lower than 0.35, moderate when between 0.36 and 0.67, strong if greater than 0.68 and very strong when higher than 0.9, Taylor, 1990).

1.3 Results

The simulated dynamics of BN (branches plant^{-1}) vs LN (leaves plant^{-1}) and AGB (Mg ha^{-1}) vs LAI (m^2 m^{-2}) in the field trials carried out in 2016-2018 are presented in Figure 1.4 and 1.5 respectively, along with measured field data and evaluation metrics. SunnGro correctly reproduced the measured dynamics of the plant variables considered in calibration under alternative combinations of sowing density (SD) and harvest time (HT), with a RMSE on flowering date equal to 3.6 days (number of trials, n=5). The model accurately simulated the evolution of biometric traits (i.e. BN and LN) along the vegetative season (Figure 1.4) in all experiments, with slight errors for the LN (RMSE=2.09 branches plant^{-1} for BN and 35.83 leaves plant^{-1} for LN; RRMSE=37.04% for BN and 27.24% for LN). Indeed, SunnGro explained the 80% and 92% of the year-to-year variability of BN and LN (EF=0.80 for BN and 0.92 for LN; r=0.90 for BN and 0.96 for LN). Larger errors corresponded to the early harvested experiment in 2016, where SunnGro underestimated LN (i.e. -95 leaves plant^{-1}), despite BN was correctly simulated (i.e. -3 branches plant^{-1}). CRM values indicated no systematic bias for BN and LN (CRM=0.067 for BN and 0.021 for LN). Nevertheless, simulation results denoted a frequent underestimation of BN at early vegetative stages (around 750 GDD from emergence), which resulted in an underestimation of LN at the same phenological stage.

The proper simulation of BN and LN led to good results for LAI and AGB dynamics during the growing season (Figure 1.5; RMSE=1.35 m^2 m^{-2} for LAI and 1.8 Mg ha^{-1} for AGB; RRMSE=33.10% for LAI and 21.36% for AGB). SunnGro was capable to describe the trends of observed AGB data in six out of nine experiments (EF=0.78; r=0.91), i.e. with the exception of ID 2, 4 (medium harvest) and 10 (late harvest), where it overestimated reference data. The LAI simulation was slightly less accurate than AGB, with EF=0.62 and r=0.84. Compared to LN, the model explanatory power was lower and decreased to 82% for AGB and 71% for LAI. The underestimation of LN in the early vegetative phase delayed the LAI increase (e.g. ID 9 and 13 in Figure 1.5) before the maximum number of branches was reached.

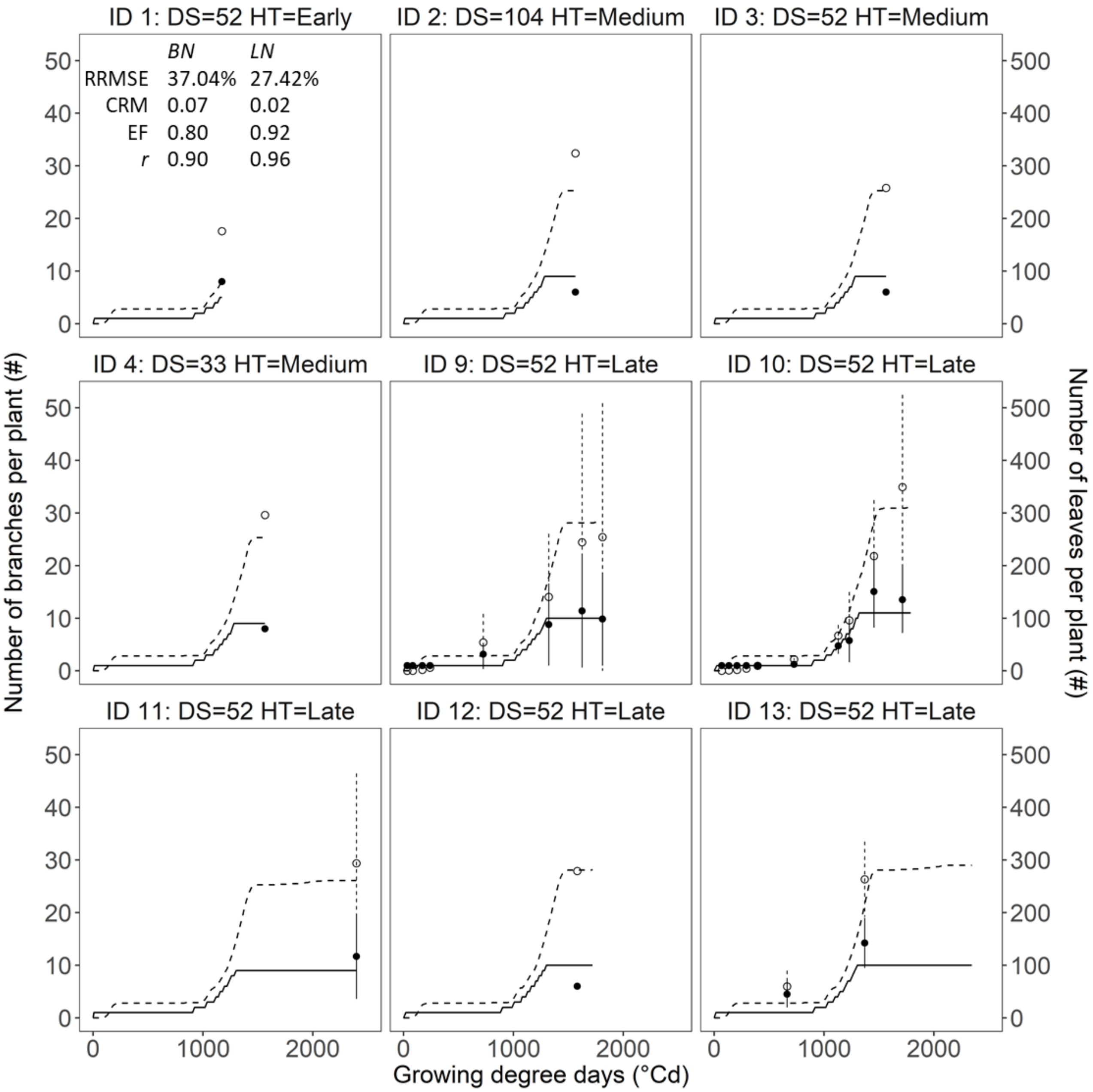

Figure 1.4 Model performances in reproducing the dynamics of the number of branches (BN, continuous line, main axis) and of leaves (LN, dashed line, secondary axis) per plant during the vegetative season of sunn hemp (May-October). Measured BN (black dots) and LN (empty dots) were collected in the period 2016-2018 at Cadriano (northern Italy) from plots with different combinations of sowing densities (SD, plants m^{-2}) and harvest times (HT). Vertical bars correspond to the standard deviation of sampled mean (n=4). The evaluation metrics reported in the top left corner are: the relative root mean square error (RRMSE, %), the modelling efficiency (EF, unitless), coefficient of residual mass (CRM, unitless) and Pearson's correlation coefficient (*r*, unitless). IDs are listed in Table 1.1.

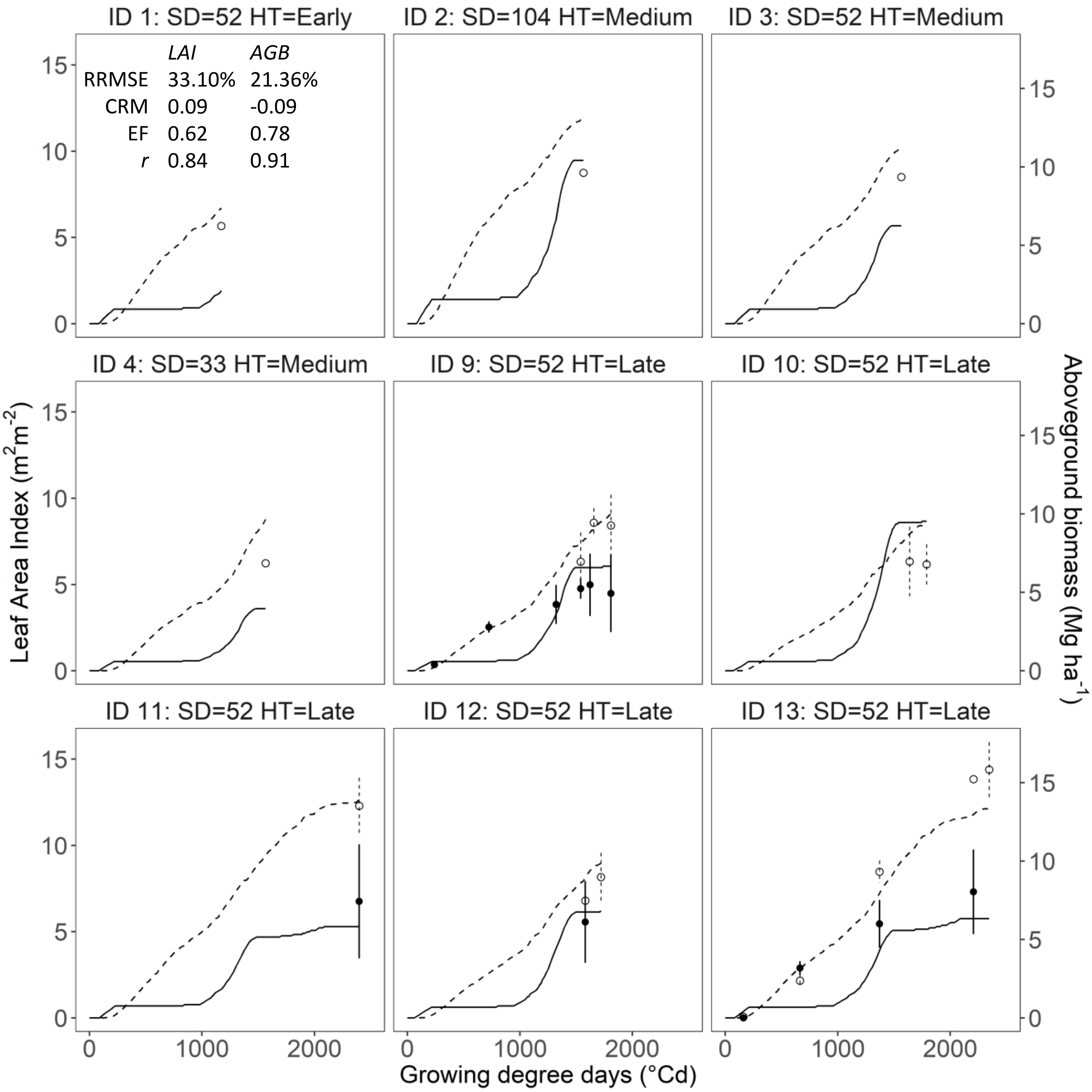

Figure 1.5 Model performances in reproducing the dynamics of the leaf area index (LAI, continuous line, main axis) and of aboveground biomass (AGB, dashed line, secondary axis) during the vegetative season of sunn hemp (May-October). Measured LAI (black dots) and AGB (empty dots) were collected in the period 2016-2018 at Cadriano (northern Italy) from plots with different combinations of sowing densities (SD, plants m^{-2}) and harvest times (HT). Vertical bars correspond to the standard deviation of sampled mean (n=4). The evaluation metrics reported in the top left corner are: the relative root mean square error (RRMSE, %), the modelling efficiency (EF, unitless), coefficient of residual mass (CRM, unitless) and Pearson's correlation coefficient (*r*, unitless). IDs are listed in Table 1.1.

SunnGro accurately reproduced the decrease in LAI and AGB according to lower SD, from high (i.e. 104 plants m^{-2}) to medium and low (i.e. 52 and 33 plants m^{-2}) SD (e.g. ID 2, 3 and 4 in Figure 1.5), as well as the higher AGB in late harvesting at medium SD (e.g. ID 1, 9 and 13 in Figure 1.5).

In summary, *Step A* activities (Figure 1.1) led to a detailed and accurate representation of the plant development and growth while markedly reducing the number of parameters from 84 (Arungro) to 38 (SunnGro).

1.3.1 Multi-site model evaluation

The comparison of measured and simulated AGB (Mg ha^{-1}) in the Aliartos, Guadajira and Cadriano experiments in the period 2016-2018 is shown as scatterplot in Figure 1.6. The model evaluation was carried out applying the model parameter set calibrated in *Step B* of this study (Figure 1.1).

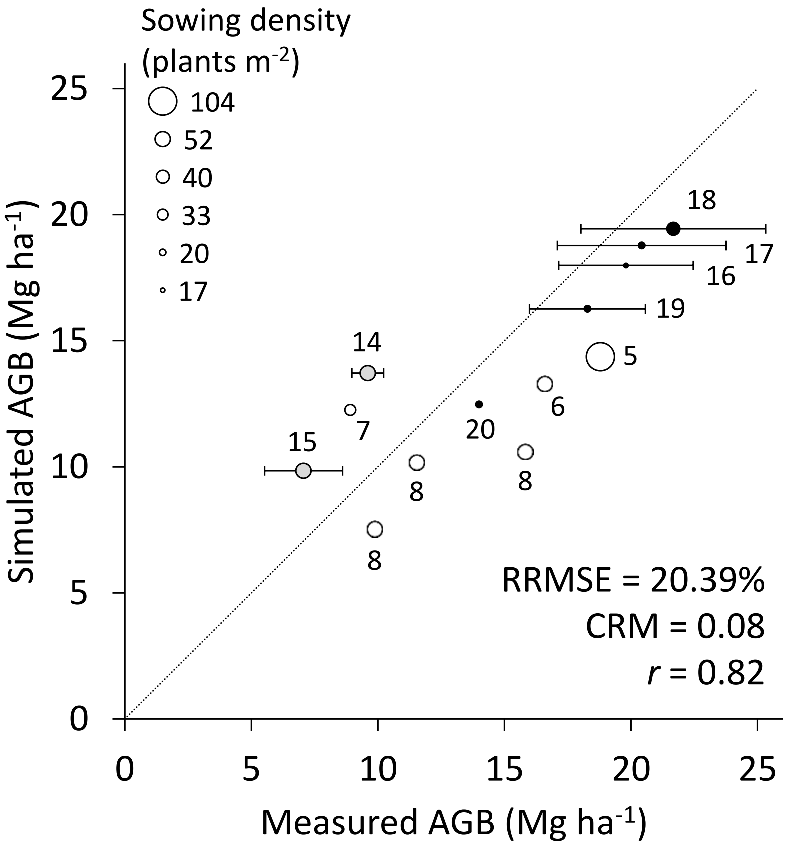

Figure 1.6 1:1 plot between measured and simulated values of aboveground biomass (AGB) of sunn hemp in Aliartos (black circles), Cadriano (empty circles) and Guadajira (grey circles) in the period 2016-2018. Samples are labelled with trial ID. Circle size is proportional to sowing density (plant m^{-2}). Horizontal bars correspond to the standard deviation of sampled mean (n=4). The evaluation metrics reported in the bottom right corner are: relative root mean square error (RRMSE, %), coefficient of residual mass (CRM, unitless) and Pearson's correlation coefficient (r, unitless). The dotted line is the 1:1 line (perfect fit).

SunnGro performances in simulating AGB were positive (r=0.82; R2=0.67), confirming its capability of reproducing the large inter-annual variability of the field experimental data in the explored conditions (RMSE=3.0 Mg ha^{-1}, RRMSE=20.39%, EF=0.6, CRM=0.08). The model correctly simulated higher AGB in the Aliartos experiments (14.0 Mg ha^{-1} < AGB < 21.7 Mg ha^{-1}), with an increasing trend from low (31.5 plant m^{-2}) to medium (46.3 plant m^{-2}) and high (89 plant m^{-2}) SD, and the lowest AGB in the late sowing experiment (ID 20, Figure 1.6). In Guadajira, SunnGro simulated lower AGB (7.0 Mg ha^{-1} <AGB <9.6 Mg ha^{-1}), despite a systematic overestimation of the experimental data (about 3.4 Mg ha^{-1}). The model also succeeded in simulating Cadriano experiments (8.9 Mg ha^{-1} < AGB <18.8 Mg ha^{-1}), except in late sowing and late harvest time trial in 2016 (ID 8 Figure 1.6, underestimation of 5.2 Mg ha^{-1}) and in the early sown, medium harvested trial in 2018 (ID 7; Figure 1.6, overestimation of 3.3 Mg ha^{-1}). The average differences between simulated and reference data fluctuated around -2.4 Mg ha^{-1} for Cadriano (-5.2 Mg ha^{-1}< AGB < 3.3 Mg ha^{-1}), 3.4 for Guadajira (2.8 Mg ha^{-1}< AGB < 4.1 Mg ha^{-1}) and -1.9 for Aliartos (-2.2 Mg ha^{-1}< AGB < -1.7 Mg ha^{-1}) and were always smaller than standard deviation of sampled mean (Figure 1.6).

1.4 Discussion

1.4.1 Rationale for model development and parameterization

SunnGro parameters related to phenology and growth were adjusted in model calibration within their biophysical ranges of variation, using literature and the experimental data collected in Cadriano. When no data for sunn hemp were available, the parameter ranges were taken from other legume crops, i.e., cowpea, pea and soybean. The base temperature for emergence (9.5 °C) was consistent with Qi et al. (1999), whereas the optimum temperature was set to 30 °C according to available data on cowpea (Craufurd et al., 1996). The thermal sum from sowing to emergence was set to 59 GDD and the range of variation of this parameter (47-64 GDD) was set according to field measurements (ID 9). A dedicated function was introduced in SunnGro to simulate the flowering date considering the photoperiod sensitivity of the short-day sunn hemp crop (Stöckle et al., 2003). The base and cutoff temperature for flowering were set at 9.4 and 28 °C according to Craufurd et al. (1997), whereas minimum and maximum day length were set at 14 and 6 hours, respectively (Stöckle et al., 2003). The dynamic of branches was reproduced via a three-parameter logistic function (Bem et al., 2017a) based on thermal time accumulation from emergence to the peak of branch population, with base (6.72 °C) and optimum temperature (38.35 °C) in line with Boons-Prins et al. (1993) and Van Heemst (1988) for soybean. The average number of leaves per plant was set at 26, varying base and optimum temperature coherently with Qi et al. (1999) on sunn hemp and Boons-Prins at al. (1993) on soybean. Average leaf length (11.7 cm) and width (3 cm) were set according to field measurements (ID 9). The maximum conversion coefficient of intercepted PAR into dry matter was calibrated to 6.55 g MJ^{-1} d^{-1} (Lecoeur and Ney, 2003; Van Oijen et al., 2010), reflecting the higher productive attitude of sunn hemp compared to other legume crops. The base temperature for photosynthesis (5.9 °C), the fraction of gross photosynthesis lost for growth respiration (23.8%), the maintenance respiration at 10 °C (0.011 Mg Mg^{-1} d^{-1}) and the base temperature for root extension (6.22 °C) were consistent with measurements of Van Heemst (1988) on cowpea and soybean. The optimum temperature for root extension (30.45°C), the increase in root length per unit of root biomass (9014 cm g^{-1}), the root depth increase per growing degree day (0.57 cm $°Cd^{-1}$) and the maximum (1.858 cm cm-3) and minimum (0.724 cm cm^{-3}) root length density were consistent with data reported by Dart and Mercer (1965), Stockle et al. (2003), Boons-Prins et al. (1993) and Moroke et al. (2005), respectively. The maximum (0.987 Mg Mg^{-1}) and minimum (0.0483 Mg Mg^{-1}) partitioning coefficients of aerial dry mass were set according to reference experimental data and studies from Bem at al. (2017a,b) and Abdul-baki et al. (2001). The PAR extinction coefficient was derived applying the Lambert-Beer equation to LAI measurements and light intercepted data from the ID 9 experiment and were in line with the reference value for cowpea (Littleton et al., 1979). Fractional increase in respiration rate per 10°C rise in temperature (Q10) was left to default value according to Boons-Prins et al. (1993) for *Pisum sativum* L. The only range taken from the Arungro model was related to the coefficient of the exponential function for aerial dry mass partitioning (between 0.51 and 0.69).

1.4.2 Model performance

The accuracy of SunnGro in simulating biometric and growth variables was higher than in most modelling studies available in literature. Best results were achieved by Bem et al. (2017a,b) who estimated leaf number per plant and total dry matter (TDM) content in the Brazilian Rio Grande do Sul State with R^2 ranging from 0.71 to 0.85 for LN and 0.53 to 0.69 for TDM. The lower accuracy of these models was probably due to the use of empirical relationships based on the number of days from sowing, without explicitly considering i) the variability of pedo-climatic conditions, ii) the processes connected to growth and development, and iii) the interactions between environment and management practices. Furthermore, the empiricism characterizing available models reduces their range of applicability, which is limited to the conditions in which they were developed (Donatelli and Confalonieri, 2011). This is an essential prerequisite for model reuse on other species/varieties, regions/locations, spatial scales (smaller/larger than in calibration) (Adams et al., 2013) as well as for climate change impact assessment studies (Cappelli et al., 2018).

A low accuracy (R^2=0.37) was obtained by Le et al. (2018), who used the EPIC model to simulate the rainfed yield of sunn hemp grown as single cover crop or intercropped with millet, in diversified crop rotations in Cambodia. These results were affected by the high complexity of the conservation system simulated, by the oversimplified approach used to represent canopy structure/development and by the lack of extensive datasets for model calibration (ten experiments). Indeed, EPIC is a generic simulator which does not consider neither the simulation of leaf size heterogeneity nor the representation of the dynamic daily evolution of branch/leaf population depending on weather and management conditions, in turns affecting light interception, photosynthesis rate and biomass accumulation. Furthermore, the calibration dataset did not include multiple in-season measurements of phenology and growth variables, as well as detailed information to define crop management and model parameterization.

All these considerations supported the development of a specific process-based model accounting for the heterogeneity of sunn hemp canopy architecture and its evolution over time. Our methodology implied the formalization of new algorithms targeting crop-specific traits and a novel parameterization supported by an extensive literature search and field data collection. This is a standard procedure in crop modelling studies, already applied for oilseed crops (Cappelli et al., 2019; Gilardelli et al., 2016; Zeleke et al., 2014) and legume species (Falconnier et al., 2019; Robertson et al., 2002). Our study allowed achieving very accurate results in simulating sunn hemp productivity across environments, while decreasing the complexity of the original model by halving the number of parameters. At field scale, the generic legume models explained about 60-81% of inter-annual AGB and yield variability, with increasing uncertainty from potential to water- and nitrogen-limited conditions. Compared to generic simulators, specific legume models (Sinclair et al., 1987; Soltani et al., 1999) performed even better, although tested with calibration datasets including a limited number of varieties and in a few sites and years.

1.4.3 Limitations and areas of improvement

In our study, the multiple-site collection of detailed input data and growth variables along crop season, allowed for an accurate and robust model development, calibration and validation under potential conditions, but does not allow extrapolating results to areas with different constraints to productivity. Although sunn hemp is a low-input crop well-adapted to different agro-environmental conditions (Lepcha et al., 2018), it shows appreciable yield decreases when exposed to severe water/nitrogen shortage and pest attacks (da Silva et al., 2016). In this context, the simulation of the impact of soil N on sunn hemp is actually constrained by the availability of i) a dedicated module for the simulation of N in soil-plant system and interactions with farming practices and ii) calibration datasets in which contrasting management and/or environmental conditions occur. Despite some approaches are available for the simulation of soil N (Benbi and Richter, 2002), crop N uptake and partitioning/remobilization to plant organs (Ma et al., 2008), their use is partly limited by a general level of empiricism (i.e. most of them do not explicitly consider the dynamics of the soil microbes and fungi involved in the N soil cycle; Donatelli and Confalonieri, 2011) and requires the collection of *ad hoc* field data to support the nitrogen-limited model implementation and evaluation.

The availability of growth data collected under different pluviometric regimes, together with i) information on soil physical (e.g. soil texture) and hydrological properties (e.g. volumetric water content at wilting point and field capacity) along the soil profile and ii) in-season multiple measurements of volumetric soil water content in the rooted zone would allow to activate and calibrate the water-limited simulation mode. This would further extend the model capability to capture the detrimental effects of low water availability in drought periods or drought-sensitive areas, which is topical under a climate change perspective. Nevertheless, the use of the hydrological model was not necessary here, since soil water retention capacity, mean seasonal cumulative precipitation (average = 224.5 mm ± 110.17 mm) and rescue irrigation, all contributed to prevent any substantial water limitation to sunn hemp production at all the experimental sites.

Significant biases in model accuracy derived instead from the lack of consideration of plant-pest interactions at the Spanish sites, where *Agriotes* spp. and *Spodoptera* spp. insects caused 10-20% yield losses due to early-season infestations (Sastre et al., 2018). Despite specific and generic insect models have been developed (Donatelli et al., 2017), the use of integrated plant-insect approaches is still limited by two main bottlenecks: i) the population dynamics are often not explicitly simulated and ii) the simulation of the impact on plants (e.g. on leaf area or assimilation reduction) is mostly simplistic and need observations on insect damages as input to the model (Donatelli and Confalonieri, 2011).

Another limitation of the study relies on the application of the model to a single variety. In this context, our future perspective is to extend the application of SunnGro to ‘Tropic Sunn’, a highly productive, long season variety, widely used in the subtropical climates of America (Schomberg et al., 2007). Despite SunnGro can be adapted via parameterization to other cultivars, the achievement of this target is currently hampered by the lack of detailed reference datasets including all the information needed to evaluate model accuracy at field level (i.e. dynamic measurements of crop phenology, LAI, BN, LN, AGB). In this perspective, the ideal dataset would include a multi-year experiment consisting of the same varieties grown in contrasting agro-environmental conditions.

1.5 Conclusions

SunnGro model proved to be capable to reproduce sunn hemp morphological traits related to canopy architecture and aboveground biomass under different combinations of management practices and pedo-climatic conditions. The main innovation in our rationale is represented by the implementation of specific algorithms to simulate crop development and the evolution of leaf size/number and branch population along the growing season, getting an excellent balance between goodness of fit, model complexity and system representation. Compared to available sunn hemp models our approach provided more accurate predictions for all simulated variables and especially for aboveground biomass, which represents the most attractive crop trait for green energy sector and related activities - i.e. bioethanol production. Furthermore, the developed modelling solution can be used to test the sunn hemp suitability to southern Europe environment, in order to assess the effect of different agronomic managements to the final yield potential into the existing site-specific cropping schemes. In this regard, the modular approach at the core of BioMA allows for an easy model application to other varieties, and fosters new model implementation, model reuse and cross-domain model integration, as well as the link with georeferenced database at an optimal spatial resolution with information on weather (current and future scenarios), soil and management practices in the area of interest. The model is fully documented and released with a sample application showing how to use it (http://www.biomamodelling.org/Components/Components.aspx?node=30057).

This study set the stage for a deeper assessment of sunn hemp productivity across other European sites during a long-time window, in order to evaluate the crop potential productivity as advanced biofuel feedstock.

CHAPTER 2
European multi-site -year sunn hemp productivity simulation under alternative management practices

2.1 Introduction

Non-biophysical sunn hemp modelling tools had been built to reproduce sunn hemp development, through generic simulator (Le et al., 2018) or empirical relationship between productive/biometric traits and time after sowing (Bem et al., 2017a,b). The limitations of the mentioned modelling approach rely in the low level of extensibility outside the specific site/year in which the model is calibrated as far as there are no specific functions relating the empirical functions to the crop biological processes. Conversely, the SunnGro process-based model (Chapter 1) was deliberately developed with tailored algorithm implementing a gross photosynthesis approach to estimate net carbon fixation, depending on PAR interception, gross CO_2 assimilation, transpiration, growth and maintenance respiration. SunnGro demonstrated his ability in reproducing the crop response to variable pedo-climatic and management conditions. Nevertheless, the sunn hemp biomass potential awareness is still weak. The importance of investigating sunn hemp suitability to European environments relies in the raising interest out of the legume native areas for its multiple uses such as cover crop (Balkom and Reeves, 2005), nematicide (Wang et al., 2002), biofumigant, weed suppressor (Cho et al., 2015; Mosjidis and Wehtje, 2011), source of nitrogen (Schomberg et al., 2007) and, above all, advanced biofuel (Cantrell et al., 2010; Paul and Chakraborty, 2018). Sunn hemp grows fast in warm summer and can reach high biomass yields in a short time (Mansoer et al., 1997; Rotar and Joy, 1983). The quick sunn hemp growth together with the urgent European demand for advanced biofuels (ICCT, 2018; Phillips et al., 2018) may set the stage for its introduction into existing cropping systems (increasing the Land Equivalent Ratio) as dedicated lignocellulosic crop to maximize the availability of local advanced biofuel feedstocks (BECOOL project, 2017). Becoming a valuable bioenergy crop is binded to yield at least as much as the food crop residues to bioenergy, which for a maize on fertile lands in Europe can reach up to 10 Mg ha^{-1} (Scarlat et al., 2010). Hence, this threshold can be adopted as a rationale reference to legitimate a food/bioenergy-based cropping system. However, there are few available studies dealing with sunn hemp cultivation in warm summer climate of Europe, among which a northern Italy one-year experiment (Parenti et al., 2019) reporting yields around 14 Mg ha^{-1}. Besides, various experiments have been carried out in three locations of southern Europe along three years (Chapter 1) under different management, outcoming aboveground dry yields ranging from 6 to 20 Mg ha^{-1}. However, the real crop potential coming from the multi-year cultivation assessment, and the impact of varying the agronomical management is not clear. The understanding of the crop response to varying agro-management practices requires time and found consuming studies that can be pre-screened by the developed sample application (Chapter 1). Moreover, the mentioned trials in two out of three sites, required high watering amount realistically unsustainable for an advanced biofuel dedicated crop. Hence, a further crop productivity assessment across other European environments performed with the mentioned modelling tools aid and aimed at testing the yield response in potential rainfed, low input sustainable cultivations under varying management will present a deeper insight for the crop potential to European temperate environments.

The objective of this study is to forecast sunn hemp potential suitability in a multi-site and -year simulation experiment as a function of the daily average temperature at variables sowing dates and densities, to pave the way for identifying the best site-specific agronomic management to maximize the biomass production, for tackling the advanced biofuel EU-28 target.

2.2 Materials and methods

The SunnGro model component as described in Chapter 1 was used to assess the uncertainty in the model's response varying the three driving factors that utmost influence the final aboveground biomass (AGB): i) the mean seasonal air temperatures ii) the sowing density and iii) the sowing date, focusing on the new developed functions for branch emission and leaf appearance as well as on AGB accumulation, in five locations of southern Europe, particularly suited for sunn hemp cultivation. The simulation was run along the last 20 years in order to capture the variability of the outputs. The Italian, Spanish and Greek sites were chosen due to their tested suitability for the crop as demonstrated by the previous Chapter, whereas a French and a Romanian sites were added to the simulation in order to assess the crop suitability in the far East and West of Europe encompassing different climates. To identify the additional sites of interest we crossed information related to the i) European climate classification according to the Köppen-Geiger taxonomy (Peel et al., 2007), ii) the presence of reliable, consistent and accessible data sources for weather and crop management and iii) the potential crop suitability to agro-climatic conditions. Although no studies are available in literature on the cultivation of sunn hemp in southern and eastern Europe, both locations are actually very suited for growing soybean crop, which shares the botanical family, similar physiologic and agronomic requirements (cultivation period, plant density, fertilization) with sunn hemp (Ciampitti et al., 2016; Rotar and Joy, 1983).

2.2.1 Simulation sites

The climatic data series 1999-2018 were all retrieved from the Prediction of Worldwide Energy Resources (POWER) at the NASA Langley Research Centre (Stackhouse, 2006), which provides global coverage at a spatial resolution of 0.5° latitude by 0.5° longitude (Figure 2.1). These data were hence pinned within the Köppen-Geiger taxonomy (KGT, Peel et al., 2007). The Guadajira (38° 51' lat. N, 6° 40' W, 222 m a.s.l.) and Aliartos (38° 22′ lat. N, 23° 10′ E, 114 m a.s.l.) sites fall in arid steppe cold climate (*Bsk*), characterized by high mean annual temperature and low precipitation with a marked dry summer season (mean annual temperature = 16.6 and 17.5 °C and mean annual precipitation = 506 and 492, respectively). Conversely, Cadriano in northern Italy (44°33' lat. N, 11° 21' E, 32 m a.s.l.) and Toulouse in southern France (43°36' lat. N, 1° 26' E, 141 m a.s.l.) are in the temperate area of Europe, the former in a more continental position with hotter summer (*Cfa*), and the latter in a marine west coast climate with higher mean annual precipitation and warm summer (*Cfb*). Drajna Nouă (44°25' lat. N, 27° 25' E, 37 m a.s.l.) in Romania is marked by summer humid subtropical climate and cold winter (*Dfa*).

The five selected environments cover a wide range of different temperatures, global solar radiation and cumulative precipitation for the southern regions of EU-28 (Figure 2.1). The simulation is performed going from utmost dry summer where a constant supplemental irrigation between 300 and 400 mm for the vegetative season was required in order to obtain an even crop establishment and development and to avoid water limiting conditions not simulated by the SunnGro model (Chapter 1) to more temperate areas, in which that amount of water is usually coming from the summertime precipitations (average of 312 mm in Drajna Nouă and 341 mm in Toulouse).

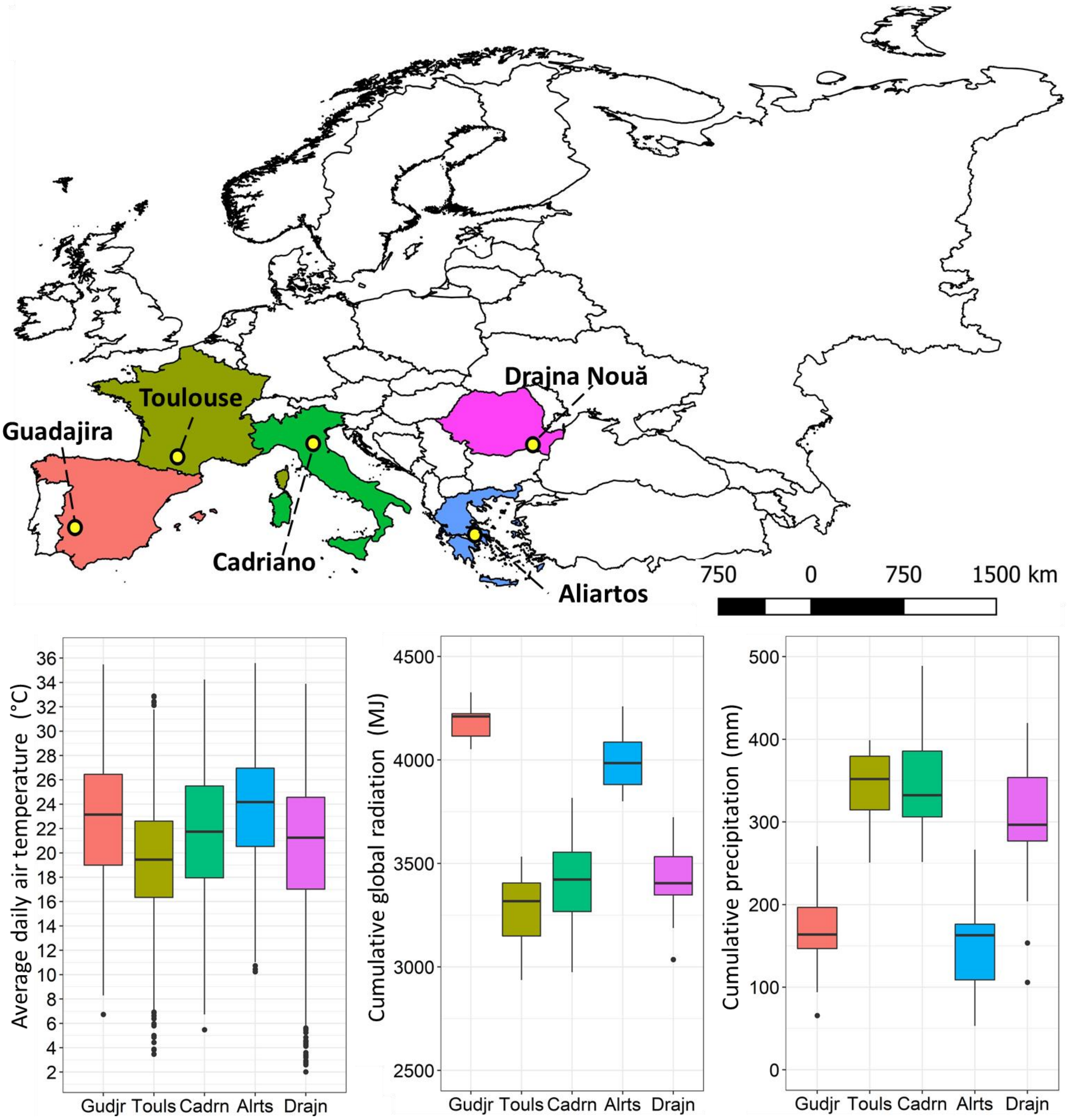

Figure 2.1 Experimental sites (yellow circles) and climatic variability during sunn hemp growing season (May-October) in the period 1999-2018. Gudjr=Guadajira, Spain; Touls=Toulouse, France; Cadrn=Cadriano, Italy; Alrts=Aliartos, Greece, Drajn= Drajna Nouă, Romania.

2.2.2 Analysis of model uncertainty

To explore model response to changes in main agro-climatic input variables determining potential BN, LN and AGB under current climate conditions, simulated outputs were visually inspected via boxplot and contour plot analyses. Uncertainty analysis was repeated for every validation site, i.e. in Italy, Spain, Greece, France and Romania.

Boxplots were drawn with ggplot2 R package, version 0.9.3 (Wickham, 2009). Boxes expand from 25th to 75th percentiles (interquartile distance, IQD), centerline is fixed at 50th percentile, whiskers expand up to the most extreme data point which is 1.5 times lower/higher than the length of the box away from the box; outliers are represented as points.

The boxplots and contour plots of i) AGB, ii) the time to reach the peak of BN and iii) the total number of days in which new leaves are emitted are presented in the results section. A contour plot is a graphic representation of the relationship among three numeric variables in two dimensions. For each experimental site, simulated outputs from Chapter 1 were used, one at a time, as target variable whereas average air temperature and sowing time were selected as explanatory weather and management input variables. For temperature, the range of variation was defined using the mean values during sunn hemp growing season in the period 1999-2018, setting 1 °C between 19 and 27 °C as class interval. As a matter of fact, a series of 20 years is usually considered enough to capture daily, seasonal and inter-annual weather fluctuations, as well as most part of the less frequent climate events that may occur in a given agro-ecosystem (Semenov and Barrow, 2002; Stöckle et al., 1999). Nine planting strategies were tested, by anticipating/delaying the standard sowing time (15 June, DOY 166) of 1-4 weeks (i.e. from 18 May - DOY 138 - to 13 July - DOY 194).

2.3 Results

The AGB values obtained from the long-term simulation experiment carried out in Spain, Greece, Italy, Hungary and France in the period 1999-2018 are presented in Figure 2.2. The AGB values were very heterogeneous and showed a large variability depending on the site, sowing date and sowing density considered. The results revealed two distinct groups of productivity, with a first group including Aliartos and Guadajira showing high average AGB values ($12.1<AGB<14.0$ Mg ha^{-1}; mean=13.3 Mg ha^{-1}) and reduced variability (0.44<average interquartile distance, IQD< 0.8 Mg ha^{-1};mean=0.6 Mg ha^{-1}) and a second group including the remaining sites with low ($8.4<AGB<11.9$ Mg ha^{-1}; mean=10.4 Mg ha^{-1}) and more uncertain ($0.7<IQD<1.4$ Mg ha^{-1}; mean=1.0 Mg ha^{-1}) AGB data. While Guadajira reported both the highest and the less variable AGB data, the most uncertain and the lowest ones were achieved at Cadriano (average IQD of 1.2 Mg ha^{-1} , 67 % higher than the mean of the other sites) and Toulouse respectively (average AGB of 9.9 Mg ha^{-1} , 17 % lower than the mean of the other locations).

In general, AGB values increase from low (mean AGB=10.3 Mg ha^{-1}), to medium (mean AGB= 11.6 Mg ha^{-1}) and high (12.7 Mg ha^{-1}) sowing density, whereas IQD decrease from 1.0 to 0.8 and 0.7 Mg ha^{-1} following the same order. The only exception is represented by Toulouse site, in which AGB variability remained practically constant at different sowing densities, with IQD ranging from 0.8 to 0.8 Mg ha^{-1}. Regardless the sowing density, average AGB values decrease linearly with delayed sowing date from 14.1 Mg ha^{-1} at DOY 138 to 9.2 Mg ha^{-1} at DOY 194, while average IQD increased from 0.8 to 1.0 Mg ha^{-1}. In this context, the most marked IQD linear increases were achieved in Guadjira, Aliartos and Cadriano ($0.57<R^2<0.67$) and, to a lesser extent, in Drajna Nouă ($R^2=0.27$) whereas in Toulouse it remained practically unchanged (R^2 very close to 0).

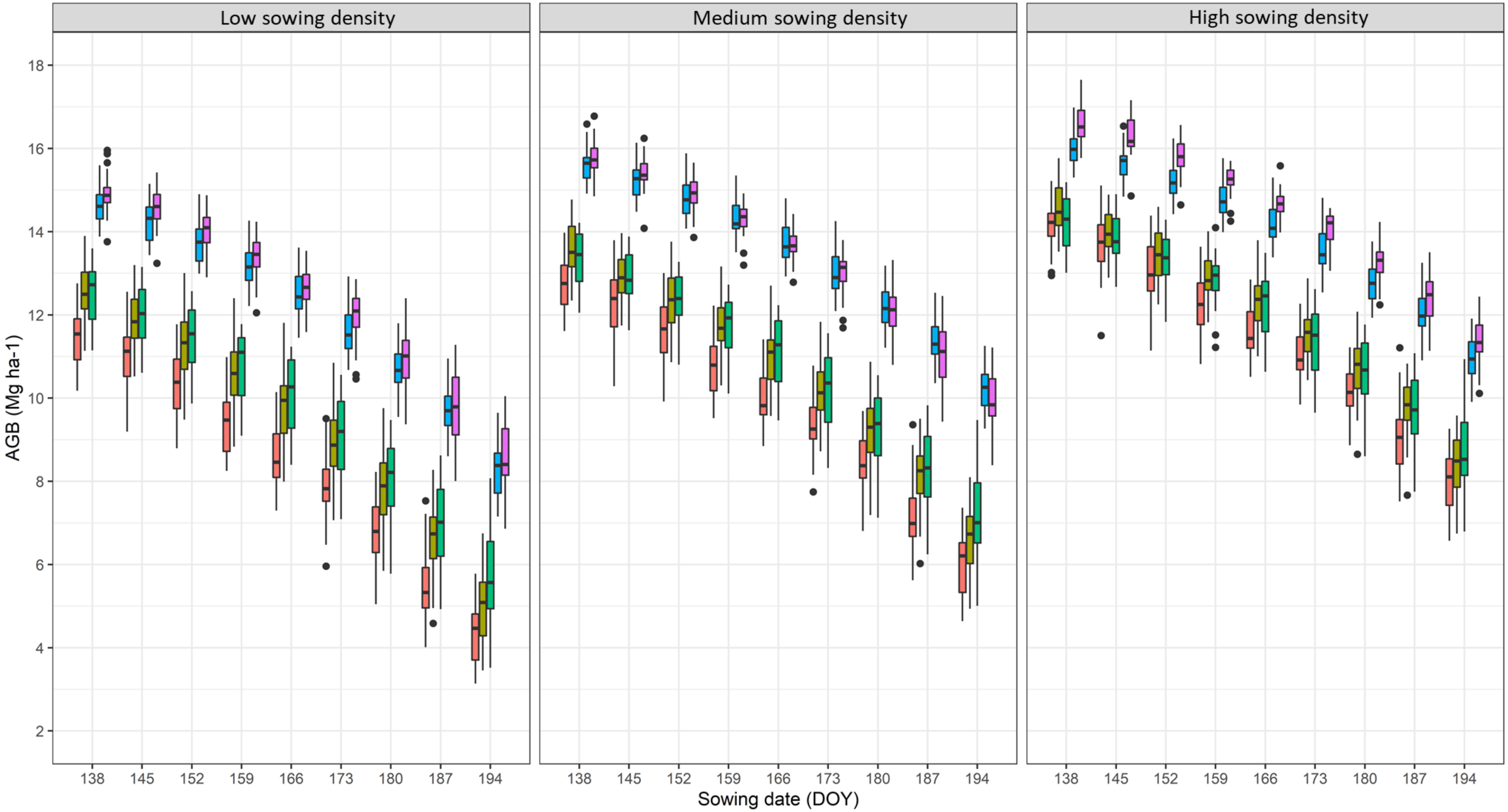

Figure 2.2 Boxplots of aboveground biomass (AGB, Mg ha^{-1}) values simulated in Guadajira (Spain - violet box), Aliartos (Greece - light blue box), Cadriano (Italy - emerald green box), Drajna Nouă (Hungary, green box) and Toulouse (France - coral box) in the period 1999-2018, by adopting different sowing times (nine dates between DOY 138 and 194) and densities (low=33 plants m^{-2}, medium=52 plants m^{-2} and high=104 plants m^{-2}). Each box is derived from the values simulated at harvest for each of the 20 years.

To investigate the combined effect of temperature and sowing date on the variability of sunn hemp productivity at different sites and sowing density simulated AGB data were mapped as contour plot in Figure 2.3.

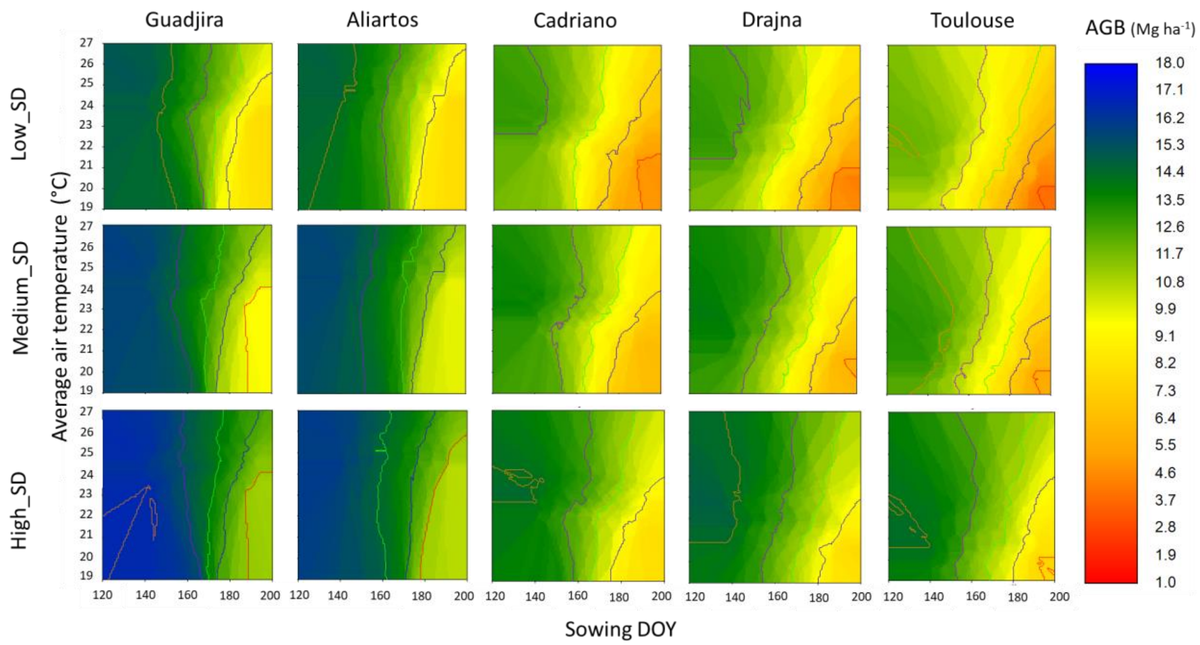

Figure 2.3 Simulated aboveground biomass (AGB, Mg ha^{-1}) as a function of (i) daily mean air temperature during the crop cycle (y-axis, °C) and ii) sowing time (x-axis; nine dates between DOY 138 and 194) at the Spanish (Guadajira), Greek (Aliartos), Italian (Cadriano); Hungarian (Drajna Nouă) and French (Toulouse) sites in the period 1999-2018. SD=Sowing density (low=33 plants m^{-2}, medium=52 plants m^{-2} and high=104 plants m^{-2}).

In general, AGB values progressively raised from late to early sowing and from low to high mean air temperatures, with increases represented by the following order: Toulouse < Drajina < Cadriano < Aliartos < Guadajira and low < medium < high sowing density.

For Guadajira and Aliartos the reduced range of colors explored along the y-axis revealed the predominance of the sowing on temperature effect and a general lower uncertainty of AGB values compared to Cadriano, Drajina and Toulouse locations.

At Spanish and Greek locations, early sowings (before DOY 160 at high SD, 150 at medium SD and 140 at low SD) led to achieve the highest AGB values regardless of temperature conditions experienced by the crop during the growing season, while reducing average uncertainty from 8.3 to 2.5 Mg ha^{-1} at Guadajira and from 7.6 to 2.5 Mg ha^{-1} at Aliartos. At both sites, late sowings (i.e. after DOY 180) allowed to obtain similar values of those achieved at Italian, Hungarian and French locations using reference planting dates (DOY 166) and medium/high sowing densities. The sites of Cadriano, Drajna and Toulouse presented very similar patterns in terms of AGB variability, characterized by higher uncertainty compared to

Spanish and Greek sites, because of a more pronounced temperature effect on productivity. In this context the uncertainty due to temperature effect on AGB variability increases by delaying sowing from 2.3 Mg ha^{-1} (DOY 138) to 4.4 Mg ha^{-1} (DOY 194) at Cadriano, from 2.5 Mg ha^{-1} (DOY 138) to 3.1 Mg ha^{-1} (DOY 194) at Drajna and from 2.4 Mg ha^{-1} (DOY 138) to 2.7 Mg ha^{-1} (DOY 194) at Toulouse, with very slight differences among sowing densities. For each degree increase in temperature, the variability of AGB values simulated at medium SD increased in a range between 0.7 (Toulouse) and 0.8 Mg ha^{-1} (Drajna) at DOY 138, and between 0.9 (Toulouse) and 1.4 Mg ha^{-1} (Cadriano) at DOY 194.

The simulation of days required to reach the peak of the branches number is presented in Figure 2.4. The Toulouse site requires an average of 11, 16, 19 and 22 more days in comparison to Drajna Nouă, Cadriano, Guadajira and Aliartos, respectively. The values decrease from the early sowings to a minimum corresponding to about mid-June, then from the end of June to mid-July the days required increase again to the original values. This trend is also displayed in the contour plot, where the effect of the average daily temperatures reduces the number of days around mid-June sowing dates. The IQD from early sowings to the late ones increases from a minimum of 0.3 to 11.5 days for Toulouse to Drajna Nouă, respectively, except for Guadajira in which the IQD decreases by 0.8 days.

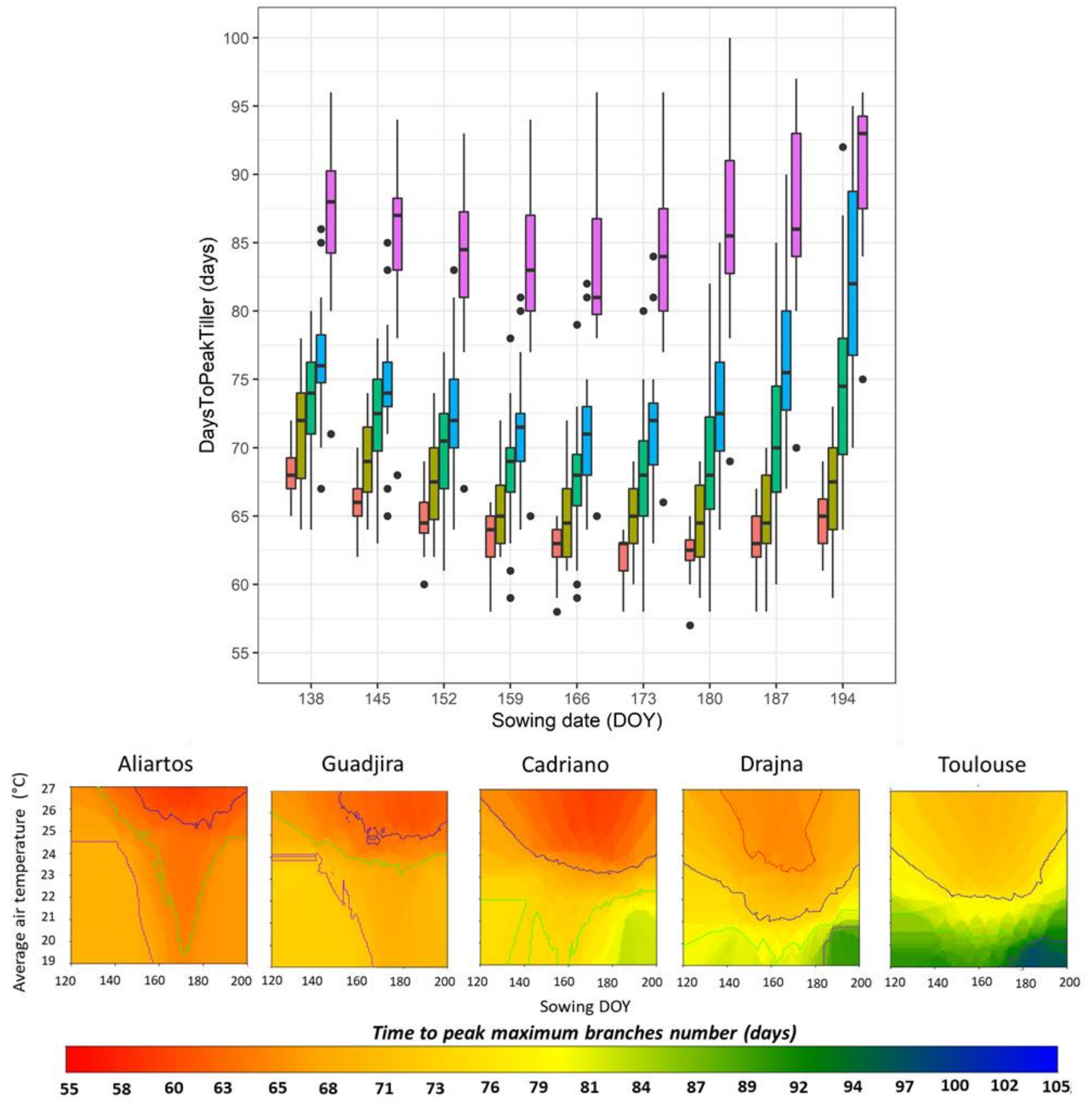

Figure 2.4 Boxplots of the time to reach the peak of branches number (above) simulated in Aliartos (Greece – coral box), Guadajira (Spain - green box), Cadriano (Italy - emerald green box), Drajna Nouă (Hungary, light blue box) and Toulouse (France - violet box) in the period 1999-2018, by adopting different sowing times (nine dates between DOY 138 and 194). Below, the corresponding contour plot as a function of (i) daily mean air temperature during the crop cycle (y-axis, °C) and ii) sowing time (x-axis; nine dates between DOY 138 and 194) at the Spanish (Guadajira), Greek (Aliartos), Italian (Cadriano); Romanian (Drajna Nouă) and French (Toulouse) sites in the period 1999-2018. Sowing density has no effect on the time to the peak of branches number per plant.

The IQD of the days to peak leaves number from early sowings to the late ones increases from a minimum of 1.75 to 9 days from Aliartos to Toulouse (Figure 2.5). The mean number of days required to reach the full leaves population has similar values in early and late sowing, whereas in the mid-June ones the number decreases to 62, 64, 68, 71 and 83 for Aliartos, Guadajira, Cadriano, Drajna Nouă and Toulouse, respectively. It is remarkable to notice how in Toulouse contour plot the effect of daily low temperatures at the late sowing dates (194 DOY) foresee a sharp reduction in the required days from about 60 to 32.

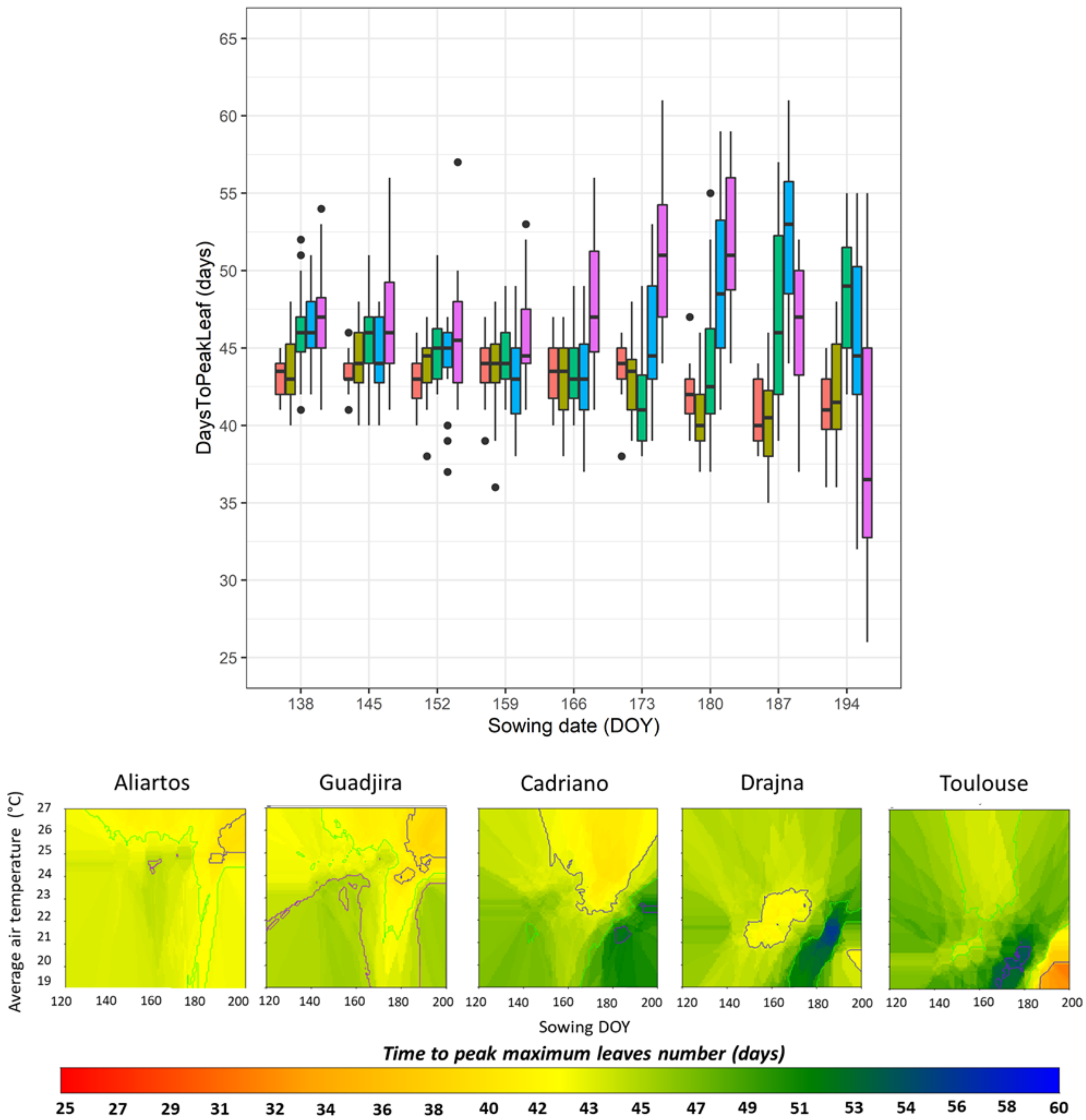

Figure 2.5 Boxplots of the time to reach the peak of leaves number (above) simulated in Aliartos (Greece – coral box), Guadajira (Spain - green box), Cadriano (Italy - emerald green box), Drajna Nouă (Hungary, light blue box) and Toulouse (France - violet box) in the period 1999-2018, by adopting different sowing times (nine dates between DOY 138 and 194). Below, the corresponding contour plot as a function of (i) daily mean air temperature during the crop cycle (y-axis, °C) and ii) sowing time (x-axis; nine dates between DOY 138 and 194) at the Spanish (Guadajira), Greek (Aliartos), Italian (Cadriano); Romanian (Drajna Nouă) and French (Toulouse) sites in the period 1999-2018. Sowing density has no effect on the time to the peak of leaves number per plant.

In Figure 2.6 the reduction of the crown size as a function of the sowing date displays how the delay of the sowing affects the final canopy of the plants. From DOY 173 the thermal time accumulation does not allow to reach the attainable final crown size with different degrees of severity following the order Toulouse > Drajna Nouă > Cadriano by a 48, 36 and 16 %, respectively. The Greek and Spanish sites are only marginally affected by the sowing delay with a reduction of about 3 %.

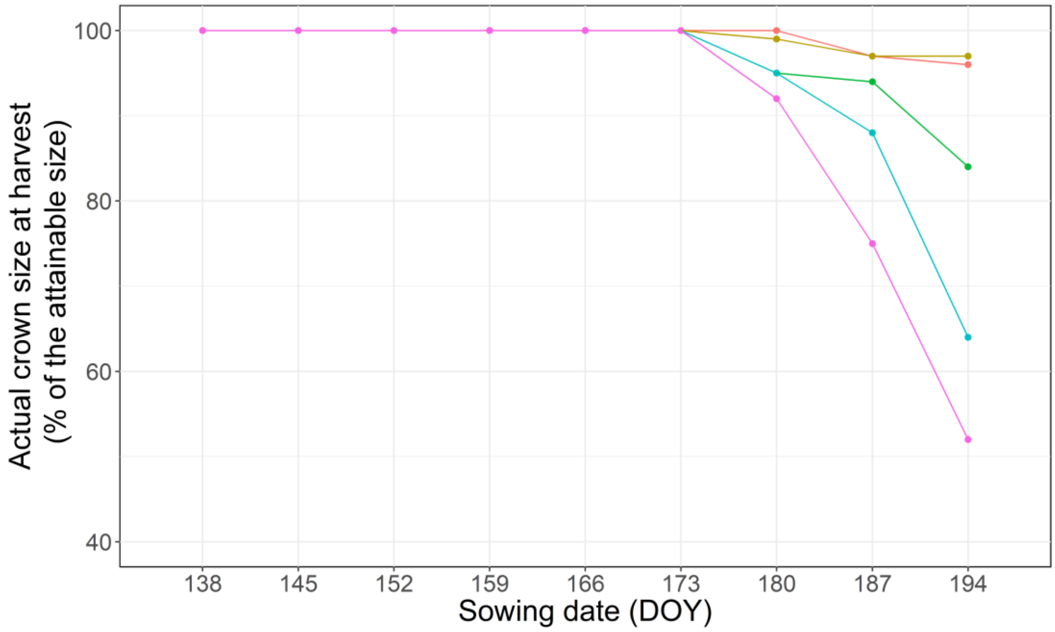

Figure 2.6 Actual crown size at harvest, expressed as percentage of the size attainable by completing thermal time accumulation, simulated in Aliartos (Greece – coral line), Guadajira (Spain - green line), Cadriano (Italy - emerald green line), Drajna Nouă (Hungary, light blue line) and Toulouse (France - violet line) in the period 1999-2018, by adopting different sowing times (nine dates between DOY 138 and 194). Each point is the mean over 20 years.

2.4 Discussion

The simulation of sunn hemp as a single crop is the starting point for the evaluation of the performances of the species in conventional and/or unconventional crop rotations, in terms of biomass production, amount of inputs required (water, nitrogen) and agronomic operations. In the framework of the BECOOL project (BECOOL project, 2017), the University of Bologna is collecting data to evaluate all these aspects, with the aim of providing input data for *in-silico* simulation experiments for the design of new food/energy cropping systems. In this context, the modular structure of the BioMA framework is aimed at fostering the extension of simulated i) processes, ii) production levels and iii) interactions between components of the systems, allowing for an easy realization of customized modelling solutions at an optimal spatial resolution, with the latter being dependent on the study purposes and available input layers. Moreover, it should be mentioned that BioMA provides to the user advanced tools for sensitivity analyses and multi-site automatic calibrations, which both can greatly facilitate model adaptation to other varieties and its application outside the conditions for which they are calibrated.

In this perspective, the results from the simulations and the analysis of uncertainty provide some general indications, which can be explained by considering the high thermal needs of sunn hemp, a species that is well-adapted to tropical, subtropical and warm temperate environments (Lepcha et al., 2018). The results point out the following sunn hemp productivity gradient Guadajira > Aliartos > Cadriano > Drajna Nouă > Toulouse. Indeed, while in hot-summer Mediterranean Spanish and Greek environments the crop is already well-suited reaching yield peaks close to the potential for the species, in marine west coast (i.e. Toulouse) and humid subtropical climates (Cadriano and Drajna Nouă) productions are quite penalized under current climate by constraints to photosynthesis due to sub-optimal temperatures. In the latter countries, projected temperature raises are expected to establish more favorable conditions for the crop by reducing the thermal limitation to solar radiation conversion and fastening leaf area expansion in the early season and, in turns, enhancing light interception. Conversely, in Aliartos and Guadajira a warmer scenario would presumably exacerbate the increase in irrigation water consumption, given that, 300-400 mm of irrigation water are already needed to reach yield potential under current scenario. The combination of sowing density and sowing time influence on the final AGB is utmost relevant. According to the initial assumption of setting AGB to 10 Mg ha^{-1} as threshold for a rationale bioenergy system, Figure 2.2 shows how the pre-condition to sunn hemp cultivation is satisfied at each site at 145, 159 and 180 DOY sowing date for the low, medium and high sowing density, respectively. Hence, considering the opportunity to double crop sunn hemp after a cash crop, the model showed that sunn hemp sowing at its highest rate can be delayed to the end of June at the latest for Cadriano, Drajna Nouă and Toulouse. Otherwise, at Aliartos and Guadajira the 10 Mg ha^{-1} are reached up to the mid-July (194 DOY) sowing date. Indeed, the AGB decreases, grouping in two: i) Cadriano, Toulouse and Drajna Nouă; ii) Aliartos and Guadajira. The Spanish and Greek locations are the most suited for sunn hemp cultivation due to the fast thermal time accumulation that even in late sowing forecasts AGB around the convenience threshold. The issue with the latter sites is related to the high water required as supplemental irrigation that challenges the cultivation sustainability in these two dry environments (see Table 1.1, Chapter 1). On the other hand, the Italian, Romanian and French environment results suitable for sunn hemp early season sowing, providing a lower AGB compared to the Spanish and Greek, although realistically in rainfed condition (Figure 2.1). Furthermore, the late sowings, simulated to test a subsequent wheat-sunn hemp scheme, results in a general increased uncertainty in final AGB due to a higher sensitivity to the year-to-year climatic variability. The simulation of the number of days to the peak of branch and leaf numbers (Figures 2.4 and 2.5) produced an alike increased uncertainty trend going from the early to the late sowings. Similarly, the reduction of the crown size (Figure 2.6) highlights that from 180 DOY sunn hemp starts to suffer the low thermal time accumulation from sowing to harvesting in comparison to the optimal thermal time accumulation required for flowering (around 1300 GDD) with different severity degrees for the different environments. It is worth to remark how the days to maximum branches number (Figure 2.4) trend decrease in every location around the end of May to mid-June, possibly due to the occurrence of the optimal temperatures for sunn hemp emergence. Indeed, a successful and quick emergence may influence the plant standing and boost the apical dominance, forcing the plants to an utmost stem elongation and consequently an overall lower number of branches that is reached in less time.

2.5 Conclusion

The results provide exhaustive examples of how SunnGro could support farmers in finding the best trade-off between crop management and productivity under current climate, as well as in anticipating crop responses to temperature variability depending on sowing date and density in different European environments. The performed simulations together with the uncertainty analysis shows that moving northern the sunn hemp aboveground biomass in optimal conditions decreases rapidly. According to the existing climatic and agronomical framework Cadriano, Drajna Nouă and Toulouse areas represent a rational choice for sunn hemp cultivation even as double crop. The balance between the warm summer paired with the adequate precipitations allow the crop to outperform the AGB reference threshold of 10 Mg ha^{-1} up to 14 Mg ha^{-1}, realistically in rainfed conditions and delayed sowings. On the other hand, Aliartos and Guadajira showed the best average temperatures for the crop growth, even though the amount of required water to balance the crop evapotranspiration is not sustainable at a field scale.

This study may therefore represent the basis to support both private and public stakeholders of agricultural sector in shifting from conventional to integrated sunn hemp-based cropping systems, while evaluating both related feasibility and sustainability in light of global warming. In this context, the consideration of key processes involved with nitrogen and water balance in the plant-soil system, pest-plant interaction and management operations (i.e. crop rotations) would allow quantifying both positive (e.g. nitrogen biological fixation) and negative (e.g. GHG emission) externalities associated with the agricultural system as a whole, and thus maximizing production via a responsible use of agricultural inputs.

CHAPTER 3
Modelling dedicated lignocellulosic annual crops integrated in a food/energy rotation in northern Italy: biomass yields and preliminary overall system performances

3.1 Introduction

At least two thirds of the 100 Mha arable land in EU-28 is dominated by conventional crops rotations, with a share of 60% of cereals (Barel et al., 2017; Eurostat, 2018). In 2011, in the Ebro valley in Spain and in the Po valley in central Italy the maize-fallow-winter wheat rotation acreage was 100,000 and 700,000 ha, respectively (Vasileiadis et al., 2011) with the soil left uncovered for many months. The chance of filling the gaps between the food crops through the cultivation of lignocellulosic crops on the same land (Land Equivalent Ratio intensification) would increase the crop diversification, the local biomass availability and contribute to the EU-28 biofuels target fulfilment (ICCT, 2018) without restricting food land. Moreover, the crop rotation diversification can contribute to the control of pests and disease, amelioration of soil structure and increase crop yield (Li et al., 2019; Liebman and Dyck, 1993). According to Gorchs et al. (2017) an industrial hemp effect on a subsequent wheat is beneficial in terms of grain yield in the first two years. Kenaf (Robinson and Cook, 2001; Russo et al., 1997; Zhang and Noe, 1996), industrial hemp (Struik et al., 2000; Zatta et al., 2012) and sunn hemp (Mosjidis and Whetje, 2011; Wang et al., 2002) have the potential to reduce weed and nematode population for the subsequent crop. For these reasons, the best-known energy crop fitting such food/energy rotations investigated in various European experiments and projects carried out in the last years in temperate environments (CROPGEN project, 2004; BIOKENAF project, Alexopoulou et al., 2004; SWEETFUEL project, Zegada and Monti 2012; FUTUROL project, Dureuil, 2008; 4FCROPS project, Alexopoulou et al., 2010; BECOOL project, Christou et al., 2018) are biomass sorghum (*Sorghum bicolor* x *Sorghum sudangrass*), kenaf (*Hibiscus cannabinus* L.), industrial hemp (*Cannabis sativa* L.) (Zegada-Lizarazu and Monti, 2011) and sunn hemp (*Crotalaria juncea* L.) (Parenti et al., 2018; see Chapter 2). Under optimal pedo-climatic conditions biomass sorghum, kenaf and industrial hemp were able to reach up to 30, 20 and 23 Mg ha^{-1}, respectively (Alexopoulou et al., 2000; Amaducci et al., 2000; Danalatos et al., 2010; Struik et al., 2000; Zegada-Lizarazu and Monti, 2012). Besides, sunn hemp was also able to yield around 14 Mg ha^{-1} in a single experiment in norther Italy (Parenti et al., 2019), although showing a wider adaptability to European climate in multi-year, multi-sites simulation experiment (Chapter 2). Each of the mentioned crops have the potential to produce up to double or triple the lignocellulosic feedstock on an annual basis compared to the potential peak of 10 Mg ha^{-1} of a maize residue to bioenergy (Scarlat et al., 2010). This threshold could be adopted as a breakeven point, in order to assess the effective biomass surplus production of the new cropping system. However, little is known on the effect of the lignocellulosic crops on a subsequent cereal grain and biomass production (Gorchs et al., 2017; Robson et al., 2002; Roth et al., 2000; Schlegel et al., 2002; Unger, 1984). Tracking down the biomass accumulation of the lignocellulosic crops is feasible through agricultural system models that, besides can help farmers identify the best management options as harvest time or reducing agronomic input improving the overall system performance. At a higher level, models can support policymakers and entrepreneurs in gathering important information across space and time to plan the evolution of the multifunctionality of agriculture (Jones et al., 2017). A three-parameters Logistic model using empirical relationships between productive/biometric traits and thermal time sum or time after sowing was successfully used to describe the sunn hemp productive traits such as number of leaves and branches (Chapter 1), aboveground biomass, plants height, stem diameter and root biomass (Bem et al., 2017a,b) demonstrating good performances in reproducing the biomass accumulation. The Logistic model limitation is due to the lack of any relation with the underlying process that strongly reduce the applicability of existing models outside the conditions for which they are calibrated. They can, otherwise, be implemented in more complex, biophysical simulation models as shown in Chapter 1. This biophysical crop simulation models can then be used as supporting tools for in—season agricultural management, as well as to forecast crop yield at regional to global level (Donatelli et al, 2002; Sinclair and Seligman, 2000). Moreover, they are used to predict the future evolution of agricultural systems in the medium-long term, being capable to forecast crop yield across different environments.

In this study an empirical Logistic model (Bem et al., 2017a,b) was used to describe the aboveground biomass and plant height dynamics of sunn hemp, biomass sorghum, kenaf and industrial hemp grown within a maize-lignocellulosic crop-wheat cropping system in a temperate European environment. The SunnGro model was set aside to compare the four lignocellulosic crops with the same tool. Moreover, SunnGro was developed to potentially estimate the suitability of unknown European environments to sunn hemp cultivation and in this context to test the different management and climatic variability effect on the final yield. Conversely, in this Chapter the interest relied in comparing sunn hemp to other lignocellulosic crops grown in a well-known environment on a single-year with the already investigated best

agro-management for the northern Italy area. Furthermore, the Logistic functions might be used as a starting point to integrate biophysical model component for biomass sorghum, kenaf and industrial hemp simulation in rotation with food crops.
The aim of the present study is to i) evaluate the goodness of a Logistic model in describing sunn hemp, biomass sorghum, kenaf and industrial hemp height and aboveground biomass dynamics during one growing season in an integrated food/energy cropping scheme in northern Italy; ii) use the developed functions for practically help decision-making at farm-scale; iii) pave the way for the integration of such developed Logistic functions within a new biophysical model for the whole cropping systems productivity simulation and iv) give a preliminary evaluation of the cropping system food/biomass potential.

3.2 Materials and methods

The Logistic model was chosen to reproduce the aboveground biomass (AGB) and plant height (PH) of the four dedicated lignocellulosic crops within the ongoing rotation framework. The simulation of the crop dynamics in a simple three-parameters Logistic function is the first step for the integration of the whole cropping schemes in a composition of coupled biophysical models tailored for the entire rotation. In Chapter 1 (see 1.2.2 section) likewise the Logistic model was fitted to describe the branches and leaves appearance along the growing season. Then, the two Logistic non-linear functions were implemented as a component of a more complex, biophysical process-based SunnGro model able to extend the simulation to variable sites and years. The present study deals with the development of non-linear functions that will be part of the modification to the rotation model simulator.

3.2.1 Logistic model and competition metrics

The Mischan and Piño (2014) Logistic model was fitted to simulate the AGB and the PH of the four dedicated lignocellulosic crops as a function of the days after sowing (DAS). The DAS were then represented as days of the year (DOY) for an easier graphical display, with the aim of comparing the crops behavior to the same reference time frame. The Logistic model was given by the following equation:

$$yi = a * e^{\left(-e^{(b-c*xi)}\right)}$$

Were, y_i is the ith observation of the dependent variable, with $I = 1, 2, \ldots$, n and n is the number of the observation; x_i is the ith observation of the independent variable; a is the asymptotic value; b is a location parameter without direct practical interpretation but with the aim of maintaining the sigmoidal shape of the model; c is a parameter associated with growth and the asymptotic plateau and e is the base of the neperiano logarithm. The Logistic model fitting was carried out through the Solver Microsoft Excel® component, setting as objective cell to minimum the sum of the square of the errors between observed and simulated data. The variable cells were set to the three model parameters (a, b, and c).

The Logistic model inflection point (IP) was calculated by:

$$xi = \frac{-b}{c}$$

$$yi = \frac{a}{2}$$

Maximum acceleration point (MAP):

$$xi = \left(\frac{-b}{c}\right) - [\left(\frac{1}{c}\right) * 1.3170]$$

$$yi = \frac{a}{4.7321}$$

Maximum deceleration point (MDP):

$$xi = \left(\frac{-b}{c}\right) + [\left(\frac{1}{c}\right) * 1.3170]$$

$$yi = \frac{a}{1.2679}$$

Asymptotic deceleration point (ADP):

$$xi = \left(\frac{-b}{c}\right) + [\left(\frac{1}{c}\right) * 2.2924]$$

$$yi = \frac{a}{1.1010}$$

The MAP indicates the moment at which the increase (acceleration) in the growth rate (velocity) is maximum. Then the IP (i.e the point at which the curve changes from being convex to concave to convex), when the production rate (velocity) tends to decay (decelerate). The

MDP indicates the moments at which the decrease (deceleration) in the growth rate (velocity) is maximum. Whereas, the ADP indicates the moment of harvest at which increases in production become insignificant (Giacomini Sari et al., 2019). Finally, the breakeven point (BEP) was fixed at 10 Mg ha^{-1} AGB assuming a conservative literature value as assessed by Scarlat (2010).

The model performances in calibration and validation were quantified with standard metrics in crop modelling studies (as Chapter 1), i.e., RMSE, relative root mean square error (RRMSE, minimum and optimum=0%; maximum=+∞, Jørgensen et al., 1986; performances can be rated as very accurate when lower than 10% of the mean, good when between 10 and 20%, acceptable if between 20 and 35 % and poor if higher than 35%, Jamieson et al., 1991; Domeneghetti et al., 2018), coefficient of residual mass (CRM, minimum=-∞, maximum=+ ∞, optimum=0, unitless, Loague and Green 1991; if positive indicates model underestimation and *vice versa*), the modelling efficiency (EF, minimum=-∞, optimum and maximum=1, unitless, Nash and Sutcliffe, 1970; if positive, the model is a better predictor than the mean of measured values and results can be considered acceptable, Moriasi et al., 2007), the coefficient of determination (R^2, minimum=0, optimum and maximum=1), and Pearson's correlation coefficient (*r*, minimum=-1, maximum=+1; extremes reveal a perfect negative or positive linear relationship; if *r* is equal to 0, no linear relationship occurs, unitless; in absolute value, correlations can be considered weak when lower than 0.35, moderate when between 0.36 and 0.67, strong if greater than 0.68 and very strong when higher than 0.9, Taylor, 1990). The model was fitted using the Solver function of Microsoft Excel, setting to minimum the sum of the square of the errors as objective cell and the three equation parameters as variable cells.

The absolute growth rate (AGR) is the growth of a crop in a given time period and it was calculated from the fitted model on a daily basis with the following formula:

$$\mathrm{AGR} = \frac{M_2 - M_1}{t_2 - t_1}$$

where M_2 and M_1 are the mass of the plant at time t_2 and t_1, respectively.

3.2.2 Agronomic practices

The cropping schemes were established in 2017 at the experimental farm of the University of Bologna in Cadriano (32 a.s.l., 44° 33' N, 11° 21' E) in a loam silty soil, neutral (pH 6.6-7.3), rich in K_2O (~159 mg kg^{-1}), with average N, P_2O_5 and organic matter contents of about 1.1 g kg^{-1}, 69 mg kg^{-1} and 1.3%, respectively. The annual average temperature and precipitation during the rotational experiment resulted 0.5 °C higher and 58 mm lower than the 20 years data series (1999-2018). Four innovative rotations were established and compared to a control rotation in a randomized block design with four replications. Each plot was settled in order to allow a complete mechanical management for the simulation of near-to-practice solutions at a field scale. The plots were 231 m^2 each, with an overall area per treatment of 924 m^2. The five systems during the three years rotation (2017-2019) were designed as follow: i) maize-fallow-wheat (C, control), ii) maize-sunn hemp-wheat (R1, rotation one), iii) maize-biomass sorghum-wheat (R2, rotation two), iv) maize-kenaf-wheat (R3, rotation three), v) maize-industrial hemp-wheat (R4, rotation four).

First year rotation (maize)

A winter ploughing, a spring disc harrowing paired with a basal fertilization with 115 kg of N as urea and a rotary harrowing were performed in order to get a firm seedbed preparation before the rotation's settlement. One chemical weed control was carried out at the end of the winter by spraying 4 kg ha^{-1} of glyphosate and a second one was required straight after maize sowing on the 22nd of March 2017 (DOY 81) by spraying a S-Metolachlor, Atrazine, Mesotrione based pre-emergence herbicide at 4 kg ha^{-1} dose. A FAO class 500 maize (Pioneer 1028) (*Zea mais*) was sown (9 seeds m^{-2}) with a pneumatic planter alongside a granular soil sterilant application lambda-cyhalothrin based 10 kg ha^{-1} and a mineral P_2O_5 fertilizers 16 kg ha^{-1} (with additional 8, 2 and 22 kg ha^{-1} of CaO, MgO and SO_2, respectively). A mechanical weed control was performed about 8 weeks after sowing together with an additional 140 kg ha^{-1} of N broadcasting. An insecticide treatment was required in the first week of July and 55 mm were sprinkled split in three different moments due to an abnormal drought occurred in June and July (+1.9 °C of air temperature and -45.7 mm of precipitation compared to the mean values of the period 1999–2018). Finally, the maize was harvested on the 24th of August 2017. The soil was hence tilled before wintertime, to follow the conventional agronomical practices of the area (one ploughing and two harrowing).

Second year rotation (dedicated lignocellulosic crops)

In 2018 the five cropping schemes started to differentiate each other, due to the sowing of the four dedicated lignocellulosic crops. Each dedicated lignocellulosic crop was sown with a pneumatic planter (varying the settings in order to obtain different sowing densities and depth according to the crop-specific characteristics). Excluding industrial hemp in R4, the other crops received a granular soil sterilant application lambda-cyhalothrin based 10 kg ha^{-1} at sowing. A preliminary glyphosate application was carried out at 4 kg ha^{-1} to the whole experimental area, then the 'Futura 75' variety of industrial hemp (*Cannabis sativa* L.) (R4) plots were fertilized with about 60 kg ha^{-1} of N and 92 kg ha^{-1} of P_2O_5, harrowed and sown at 157 seeds m^2 on the 24th of April 2018 (DOY 114). Four days later, the 'Bulldozer' (by KWS) biomass sorghum hybrid (*Sorghum bicolor* x *Sorghum sudangrass*) (R2) was sown at 19 seeds m^2 on the 27th of April 2018 (DOY 117). About one month later the R2 plots were mechanically weeded and fertilized incorporating 120 kg ha^{-1} of N. In R3 plots the Indian 'H328' kenaf (*Hibiscus cannabinus*) variety was coated with an iprodione based fungicide and sown (25 seeds m^2) on the 8th of May 2018 (DOY 128). About one month later kenaf was mechanically weeded and fertilized adding 37 kg ha^{-1} of N. Finally, on R1 plots an additional 4 kg ha^{-1} glyphosate spraying on the 25th of May 2018 (DOY 145) occurred, and the same day the 'Ecofix' variety of sunn hemp (*Crotalaria juncea*) was sown at 52 seeds m^{-2}. Likewise, sunn hemp was mechanically weeded between the rows about one month after sowing, even though it didn't receive any further nitrogen input. The late sunn hemp sowing occurred due to wild rabbit that destroyed the first crop establishment at the beginning of May, hence a metallic fence was placed around R1 plots for the first month after emergence. The late R1 sowing, required a supplemental 15 mm of sprinkler irrigation on the 30th of May. On the 6th of July a violent storm caused a severe lodging to the biomass sorghum, whereas the other crops did not report any damage. On the 20th of August 2018 (DOY 232) industrial hemp was manually and mechanically harvested, whereas for hemp and sunn hemp, biomass sorghum and kenaf the harvest occurred on the 25th of September 2018 (DOY 268).

Third year rotation (wheat)

Straight after harvesting, the plots were all tilled with a spading machine and each of them was immediately sown on the 19th November 2018 (DOY 323) with a medium-early winter wheat (*Triticum aestivum*) 'Starpan' variety (marketed by RAGT) at 200 kg seeds ha^{-1} with a mechanical seeder. Along the vegetative wheat growing season three nitrogen fertilization were applied in i) mid-January (69 kg ha^{-1} of N), ii) during the elongation in mid-March (100 kg ha^{-1} N) and iii) at the inflorescence emergence (40 kg ha^{-1} N). One herbicide treatment was performed in mid-March encompassing both broad and narrow leaf weed control. Two insecticide and two fungicide treatments were applied in mid- and the end of May, following the agronomical practices of the neighbor farmers. The harvest was carried out on the 2nd of July 2019.

3.2.3 Field measurements

Plant density (PD, plants m^{-2}) and dry AGB (Mg ha^{-1}) were measured post-emergence and at harvest, respectively on a representative randomly selected area per reps of 8 m^2 for maize (on the 24th of August 2017), sunn hemp, biomass sorghum, kenaf (25th September 2018) and industrial hemp (20th August 2018), conversely on 1 m^2 on wheat (02 July 2019). The harvest was carried out by manually cut and weight the plants in the sample area at about 3 cm from the soil surface. Then, the dry biomass was determined by oven-drying the fresh mass at 105°C until constant weight. Ten plants per rep were then selected and weighted for the leaves, stems and grain components partitioning. Additional biometric parameters were periodically monitored in 2018 on the dedicated lignocellulosic crops in order to calibrate the Logistic model. The height (PH) was monitored measuring ten randomly selected plants five times during the vegetative season. The AGB, plant components and Leaf Area Index (LAI) were recorded four times about once per month sampling an area of 0.3 m^2 per plot, at each sampling date. The LAI was determined by destructive method using a LI-COR LI 3100C area meter.

3.3 Result

Logistic model evaluation

The Logistic model correctly reproduced the measured dynamics of the plant variables considered (Figure 3.1). The model performances in simulating the evolution of PH and AGB along the vegetative season proved to be accurate for all the four dedicated lignocellulosic crops, with slight deviations from the measured data, especially for PH (RMSE=23.08 cm for PH and 0.4 Mg ha^{-1} for AGB; RRMSE=16.23% for PH and 4.28% for AGB). Indeed, the Logistic model that will be implemented in composition of biophysical model for the whole rotation, succeeded in reproducing the variability of the different crops (EF=0.998 for AGB and 0.959 for PH; r=0.9994 for AGB and 0.982 for PH) with an exploratory power of about 99 and 98%, respectively.

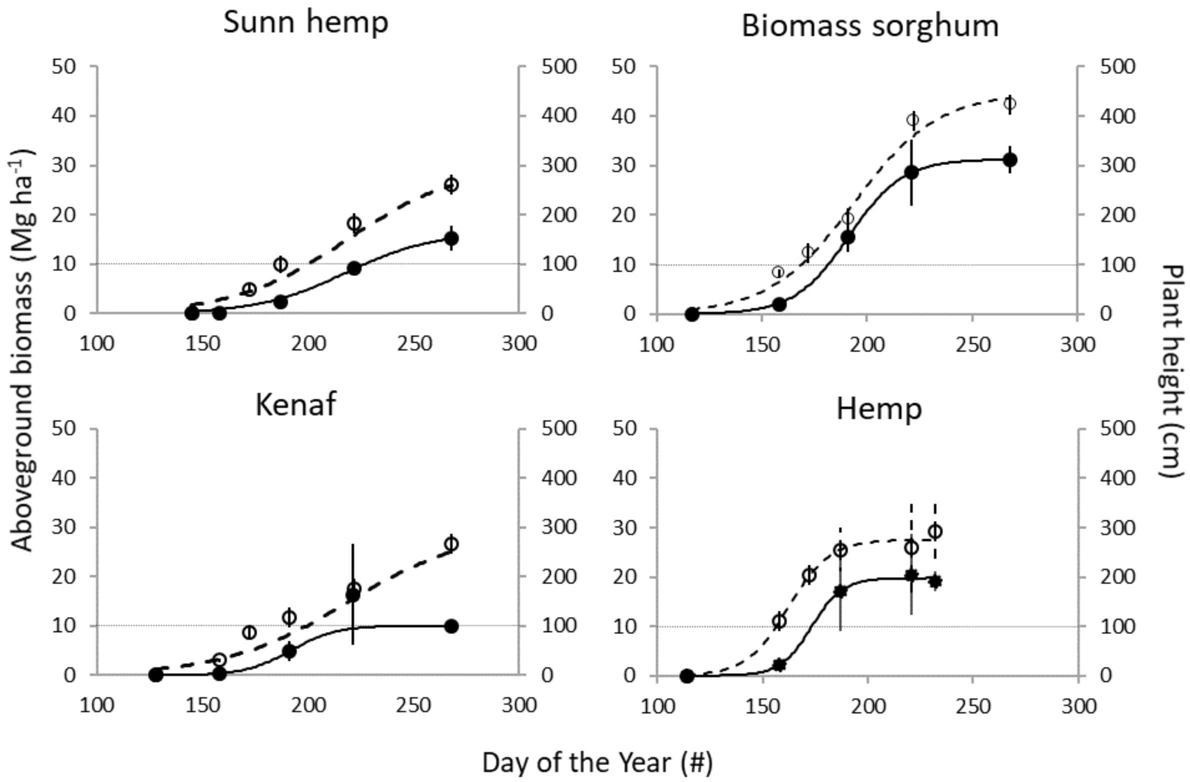

Figure 3.1 Reproduction of the dynamics of the aboveground biomass (AGB, continuous line, main axis) and of plants height (dashed line, secondary axis) during the vegetative season (May-October) of sunn hemp (R1), biomass sorghum (R2), kenaf (R3) and industrial hemp (R4). Measured AGB (black dots) and plants height (empty dots) were collected in 2018 at Cadriano. The lignocellulosic crops were sown at different days of the year (DOY, horizontal axis). Horizontal line represents the breakeven point, assumed as reference for a satisfactory biomass production. Vertical bars correspond to the standard deviation of sampled mean (n=4).

Major differences between simulated and observed values emerged at the first sampling dates, which showed a slight overestimation for AGB (CRM=-0.01) and underestimation for PH (CRM=0.03). However, CRM values were very close to 0 revealing no systematic bias in the simulation of the two variables. In general, the differences between simulated and reference AGB data (Figure 3.2) fluctuated around 0.5 Mg ha^{-1} for sunn hemp (−0.2 Mg ha^{-1}< AGB < 0.8 Mg ha^{-1}), 0.06 for biomass sorghum (-0.02 Mg ha^{-1}< AGB < 0.09 Mg ha^{-1}), 0.02 for kenaf (-0.003 Mg ha^{-1}< AGB < 0.026 Mg ha^{-1}) and 0.7 for industrial hemp (-0.7 Mg ha^{-1}< AGB < 0.7 Mg ha^{-1}) and were always smaller than standard deviation of sampled mean. Likewise, the PH simulated against observed data ranged around 41 cm for sunn hemp (−70 cm< PH < 12 cm), 32 for biomass sorghum (-30 cm< PH < 34 cm), 18 for kenaf (-20 cm< PH < 15 cm) and 16 for hemp (-16 cm< PH < 16 cm).

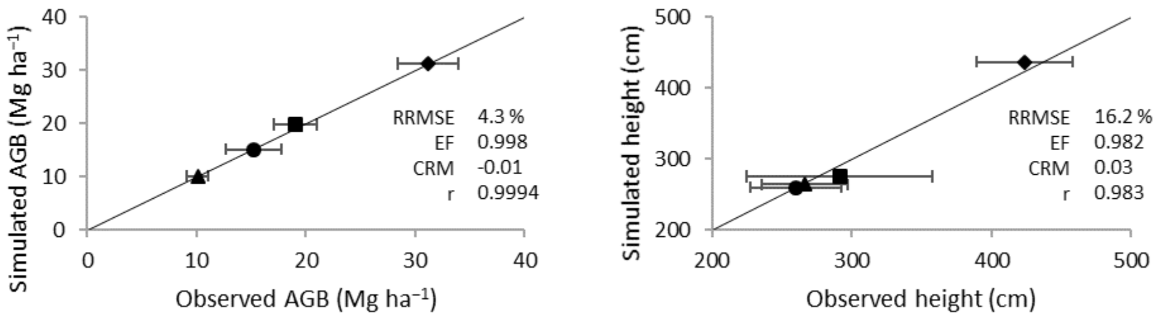

Figure 3.2 1:1 plot between measured and simulated values of aboveground biomass (AGB, left-side) and plants height (PH, right-side) of sunn hemp (dots), biomass sorghum (rhombus), kenaf (triangle) and hemp (square). The evaluation metrics reported in the bottom right corner are: relative root mean square error (RRMSE, %), modelling efficiency (EF, unitless), coefficient of residual mass (CRM, unitless) and Pearson's correlation coefficient (r, unitless). The dotted line represents the 1:1 line (perfect fit). Horizontal bars correspond to the standard deviation of the observed sampled mean (n=4)

Lignocellulosic crops growth dynamics and model critical points

The Logistic model insight on AGB accumulation of the simulated crops (Figure 3.2), allows to inference the time required to the breakeven point (BEP) to the adequate AGB yields for each simulated crop (Table 3.1).

Table 3.1 Model parameters (a, b, c), Inflection point (IP), Maximum acceleration point (MAP), Maximum deceleration point (MDP), Asymptotic deceleration point (ADP), Breakeven point (BEP) and the criteria for the evaluation of the fitting quality: relative root mean square error (RRMSE, %), root mean square error (RMSE, Mg ha^{-1}), modelling efficiency (EF, unitless) and coefficient of determination (R^2, unitless).

		Unit	Sunn hemp	Biomass sorghum	Kenaf	Hemp
a		unitless	16.5	31.3	10.1	19.8
b		unitless	-3.5	-5.8	-6.0	-8.1
c		unitless	0.05	0.09	0.09	0.14
IP	x_i	DAS	73	74	64	59
	y_i	Mg ha^{-1}	8.3	15.6	5.1	9.9
MAP	x_i	DAS	45	57	50	50
	y_i	Mg ha^{-1}	3	7	2	4
MDP	x_i	DAS	100	91	78	69
	y_i	Mg ha^{-1}	13	25	8	16
ADP	x_i	DAS	120	103	88	76
	y_i	Mg ha^{-1}	15	28	9	18
BEP	x_i	DAS	82	65	114	60
	y_i	Mg ha^{-1}	10	10	10	10
RRMSE		%	11.1	0.3	0.4	4.2
RMSE		unitless	0.534	0.043	0.013	0.446
EF		unitless	0.992	0.99999	0.99999	0.997
R^2		unitless	0.999	0.99999	0.99999	0.997

Industrial hemp turned out to be the quickest in reaching the BEP, requiring only 60 DAS (174 DOY) to be able to provide 10 Mg ha^{-1} of dry mass, whereas biomass sorghum, sunn hemp and kenaf 65, 82 and 114 DAS (182, 227 and 242 DOY), respectively. The PH in relation to the BEP varied widely between the four dedicated crops, indeed it was met at 161 cm for biomass sorghum, 174 cm for sunn hemp, 205 cm for kenaf and 213 cm for industrial hemp. However, the difference in the absolute time from the maximum acceleration point (MAP) to the maximum deceleration point (MDP) and from MAP to the asymptotic deceleration point (ADP) highlighted a different speed chart in the AGB accumulation. Industrial hemp was capable of an utmost rough acceleration in the MAP-MDP and MAP-ADP interval accumulating 12 and 14 Mg ha^{-1} of AGB in 19 and 26 days, respectively (Table 3.1) with a peak absolute growth rate (AGR) of 0.7 Mg ha^{-1} d^{-1} at 173 DOY (Figure 3.3). Biomass sorghum had a MAP-MDP and MAP-ADP interval in which it grew 18 and 21 Mg ha^{-1} AGB in 34 and

46 days, with a peak AGR of 0.6 Mg ha^{-1} d^{-1} at 191 DOY. Sunn hemp registered the widest growth MAP-MDP and MAP-ADP interval (55 and 75 days, in which it accumulated 10 and 12 Mg ha^{-1} of AGB) reaching an AGR of 0.2 Mg ha^{-1} d^{-1} at 218 DOY. Conversely, kenaf in the MAP-MDP and MAP-ADP interval accumulated the lowest AGB, 6 and 7 Mg ha^{-1} in 28 and 38 days, respectively, with an AGR of 0.2 Mg ha^{-1} d^{-1} at 192 DOY.

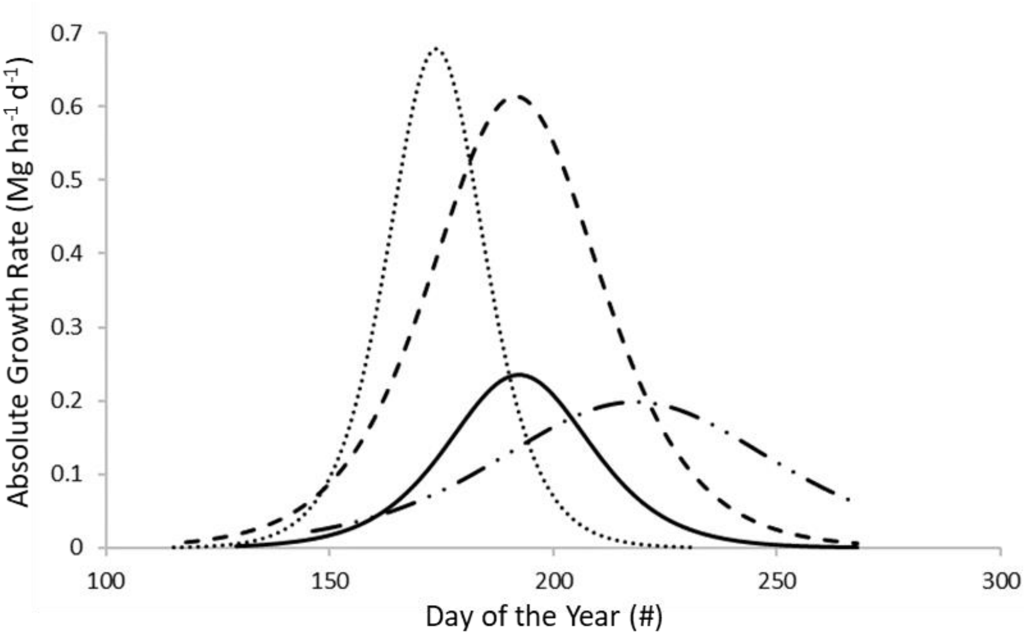

Figure 3.3 Absolute growth rate (AGR, Mg ha^{-1} d^{-1}) of AGB during the second-year rotation (2018) for sunn hemp (R1, long dash dot dot line), biomass sorghum (R2, dash line), kenaf (R3, continuous line) and hemp (R4, round dot line), plotted against the day of the year (DOY) during the growing season.

The AGB components (i.e leaf and stems) and LAI (Figure 3.4) at the final harvest for sunn hemp outcame with 12.4, 2.8 Mg ha^{-1} of stems and leaves dry biomass, respectively (stems representing the 82% of the AGB). Biomass sorghum produced 25.8 Mg ha^{-1} of stems, 3.7 of leaves and 1.7 of grain dry biomass (stems about 83% of AGB). Kenaf averaged 8.6, 1.5 Mg ha^{-1} of stems and leaves dry biomass, respectively (stems about 85% of AGB). Finally, industrial hemp yielded 15.2, 3.9 Mg ha^{-1} of stems and leaves dry biomass (stems about 80% of AGB). The final LAI was greatest for industrial hemp that reached 10.7 m^2 m^{-2}, then sunn hemp, kenaf and biomass sorghum with 7.3, 4.6 and 2.4 m^2 m^{-2} respectively.

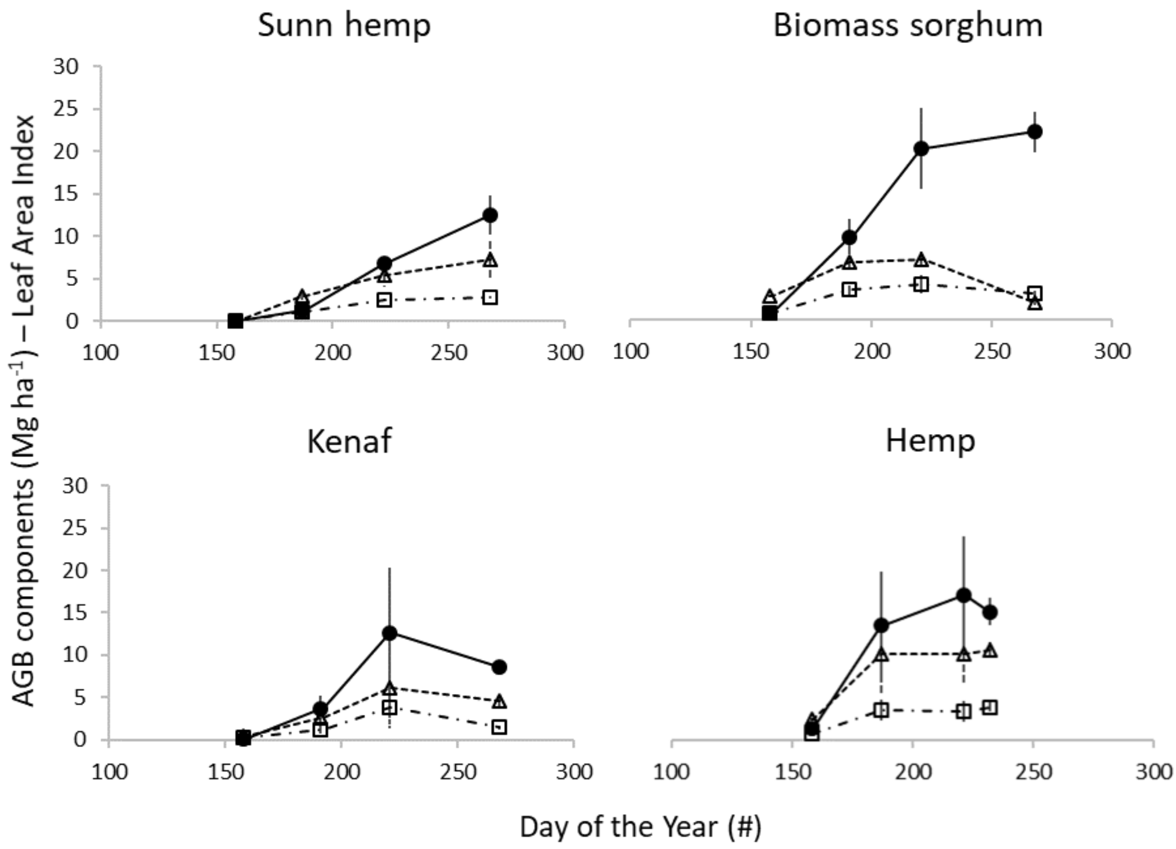

Figure 3.4 Stems (black dots with continuous trendline), leaves (empty triangles with square dot trendline) dry biomass and LAI (empty squares with dash dot trendline) at each of the four sampling dates. The data were collected during the second-year rotation (2018) for sunn hemp (R1), biomass sorghum (R2), kenaf (R3) and industrial hemp (R4).

The productive traits of the five tested crop rotations are presented in Figure 3.5. The left column is to indicate the total amount of food produced by each rotation during the whole cropping system. No statistically significant differences ($P < 0.05$) were found in the grain production in any of the three year, with each rotation averaging about 16 Mg ha^{-1} of dry grain.

Preliminary rotations results

However, looking at the cumulative biomass mobilization capacity, the R2 was able to reach 44.5 Mg ha^{-1} dry AGB, (average of about 14.8 Mg ha^{-1} per year). R4 and R1 were able to yield a similar amount of AGB, 33.7 and 30.4 Mg ha^{-1}, respectively (11.2 and 10.1 Mg ha^{-1} per year). R3 resulted to have the lowest overall AGB production within the higher LER schemes, yielding 25.4 Mg ha^{-1} along the three years and 8.5 Mg ha^{-1} average per year. The control rotation mobilized an overall AGB of 14.9 Mg ha^{-1} (5.0 Mg ha^{-1} per year).

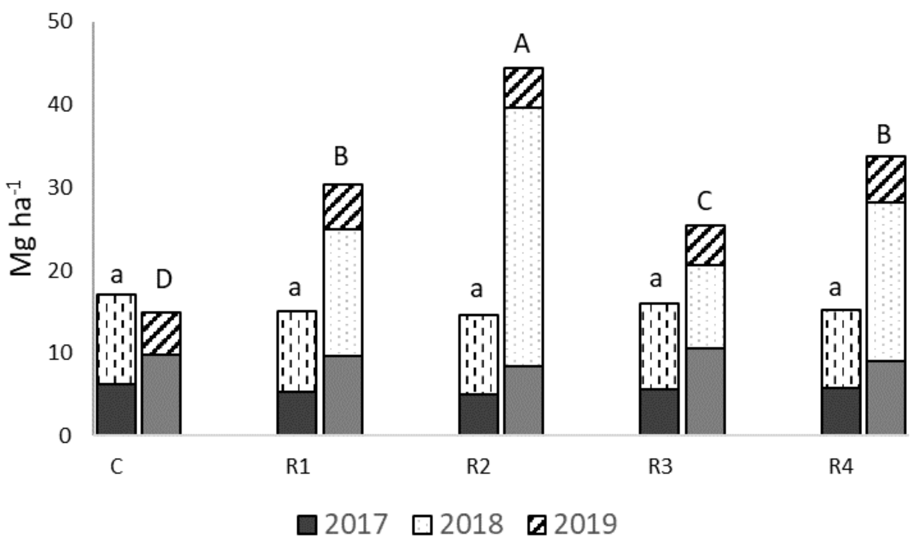

Figure 3.5 Cumulated grain yields (left-column) and AGB (right-column) by rotation. The solid-color pattern stands for the first-year rotation (2017), the dotted pattern for the second-year (2018), the vertical and diagonal stripes pattern for the third-year (2019). All parameters were subjected to the analysis of variance ($P < 0.05$) and the LSD test was used for means comparison separately for grain and AGB production.

The gap between the biomass mobilization of the five systems is chiefly due to the diverse AGB accumulation of the dedicated bioenergy crop during the growing season (see dots in Figure 3.1). Biomass sorghum was able to outperform industrial hemp, sunn hemp and kenaf by yielding 63, 105 and 209% more AGB. Regardless, the effect of the dedicated lignocellulosic crop on the subsequent wheat produced a significant decrease in the harvested wheat straw at the end of the rotation for the R3 compared to R4 and R1 by 3.5 and 3.4 Mg ha^{-1}, respectively; whereas similar to R2 and C. Otherwise, the wheat grain production was unaffected.

3.4 Discussion

Given the scope of the present study the most effective way to compare the four lignocellulosic crops was the choice of a common tool. SunnGro was designed to simulate sunn hemp potentiality in unknown environment under different pedo-climatic and agro-management. The Cadriano site is well-known and already used in the SunnGro calibration dataset, besides SunnGro is unable to simulate biomass sorghum, kenaf and industrial hemp. Due to these reasons the Logistic function (Bem et al., 2017a,b), previously used in Chapter 1 (see section 1.2.2) that proved high performances in simulating leaf and branch population based on the thermal time daily accumulated from emergence, was chosen. A further step will be to include SunnGro in a modelling solution able to simulate the whole crop rotation. In this context, the new modelling solution will contain a suite of crop models each one specifically designed to reproduce the crop cycle of one or more species along the rotation.

According to Jamieson (1991) and Domeneghetti (2018) the fitted three-parameter Logistic function was able to simulate AGB and PH of the four dedicated lignocellulosic crops with a 'very accurate' and 'good' rating, respectively. The other model evaluation parameters support the goodness of the fitting with low RMSE, high EF, R^2 and CRM very close to 0. According to Taylor (1990) the Pearson's correlation coefficient higher than 0.9 highlighted a 'very strong linear' correlation between measured and observed data both for AGB and PH. The calculation of the critical curve points MAP, IP, BEP, MDP, ADP allow an in-field ready-to-use tool that can help increase farmers decision-making efficiency. In particular, the BEP represents the ideal moment in which the AGB of the lignocellulosic crop exceed the biomass yield to bioenergy of a grain/silage maize. Likewise, the ADP is of utmost importance as far as it indicates the moment at which the harvesting should be carried out since increases in production become insignificant. The fitted AGB curves display marked differences in biomass accumulation between the four crops. Industrial hemp was the quickest in reaching the BEP fixed to 10 Mg ha^{-1} not only because it was the first crop to be sown, but rather due to the highest AGR. The mid-late April sown for industrial hemp is a feasible practice in northern Italy, due to its lower germination temperature requirement compared to the others. The early sowing allows industrial hemp to benefit from the higher soil water content, precipitations and lower weed competition. Hence, industrial hemp was able to meet the BEP the 24th of June and on the 10th of July reached the ADP with 18 Mg ha^{-1}. The importance of an early harvest is the key to an optimal and fast field drying window, providing to farmers longer time-frame for the following crop soil preparation. Biomass sorghum is slightly slower in the AGR than industrial hemp, although it is the absolute highest biomass yielding crop of the experiment. The ADP was reached on the 8th of August at 28 Mg ha^{-1} AGB, suggesting that the optimal harvesting for biomass maximization was met early in the season, allowing a longer field drying phase. Nevertheless, the entire plots were completely lodged hampering the manual harvest and most likely, slowing down the mechanical one, demonstrating a higher biomass sorghum susceptibility to lodging compared to the other crops. Sunn hemp and kenaf flatter growth curve suggest that their temperature requirements are not fully accomplished during the growing season. However, sunn hemp reached high AGB, overtaking the BEP much earlier than kenaf on the 15th of August versus the 30th of August, even though it was sown 17 days later. The AGB components reveals the fibrous nature of the dedicated lignocellulosic crops with a high (about 4:1) stems to leaves ratio, which means that the feedstock for advanced biofuel is to a higher extent made of stems. The stems tissues mineral composition has a higher advanced biofuel conversion suitability with regard to leaf tissues (Angelini et al., 2014; Cantrell et al., 2010; Fernando et al., 2007; Monti et al., 2008; Singh et al., 2012). The PH simulation represents an easy and quick estimation of the overall production at a field-scale, allowing prompt action in order to plan the best harvest time during the season without delaying the subsequent crops. It was, indeed, very practical to know with an utmost accuracy that when sunn hemp, biomass sorghum, kenaf and industrial hemp reached about 256, 354, 141 and 260 cm height they were approaching the AGB accumulation plateau in a growing season with +0.7 °C and -19 mm of precipitations compared to the average 20 years data series of the Cadriano's site. The model usefulness is stressed from the perspective of the crop sequencing time which in a crop intensification scenario is of utmost importance. In this light, the Logistic model and its calculated critical points gives practical information on the lignocellulosic crops, allowing to save time for a better soil bed preparation of the succeeding crop. Indeed, the whole cropping system will benefit from more efficient and conscious management.

Even though the mentioned inference could be considered a good reality approximation, it is worldwide known that many biological, environmental and agronomic drivers interacts in the year-to-year crop production variability. For this reason, the future simulation of the whole integrated rotation will take into account some of the biophysical factors improving the extensibility of the prediction capacity through time and space. The flaws of the empirical Logistic function are related to the lack of any relation between the parameters with the underlying process, that strongly reduce the applicability of the models outside the conditions for which they are calibrated. In this light, the agronomic data presented in this research were collected to supplement the modelling output, allowing a deeper insight in the lignocellulosic biomass components (highly valuable for advanced biofuel purpose) and to preliminary evaluate the rotation production potential. These additional agronomic data were presented as far as they will be the benchmark of the calibration/validation of the further modelling activity. The lignocellulosic crops AGB and PH simulation for streamlining the harvest time is important in a crop rotation framework where the management of the preceding crop is reflected on the yield of the subsequent one. Indeed, wheat was sown quite late (19th of November) compared to the usual timing for the area (mid-October) to allow the precedent lignocellulosic crops to grow longer and fit the Logistic model. The performed simulation demonstrates that at least industrial hemp, biomass sorghum and kenaf could have been harvested much earlier without affecting their AGB production. Sowing wheat in mid-October seems to be a feasible practice even though it is subsequent to biomass sorghum, kenaf or industrial hemp. Conversely, sunn hemp seems to require up to mid-September to reach its ADP. Wheat sown was not differentiated across the five rotations, hence the reduction in the wheat straw biomass assessed in R3 compare to R1 and R4 is related to the rotational effect of kenaf on wheat. According to Gorchs et al. (2017) an industrial hemp effect on a subsequent wheat is beneficial in terms of grain yield in the first two years, whereas no information are available on the other dedicated lignocellulosic crops preceding wheat (Zegada and Monti, 2011) regardless the effect on the reduction of weed pressure, insects and nematodes (sunn hemp, kenaf and industrial hemp), increase of crop diversification (sunn hemp, kenaf and industrial hemp) and soil structure amelioration (industrial hemp). Moreover, sunn hemp, might have add some biologically fixed nitrogen (Ashworth et al., 2015; Mappaona et al., 1995) into the soil for the following wheat.

Finally, the AGB and grain three-years overall yields for the four integrated rotations demonstrated the chance to significantly increase the local biomass availability at the farm-scale without affecting the subsequent cereal grain yield. Further studies are needed in order to investigate the long-term effect of such cropping schemes on soil organic matter, nutrient contents, water flows and AGB.

3.5 Conclusion

The Logistic function provides high performances in the annual simulation of dedicated lignocellulosic crops aboveground biomass and plants height. The leverage is given by the easiness of a three-parameter function quickly adaptable through the Solver Excel function from case to case. By contrast, the main limit of logistic functions are the low level of extensibility outside the site/year in which the model is generated as far as there are no specific links relating the empirical model to the crop biological processes. Practically speaking, some site-specific biometric/productive measured data will always be needed to implement the Logistic functions. Nevertheless, their extensibility will be given by the implementation within tailored biophysical model for the cropping schemes simulation. In general, the new crop rotations resulted in 1.5 to 3 higher biomass productions compared to reference scenario (maize/wheat), without decreasing food production. The maize-industrial hemp-wheat rotation provided interesting results; however, industrial hemp harvesting seems a serious technical constrain for this crop. Although sunn hemp produced half biomass than biomass sorghum, a number of potential advantages should be taken into account for this species: sunn hemp, being a legume, does not require N fertilization, it was less prone to lodging than sorghum, and last but not least it may couple the lignocellulosic production with protein production once the site-specific variety has been selected. The fitted functions can support farmers decision-making for setting up the best agricultural practices.

General conclusions and future perspectives

If I was to see a rationale behind the study, this would be: "*in the future, we cannot imagine two separate 'agricultures' for food and biofuels (or more generally, bioenergy), but smart agriculture in which conventional (food/feed) and new uses of agricultural products are integrated and synergic"*.

On this basis, the present study aimed at providing innovative cropping schemes for Europe to increase lignocellulosic feedstocks per unit land without reducing food or feed land use. The model SunnGro was developed to simulate sunn hemp productivity across Europe, an interesting legume crop that may be introduced into conventional crop rotations enable to increase lignocellulosic biomass without reducing land for food/feed crop land. By implementing SunnGro model, the sunn hemp productivity was estimated in different European environments for 20 years. The innovation relies in the possibility to test sunn hemp through a simple, open-source and user-friendly Software Development Kit (SDK) available on http://www.biomamodelling.org/Components/Components.aspx?node=30057. The SDK contains a help file with the documentation of algorithms and models, and a sample application illustrating how to use the component. The model input to provide are a meteo.xlxs and a soil.xlxs files, then a sowing date, harvest time and sowing density. The findings support the introduction of sunn hemp in three out of the five tested environments even though its integration into food/enegy crop rotations requires additional investigations.

In this light a further step was carried out in Chapter 3 in which sunn hemp together with other 3 best-known lignocellulosic crops were simulated within a rotation framework. Sunn hemp, biomass sorghum, kenaf and industrial hemp comparison as potential feedstocks for advanced biofuel within a food/energy integrated crop rotation is first-of-a-kind study to the best of our knowledge. Overall, the rotation with biomass sorghum resulted the highest in biomass yield; the rotations with industrial hemp and sunn hemp are also very promising in the north Italian environment.

This study may therefore represent the basis to support both private and public stakeholders of agricultural sector in shifting from conventional to integrated food/biofuel systems. Significant environmental benefits associated with such innovative crop rotations should be also recognized (nitrogen and water balance, pest-plant interaction, biodiversity and crop diversification, GHG emission, etc.). A further step will be to include all four lignocellulosic crop simulations in a modelling solution able to simulate the whole crop rotation. In this context, the new modelling solution will contain a suite of crop models (e.g. SunnGro, CropSyst v4,..), each one specifically designed to reproduce the crop cycle of one or more species along the rotation, coupled with the same water balance component dealing with the simulation of crop water uptake and soil water redistribution in the soil profile. In this regard, the modular approach at the core of BioMA allows for an easy model application to other varieties, and fosters new model implementation, model reuse and cross-domain model integration, as well as the link with georeferenced database at an optimal spatial resolution with information on weather (current and future scenarios), soil and management practices in the area of interest.

Acknowledgments

This study received financial support from the (i) European Union's Horizon 2020 Research and Innovation Programme under grant agreement 744821 (BECOOL; https://www.becoolproject.eu/) from which the multi-site -year data used in the following thesis were retrieved.

References

Abdul-baki, A.A., Bryan, H.H., Zinati, G.M., Klassen, W., Codallo, M., Heckert, N., 2001. Biomass yield and flower production in sunn hemp: effect of cutting the main stem. J. Veg. Crop Prod. 7, 83–104. https://doi.org/10.1300/j068v07n01_10

Acutis, M., Confalonieri, R., 2006. Optimization algorithms for calibrating cropping systems simulation models. A case study with simplex-derived methods integrated in the WARM simulation environment. Ital. J. Agrometeorol. 11, 26–34.

Adams, H.D., Williams, A.P., Xu, C., Rauscher, S.A., Jiang, X., McDowell, N.G., 2013. Empirical and process-based approaches to climate-induced forest mortality models. Front. Plant Sci. 4 (438), 1-5. https://doi.org/10.3389/fpls.2013.00438

Alexopoulou, E., Christou, M., Eleftheriadis, I., 2010 Role of 4F cropping in determining future biomass potentials, including sustainability and policy related issues. A publication as part of the Biomass Futures project (IEE 08 653 SI2. 529 241) funded by the European Union's Intelligent Energy Programme.

Alexopoulou, E., Christou, M., Mardikis, M., Chatziathanassiou, A., 2000. Growth and yields of kenaf varieties in central Greece. Ind. Crop. Prod. 11, 163-72. https://doi.org/10.1016/S0926-6690(99)00064-3

Alexopoulou, E., Christou, M., Nicholaou, A., Mardikis, M., 2004. BIOKENAF: a network for industrial products and biomass for energy from kenaf. In: Van Swaalj, W.P.M. (Ed.), Biomass for Energy, Industry and Climate Protection. Proceedings of the 2nd World Biomass Conference. 10–14 May, Roma, Italy, 2040–2043.

Allen, B., Kretschmer, B., Baldock, D., Menadue, H., Nanni, S., Tucker, G., 2014. Space for energy crops – assessing the potential contribution to Europe's energy future. Report produced for BirdLife Europe, European Environmental Bureau and Transport & Environment. IEEP, London.

Amaducci, S., Amaducci, M.T., Benati, R., Venturi, G., 2000. Crop yield and quality parameters of four annual fibre crops (hemp, kenaf, maize and sorghum) in the North of Italy. Ind. Crop. Prod. Prod. 11, 179–186. https://doi.org/10.1016/S0926-6690(99)00063-1

Angelini, L.G., Tavarini, S., Cestone, B., Beni, C., 2014. Variation in mineral composition in three different plant organs of five fibre hemp (*Cannabis sativa* L.) cultivars. Agrochimica 58, 1–18.

Ashworth, A.J., West, C.P., Allen, F.L., Keyser, P.D., Weiss, S.A., Tyler, D.D., Taylor, A.M., Warwick, K.L., Beamer, K.P., 2015. Biologically fixed nitrogen in legume intercropped systems: comparison of nitrogen-difference and nitrogen-15 enrichment techniques. Agron. J. 107, 2419–2430. https://doi.org/10.2134/agronj14.0639

Balat, M., 2007. An overview of biofuels and policies in the European union. Energy Sources, Part B Econ. Plan. Policy 2, 167–181. https://doi.org/10.1080/15567240500402701

Balkcom, K.S., Reeves, D.W., 2005. Sunn-hemp utilized as a legume cover crop for corn production. Agron. J. 97, 26–31. https://doi.org/10.2134/agronj2005.0026

Banghoo, M., Tehnani, H., Handerson, J., 1986. Effect of planting date, nitrogen levels, row spacing and plant population on kenaf performance in the San Joaquin Valley, California. Agron. J. 78, 600– 604. https://doi.org/10.2134/agronj1986.00021962007800040009x

Barel, S., Capkovicova, A., Hélaine, S., Lanos, B., Londero, P., Mondelaers, K., Van Doorslaer, B., Van Schagen, M., Pérez, D.Z., 2017. EU agricultural outlook for markets and income 2018-2030. EC. Agriculture and rural development. https://ec.europa.eu/agriculture/markets-and-prices/medium-term-outlook_en

BECOOL project, 2017. Brazil-EU Cooperation for Development of Advanced Lignocellulosic Biofuels. URL: https://www.becoolproject.eu/

Bem, C.M., Filho, A.C., Chaves, G.G., Kleinpaul J.A., Pezzini, R.V., Lavezo, A., 2017b. Gompertz and logistic models to the productive traits of sunn hemp. J. Agric. Sci. 10, 225-238. https://doi.org/10.5539/jas.v10n1p225

Bem, C.M., Filho, A.C., Facco, G., Schabarum, D.E., Silveira, D.L., Simões, F.M., Uliana, D.B., 2017a. Growth models for morphological traits of sunn hemp. Semina: Cien. Agrar. 38, 2933-2944. https://doi.org/10.5433/1679-0359.2017v38n5p2933

Benbi, D.K., Richter, J., 2002. A critical review of some approaches to modelling nitrogen mineralization. Biology and Fertility of Soils, 35(3), 168-183. https://doi.org/10.1007/s00374-002-0456-6

Benson, G.O., 1985. Why the reduced yields when corn follows corn and possible management responses? Proc. Corn Sorghum Res. Conf., Chicago, 161-174.

Bhardwaj, H.L., Webber, C.L., Sakamoto, G.S., 2005. Cultivation of kenaf and sunn hemp in the mid-Atlantic United States. Ind. Crops Prod. 22, 151–155. https://doi.org/10.1016/j.indcrop.2004.08.002

Biederbeck, V.O., Bouman, O.T., 1994. Water use by annual green manure legumes in dryland cropping systems. Agron. J. 86, 543–549. https://doi.org/10.2134/agronj1994.00021962008600030016x

Boons-Prins E.R., De Koning G.H.J., Van Diepen C.A., 1993. Crop-specific simulation parameters for yield forecasting across the European Community (No. 32). CABO-DLO.

Boote, K.J., Minguez, M.I., Sau, F., 2002. Adapting the CROPGRO legume model to simulate growth of faba bean. Agron. J. 94, 743-756.

Bullock, D.G., 1992. Crop rotation. CRC. Crit. Rev. Plant Sci. 11, 309–326. https://doi.org/10.1080/07352689209382349

Bybee-Finley, K.A., Mirsky, S.B., Ryan, M.R., 2016. Functional diversity in summer annual grass and legume intercrops in the northeastern United States. Crop Sci. 56, 2775–2790. https://doi.org/10.2135/cropsci2016.01.0046

Cantrell, K.B., Bauer, P.J., Ro, K.S., 2010. Utilization of summer legumes as bioenergy feedstocks. Biomass and Bioenergy 38, 261–273. https://doi.org/10.1080/00380768.1995.10419623

Cappelli, G., Confalonieri, R., Romani, M., Feccia, S., Pagani, M.A., Cappa, C., Bocchi, S., Bregaglio, S., 2018. Boundaries and perspectives from a multi-model study on rice grain quality in Northern Italy. Field Crop. Res. 215, 140–148. https://doi.org/10.1016/j.fcr.2017.10.014

Cappelli, G., Zanetti, F., Ginaldi, F., Righini, D., Monti, A., Bregaglio, S., 2019. Development of a process-based simulation model of camelina seed and oil production: A case study in Northern Italy. Ind. Crop. Prod. 134, 234-243. https://doi.org/10.1016/j.indcrop.2019.03.046

Chatskikh, D., Olesen, J.E., 2007. Soil tillage enhanced CO_2 and N_2O emissions from loamy sand soil under spring barley. Soil Tillage Res. 97, 5–18. https://doi.org/10.1016/j.still.2007.08.004

Cherr, C.M., Scholberg, J.M.S., McSorley, R., 2006. Green manure as nitrogen source for sweet corn in a warm-temperate environment. Agron. J. 98, 1173–1180. https://doi.org/10.2134/agronj2005.0036

Cho, A.H., Chase, C.A., Treadwell, D.D., Koenig, R.L., Morris, J.B., Morales-Payan, J.P., 2015. Apical dominance and planting density effects on weed suppression by sunn hemp (*Crotalaria juncea* L.). HortScience 50, 263–267.

Christou, M., Alexopoulou, E., Monti, A., Zegada-Lizarazu, W., Parenti, A., Carrasco, J., Ciria, C.S., Pari, L., Suardi, A., 2018. Biomass production and feedstock diversification for advanced biofuels: the BECOOL project. in: 26th European Biomass Conference & Exhibition, Copenhagen, 14–17. https://doi.org/10.5071/26thEUBCE2018-1BV.8.26

Ciampitti, I.A., Schapaugh, W.T., Shoup, D., Duncan, S., Diaz, D.R., Peterson, D., Rogers, D.H., Whitworth, J., Schwarting, H., Jardine, D., Harner, J., Taylor, M., O'Brien, D.M., O'Neil, J., Sharda, A., Haag, L., 2016. Soybean production handbook. Kansas State University Agricultural Experiment Station and Cooperative Extension Service. https://doi.org/10.1021/ac60320a016

Colauzzi, M., Serra, P., Amaducci, S., 2018. Variety earliness effect on field drying of biomass sorghum. Biomass and Bioenergy 115, 160–173. https://doi.org/10.1016/j.biombioe.2018.04.011

Connor, D.J., Cassman, K.G., Loomis, R.S. (Eds.), 2011. Agricultural systems. In: Crop ecology: productivity and management in agricultural systems. Cambridge University Press, Cambridge, 3–22. https://doi.org/10.1017/CBO9780511974199.003

Cook, C.G., White, G.A., 1996. *Crotalaria juncea*: a potential multi-purpose fiber crop. Prog. new Crop. J. Janick, 389–394.

Craufurd, P.Q., Ellis, R.H., Summerfield, R.R.J., Menin, L., 1996. Development in cowpea (*Vigna unguiculata*). I. The influence of temperature on seed germination and seedling emergence. Exp. Agric. 32, 1–12. https://doi.org/10.1017/s0014479700025801

Craufurd, P.Q., Summerfield, R.J., Ellis, R.H., Roberts, E.H., 1997. Photoperiod, temperature, and the growth and the development of cowpea. In: Singh B.B., Mohan Raj D.R., Dashiell K.E., Jackai L.E.N. (Eds.), Advances in cowpea research, 75-86. IITA and JIRCAS. Ibadan, Nigeria.

CROPGEN project, 2004. Renewable energy from crops and agrowastes. URL: http://www.cropgen.soton.ac.uk/

da Silva, G. P., de Mello Prado, R., Moda, L.R., Silva, S.L.O., 2016. Growth, nutrient accumulation and nutritional efficiency of sunn hemp in function of nutrient omission. Afr. J. Agr. Res. 11, 494-499. https://doi.org/10.5897/AJAR2015.10446

Danalatos, N.G., Archontoulis, S.V., 2010. Growth and biomass productivity of kenaf (*Hibiscus cannabinus*, L.) under different agricultural inputs and management practices in central Greece. Ind. Crops Prod. 32, 231–240. https://doi.org/10.1016/j.indcrop.2010.04.013

Dart, P.J., Mercer, F. V., 1965. The effect of growth temperature, level of ammonium nitrate, and light intensity on the growth and nodulation of cowpea (*Vigna sinensis* endl. ex hassk.). Aust. J. Agric. Res. 16, 321–345. https://doi.org/10.1071/AR9650321

Directive (EU) 2015/1513 of the European Parliament and of the Council of 9 September 2015 amending Directive 98/70/EC relating to the quality of petrol and diesel fuels and amending Directive 2009/28/EC on the promotion of the use of energy from renewable sources. Official Journal of the European Union L 239/1, 15.9.2015.

Directive (EU) 2018/2001 of the European Parliament and of the Council of 11 December 2018 on the promotion of the use of energy from renewable sources. Official Journal L 382/82, 23.

Domeneghetti, A., Tarpanelli, A., Grimaldi, L., Brath, A., Schumann, G., 2018. Flow duration curve from satellite: potential of a fifetime SWOT mission. Remote Sens. 10, 1107; 23. https://doi.org/10.3390/rs10071107

Donatelli, M., Bregaglio, S., Confalonieri, R., De Mascellis, R., Acutis, M., 2014. A generic framework for evaluating hybrid models by reuse and composition - A case study on soil temperature simulation. Environ. Model. Softw. 62, 478–486. https://doi.org/10.1016/j.envsoft.2014.04.011

Donatelli, M., Confalonieri, R., 2011. Biophysical models for cropping system simulation. In: Flichman, G. (Ed.), Bio-Economic Models Applied to Agricultural Systems. Springer, 59–87.

Donatelli, M., Magarey, R.D., Bregaglio, S., Willocquet, L., Whish, J.P.M., Savary, S., 2017. Modelling the impacts of pests and diseases in agricultural systems. Agr. Syst. 155, 213-224. https://doi.org/10.1016/j.agsy.2017.01.019

Donatelli, M., Srivastava, A.K., Duveiller, G., 2012. "Estimating impact assessment and adaptation strategies under climate change scenarios for crops at EU27 scale". International Congress on Environmental Modeling and Software Managing Resources of a Limited Planet.

Donatelli, M., Van Ittersum, M., Bindi, M., Porter, J., 2002. Modelling cropping systems - Highlights of the symposium and preface to the special issues. Eur. J. Agron. 18, 1–11. https://doi.org/10.1016/S1161-0301(02)00095-3

Dureuil, A., 2008. File on the environment. Futurol addresses the development and production of 2nd generation bioethanol. Info Chim. Mag. 45, 48–49.

EC (European Commission), 2011. 885 final. Results of the public consultation on the “Energy Roadmap 2050”. 15 December Brussels.

EEA (European Environmental Agency), 2015. Agri-environmental indicator. Greenhouse gas emissions. URL: https://ec.europa.eu/eurostat/statistics-explained/index.php/Main_Page

Eurostat regional yearbook 2018 edition. URL: https://doi.org/10.2785/29084

Falconnier, G.N., Journet, E.-P., Bedoussac, L., Vermue, A., Chlébowski, F., Beaudoin, N., Justes, E., 2019. Calibration and evaluation of the STICS soil-crop model for faba bean to explain variability in yield and N_2 fixation. Eur. J. Agron. 104, 63-77. https://doi.org/10.1016/j.eja.2019.01.001

Fernando, A.L., Duarte, M.P., Morais, J., Catroga, A., Serras, G., Mendes, B., Oliveira, J.F.S., 2007. Characterization of kenaf potential in Portugal as an industrial and energy feedstock, in: New and Renewable Energy Technologies for Sustainable Development, 87–94. https://doi.org/10.1142/9789812707437_0008

French, J., 1978. The effect of fallowing on the yield of wheat. I. The effect on soil water storage and nitrate supply. Aust. J. Agric. Res. 29, 653–668. https://doi.org/10.1071/AR9780653

Gawel, E., Ludwig, G., 2011. The iLUC dilemma: how to deal with indirect land use changes when governing energy crops? Land use policy 28, 846–856. https://doi.org/10.1016/j.landusepol.2011.03.003

Gebremedhin, B., Schwab, G., 1998. The economic importance of crop rotation systems: Evidence from the literature. Dep. Agric. Econ. Michigan State Univ. https://doi.org/10.22004/ag.econ.11690

Giacomini Sari, B., Dal'Col Lúcio, A., Souza Santana, C., Olivoto, T., Diel, M.I., Ketzer Krysczun, D., 2019. Nonlinear growth models: an alternative to ANOVA in tomato trials evaluation. Eur. J. Agron. 104, 21–36. https://doi.org/10.1016/j.eja.2018.12.012

Gilardelli, C., Stella, T., Frasso, N., Cappelli, G.A., Bregaglio, S., Chiodini, M.E., Scaglia, B., Confalonieri, R., 2016. WOFOST-GTC: a new model for the simulation of winter rapeseed production and oil quality. Field Crop. Res. 197, 125–132. https://doi.org/10.1016/j.fcr.2016.07.013

Giller, K.E., Beare, M.H., Lavelle, P., Izac, A.M.N., Swift, M.J., 1997. Agricultural intensification, soil biodiversity and agroecosystem function. Appl. Soil Ecol. 6, 3–16. https://doi.org/10.1016/S0929-1393(96)00149-7

Gorchs, G., Lloveras, J., Serrano, L., Cela, S., 2017. Hemp yields and its rotation effects on wheat under rainfed Mediterranean conditions. Agron. J. 109, 1551–1560. https://doi.org/10.2134/agronj2016.11.0676

Havlin, J.L., Kissel, D.E., Maddux, L.D., Claassen, M.M., Long, J.H., 1990. Crop rotation and tillage effects on soil organic carbon and nitrogen. Soil Sci. Soc. Am. J. 54, 448. https://doi.org/10.2136/sssaj1990.03615995005400020026x

Heitman, A.J., Castillo, M.S., Smyth, T.J., Crozier, C.R., 2018. Stem, leaf, and panicle yield and nutrient content of biomass and sweet sorghum. Agron. J. 110, 1659–1665. https://doi.org/10.2134/agronj2018.03.0178

ICCT (International Council of Clean Transportation), 2014. Wasted, Europe's untapped resource, an assessment of advanced biofuels from wastes & residues (https://theicct.org/sites/default/files/publications/WASTED-final.pdf).

ICCT (International Council of Clean Transportation), 2018. Final recast Renewable Energy Directive for 2021-2030 in the European Union. https://theicct.org/sites/default/files/publications/EU_Fuels_Policy_Update_20180719.pdf P. 3.

IEA (International Energy Agency), 2019. Tracking transport. Retrieved from: https://www.iea.org/reports/tracking-transport-2019

IRENA (International Renewable Energy Agency), 2016. Boosting biofuels: sustainable paths to greater energy security. URL: www.irena.org/publications.

Jamieson, P.D., Porter, J.R., Wilson, D.R., 1991. A test of computer simulation model ARCWHEAT1 on wheat crops grown in New Zealand. Field Crop. Res. 27, 337–350. https://doi.org/10.1016/0378-4290(91)90040-3

Johnson, J.M.F., Novak, J.M., Varvel, G.E., Stott, D.E., Osborne, S.L., Karlen, D.L., Lamb, J.A., Baker, J., Adler, P.R., 2014. Crop residue mass needed to maintain soil organic carbon levels: can it be determined? BioEnergy Res. 7, 481–490. https://doi.org/10.1007/s12155-013-9402-8

Jones, J.W., Antle, J.M., Basso, B., Boote, K.J., Conant, R.T., Foster, I., Godfray, H.C.J., Herrero, M., Howitt, R.E., Janssen, S., Keating, B.A., Munoz-Carpena, R., Porter, C.H., Rosenzweig, C., Wheeler, T.R., 2017. Brief history of agricultural systems modeling. Agric. Syst. 155, 240–254. https://doi.org/10.1016/j.agsy.2016.05.014

Jørgensen, S.E., Kamp-Nielsen, L., Christensen, T., Windolf-Nielsen, J., Westergaard, B., 1986. Validation of a prognosis based upon a eutrophication model. Ecol. Modell. 35, 165–182. https://doi.org/10.1016/0304-3800(86)90024-4

Kamireddy, S.R., Li, J., Abbina, S., Berti, M., Tucker, M., Ji, Y., 2013. Converting forage sorghum and sunn hemp into biofuels through dilute acid pretreatment. Ind. Crops Prod. 49, 598–609. https://doi.org/10.1016/j.indcrop.2013.06.018

Karlen, D.L., Varvel, G.E., Bullock, D.G., Cruse, R.M., 1994. Crop rotations for the 21st century. Adv. Agron. 53. https://doi.org/10.1016/S0065-2113(08)60611-2

Khawaja, C., Janssen, R., 2014. S2Biom: Sustainable supply of non-food biomass for a resource efficient bioeconomy. © 2014 by WIP - Renewable Energies. URL: www.s2biom.eu

Larson, W.E., Clapp, C.E., Pierre, W.H., Morachan, Y.B., 2010. Effects of increasing amounts of organic residues on continuous corn: II. Organic carbon, nitrogen, phosphorus, and sulfur. Agron. J. 64, 204. https://doi.org/10.2134/agronj1972.00021962006400020023x

Le, K.N., Jeong, J., Reyes, M.R., Jha, M.K., Gassman, P.W., Doro, L., Hok, L., Boulakia, S., 2018. Evaluation of the performance of the EPIC model for yield and biomass simulation under conservation systems in Cambodia. Agr. Syst. 166, 90-100. https://doi.org/10.1016/j.agsy.2018.08.003

Lecoeur J., Ney B., 2003. Change with time in potential radiation-use efficiency in field pea. Eur. J. Agron., 19(1): 91-105. https://doi.org/10.1016/S1161-0301(02)00019-9

Lepcha, I., Naumann, H.D., Fritschi, F.B., Kallenbach, R.L., 2018. Herbage accumulation, nutritive value, and regrowth potential of sunn hemp at different harvest regimens and maturity. Crop Sci. 59, 413-421. https://doi.org/10.2135/cropsci2017.09.0589

Li, J., Huang, L., Zhang, J., Coulter, J.A., Li, L., Gan, Y., 2019. Diversifying crop rotation improves system robustness. Agron. Sustain. Dev. 39, 38. https://doi.org/10.1007/s13593-019-0584-0

Liebman, M., Dyck, E., 1993. Crop rotation and intercropping strategies for weed management. Ecol. Appl. 3, 92–122. https://doi.org/10.2307/1941795

Littleton E.J., Dennett M.D., Monteith J.L., Elstonff J., 1979. The growth and development of cowpeas (*Vigna unguiculata*) under tropical field conditions: 2. Accumulation and partition of dry weight. The Journal of Agricultural Science, 93(2): 309-320. https://doi.org/10.1017/S0021859600036868

Loague, K., Green, R.E., 1991. Statistical and graphical methods for evaluating solute transport models: overview and application. J. Contam. Hydrol. 7, 51–73. https://doi.org/10.1016/0169-7722(91)90038-3

Ma, L., Bruulsema, T., Ahuja, L.R., 2008. Quantifying and understanding plant nitrogen uptake for systems modeling. CRC Press.

MacRae, R.J., Mehuys, G.R., 1985. The effect of green manuring on the physical properties of temperate-area soils. Adv. Soil Sci. 3, 71–94. https://doi.org/10.1007/978-1-4612-5090-6_2

Malézieux, E., Crozat, Y., Dupraz, C., Laurans, M., Makowski, D., Ozier-Lafontaine, H., Rapidel, B., de Tourdonnet, S., Valentin-Morison, M., 2009. Mixing plant species in cropping systems: concepts, tools and models. A review. Agron. Sustain. Dev. 29, 43–62. https://doi.org/10.4995/agt.2018.7146

Mansoer, Z., Reeves, D.W., Wood, C.W., 1997. Suitability of sunn hemp as an alternative late-summer legume cover crop. Soil Sci. Soc. Am. J. 61, 246–253. https://doi.org/10.2136/sssaj1997.03615995006100010034x

Mappaona, Yoshida, S., Mappaona, 1995. Growth and nitrogen fixation of *Sesbania cannabina*, *Crotalaria juncea*, and *Cassia tora* under the application of various forms of phosphorus. Soil Sci. Plant Nutr. 41, 613–619. https://doi.org/10.1080/00380768.1995.10419623

Metzger, M.J., Bunce, R.G.H., Jongman, R.H.G., Mücher, C.A., Watkins, J.W., 2005. A climatic stratification of the environment of Europe. Glob. Ecol. Biogeogr. 14, 549–563. https://doi.org/10.1111/j.1466-822X.2005.00190.x

Mischan, M. M., Pinho, S. Z., 2014. Modelos não lineares: Funções assintóticas de crescimento (1st ed.). São Paulo: Cultura Acadêmica.

Montgomery, B., 1954. Sunn fiber. In H.R. Mauersberger (ed.) Mathew's texile fibers. 6th ed. John Wiley & Sons, New York. 323-327.

Monti, A., Di Virgilio, N., Venturi, G., 2008. Mineral composition and ash content of six major energy crops. Biomass and Bioenergy 32, 216–223. https://doi.org/10.1016/j.biombioe.2007.09.012

Moriasi, D.N., Arnold, J.G., van Liew, M.W., Bingner, R.L., Harmel, R.D., Veith, T.L., 2007. Model evaluation guidelines for systematic quantification of accuracy in watershed simulations. Trans. ASABE 50, 885–900.

Moroke, T.S., Schwartz, R.C., Brown, K.W., Juo, A.S.R., 2005. Soil water depletion and root distribution of three dryland crops. Soil Sci. Soc. Am. J. 69, 197. https://doi.org/10.2136/sssaj2005.0197

Mosjidis, J.A., Balkcom, K.S., Burke, J.M., Casey, P., Hess, J.B., Wehtje, G., 2013. Production of the sunn hemp cultivars 'AU Golden' and 'AU Durbin' developed by Auburn University. Alabama agricultural experimental station. https://doi.org/10.13140/2.1.5187.0402

Mosjidis, J.A., Wehtje, G., 2011. Weed control in sunn hemp and its ability to suppress weed growth. Crop Prot. 30, 70–73. https://doi.org/10.1016/j.cropro.2010.08.021

Muth, D.J., Bryden, K.M., Nelson, R.G., 2012. Sustainable agricultural residue removal for bioenergy: a spatially comprehensive US national assessment. Appl. Energy 102, 403–417. https://doi.org/10.1016/j.apenergy.2012.07.028

Nash, J.E., Sutcliffe, J.V., 1970. River flow forecasting through conceptual models, part I. A discussion of principles. J. Hydrol. 10, 282–290. https://doi.org/10.1016/0022-1694(70)90255-6

Nelder, J.A., Mead, R., 1965. A Simplex Method for Function Minimization Comput. The Computer Journal 7 (4), 308–3013. https://doi.org/10.1093/comjnl/7.4.308

Oehmichen, K., Majer, S., Thrän, D., Elbersen, B., Annevelink, B., Forsell, N., di Fulvio, F., 2018. Brazil-EU Cooperation for Development of Advanced Lignocellulosic Biofuels - Deliverable D5.3 Description of plausible value chains. https://doi.org/10.1177/1538574418797223

Papastylianou, P., Kakabouki, I., Travlos, I., 2018. Effect of nitrogen fertilization on growth and yield of industrial hemp (*Cannabis sativa* L.). Not. Bot. Horti Agrobot. Cluj-Napoca 46, 197–201. https://doi.org/10.15835/nbha46110862

Parenti, A., Zegada-Lizarazu, W., Borghesi, A., Monti, A., 2019. Intercropping dedicated grass and legume crops for advanced biofuel production, in: 27th European Biomass Conference & Exhibition, Lisbon., 105–107. https://doi.org/10.5071/27thEUBCE2019-1BO.9.5

Parenti, A., Zegada-Lizarazu, W., Monti, A., 2018. Evaluation of sunn hemp productivity after wheat under no tillage conditions, in: 26th European Biomass Conference & Exhibition, Copenhagen, 2018–2020. https://doi.org/10.5071/26thEUBCE2018-1DV.5.11

Pari, L., Assirelli, A., Acampora, A., Suardi, A., Santangelo, E., 2015. A mower-conditioner to improve fiber sorghum plant drying. Appl. Eng. Agric. 31, 733–740. https://doi.org/10.13031/aea.31.11030

Paul, S.K., Chakraborty, S., 2018. Microwave-assisted ionic liquid-mediated rapid catalytic conversion of non-edible lignocellulosic sunn hemp fibres to biofuels. Bioresour. Technol. 253, 85–93. https://doi.org/10.1016/j.biortech.2018.01.010

Peel, M.C., Finlayson, B.L., McMahon, T. A., 2007. Updated world map of the Köppen–Geiger climate classification. Hydrol. Earth Syst. Sci. 11, 1633–1644. https://doi.org/10.5194/hess-11-1633-2007

Phillips, S., Flach, B., Lieberz, S., Lappin, J., Bolla, S., 2018. EU-28 Biofuels Annual 2018.

Porter, J.R., Semenov, M.A., 2005. Crop responses to climatic variation. Philos. T. R. Soc. B 360, 2021–2035.

Qi, A., Wheeler, T.R., Keatinge, J.D.H., Ellis, R.H., Summerfield, R.J., Craufurd, P.Q., 1999. Modelling the effects of temperature on the rates of seedling emergence and leaf appearance in legume cover crops. Exp. Agric. 35, 327–344. https://doi.org/10.1017/S0014479799003099

Robertson, M.J., Carberry, P.S., Huth, N.I., Turpin, J.E., Probert, M.E., Poulton, P.L., Bell, M., Wright, G.C., Yeates, J., Brinsmead, R.B., 2002. Simulation of growth and development of diverse legume species in APSIM. Aust. J. Agr. Res. 53, 429 - 446. https://doi.org/10.1071/AR01106

Robinson, A.F., Cook, C.G., 2001. Root-knot and reniform nematode reproduction on kenaf and sunn hemp compared with that on nematode resistant and susceptible cotton. Ind. Crop. Prod. 13, 249 – 264. https://doi.org/10.1016/S0926-6690(00)00082-0

Robson, M.C., Fowler, S.M., Lampkin, N.H., Leifert, C., Leitch, M., Robinson, D., Watson, C.A., Litterick, A.M., 2002. The agronomic and economic potential of break crops for ley/arable rotations in temperate organic agriculture. Adv. Agron. 77, 369–427. https://doi.org/10.1016/S0065-2113(02)77018-1

Rooney, W.L., Blumenthal, J., Bean, B., Mullet, J.E., 2007. Designing sorghum as a dedicated bioenergy feedstock. Biofuels, Bioprod. Biorefining 1, 147–157. https://doi.org/10.1002/BBB

Rotar, P.P., Joy, R.J., 1983. "Tropic sun" sunn hemp, *Crotalaria juncea* L., Univ. of Hawaii, College of Tropical Agr. and Human Resources, Institute of Tropical Agr. and Human Resources Research Extension Series 36.

Roth, C. M., Shroyer, J. P., Paulsen, G. M., 2000. Allelopathy of sorghum on wheat under several tillage systems. Agron. J. 92, 855-860.

Russo, V. M., Webber III, C. L., Myers, D. L., 1997. Kenaf extract affects germination and post-germination development of weed, grass and vegetable seeds. Ind. Crop. Prod. 6, 59 – 69. https://doi.org/10.1016/S0926-6690(96)00206-3

Sastre, C.M, Ciria, C.S., Ciria, P., Carrasco, J., 2018. WP1: Biomass production and feedstock diversification for advanced biofuels. Oral presentation at BECOOL 3rd technical meeting. 13-14 June 2018. Borgo San Lorenzo (Italy).

Scarlat, N., Fahl, F., Lugato, E., Monforti-Ferrario, F., Dallemand, J.F., 2019. Integrated and spatially explicit assessment of sustainable crop residues potential in Europe. Biomass and Bioenergy 122, 257–269. https://doi.org/10.1016/j.biombioe.2019.01.021

Scarlat, N., Martinov, M., Dallemand, J.F., 2010. Assessment of the availability of agricultural crop residues in the European Union: Potential and limitations for bioenergy use. Waste Manag. 30, 1889–1897. https://doi.org/10.1016/j.wasman.2010.04.016

Schils, R., Olesen, J.E., Kersebaum, K.C., Rijk, B., Oberforster, M., Kalyada, V., Khitrykau, M., Gobin, A., Kirchev, H., Manolova, V., Manolov, I., Trnka, M., Hlavinka, P., Paluoso, T., Peltonen-Sainio, P., Jauhiainen, L., Lorgeou, J., Marrou, H., Danalatos, N., Archontoulis, S., Fodor, N., Spink, J., Roggero, P.P., Bassu, S., Pulina, A., Seehusen, T., Uhlen, A.K., Żyłowska, K., Nieróbca, A., Kozyra, J., Silva, J.V., Maçãs, B.M., Coutinho, J., Ion, V., Takáč, J., Mínguez, M.I., Eckersten, H., Levy, L., Herrera, J.M., Hiltbrunner, J., Kryvobok, O., Kryvoshein, O., Sylvester-Bradley, R., Kindred, D., Topp, C.F.E., Boogaard, H., de Groot, H., Lesschen, J.P., van Bussel, L., Wolf, J., Zijlstra, M., van Loon, M.P., van Ittersum, M.K., 2018. Cereal yield gaps across Europe. Eur. J. Agron. 101, 109–120. https://doi.org/10.1016/j.eja.2018.09.003

Schlegel, A. J., Dumler, T. J., Thompson, C. R., 2002. Feasibility of four-year crop rotations in the central high plains. Agron. J. 94, 509-517.

Schomberg, H.H., Martini, N.L., Diaz-Perez, J.C., Phatak, S.C., Balkcom, K.S., Bhardwaj, H.L., 2007. Potential for using sunn hemp as a source of biomass and nitrogen for the Piedmont and Coastal Plain Regions of the Southeastern USA. Agron. J. 99, 1448–1457. https://doi.org/10.2134/agronj2006.0294

Schrader, W. D., Fuller, W. A., and Cady, F. B., 1966. Estimation of a common nitrogen response function for corn (*Zea mays*) in different crop rotations. Agron. J. 58, 397. https://doi.org/10.2134/agronj1966.00021962005800040010x

Semenov, M.A., Barrow, E.M., 2002. LARS-WG. A stochastic weather generator for use in climate impact studies. User manual. Rothamsted Research, Harpenden, Hertfordshire AL5 2JQ, UK, 27.

Sinclair, T.R., 1986. Water and nitrogen limitations in soybean grain production. I Model development. Field Crop. Res. 15, 125-141. https://doi.org/10.1016/0378-4290(86)90082-1

Sinclair, T.R., Muchow, R.C., Ludlow, M.M., Leach, G.J., Lawn, R.J., Foale, M.A., 1987. Field and model analysis of the effect of water deficit on carbon and nitrogen accumulation by soybean, cowpea and black gram. Field Crop. Res. 17, 121-140. https://doi.org/10.1016/0378-4290(87)90087-6

Sinclair, T.R., Seligman, N., 2000. Criteria for publishing papers on crop modeling. Field Crops Res. 68, 165-172. https://doi.org/10.1016/S0378-4290(00)00105-2

Singh, M.P., Erickson, J.E., Sollenberger, L.E., Woodard, K.R., Vendramini, J.M.B., Fedenko, J.R., 2012. Mineral composition and biomass partitioning of sweet sorghum grown for bioenergy in the southeastern USA. Biomass and Bioenergy 47, 1–8. https://doi.org/10.1016/j.biombioe.2012.10.022

Soltani, A., Ghassemi-Golezani, K., Khooie, F.R., Moghaddam, M., 1999. A simple model for chickpea growth and yield. Field Crop. Res. 62, 213-224. https://doi.org/10.1016/S0378-4290(99)00017-9

Stackhouse, P., 2006. Prediction of worldwide energy resource. Available at http://power.larc.nasa.gov. NASA Langley Research Center, Hampton, VA.

Stella, T., Francone, C., Yamac¸ S.S., Ceotto, E., Pagani, V., Pilu, R., Confalonieri, R., 2015. Reimplementation and reuse of the Canegro model: from sugarcane to giant reed. Comput. Electron. Agr. 113, 193-202. https://doi.org/10.1016/j.compag.2015.02.009

Stöckle, C.O., Campbell, G.S., Nelson, R., 1999. ClimGen Manual. Biological Systems Engineering Department, Washington State University, Pullman, WA.

Stöckle, C.O., Donatelli, M., Nelson, R., 2003. CropSyst, a cropping systems simulation model. Eur. J. Agron. 18, 289-307. https://doi.org/10.1016/S1161-0301(02)00109-0

Stöckle, C.O., Kemanian, A.R., Nelson, R.L., Adam, J.C., Sommer, R., Carlson, B., 2014. CropSyst model evolution: From field to regional to global scales and from research to decision support systems. Environ. Model. Softw. 62, 361–369. https://doi.org/10.1016/j.envsoft.2014.09.006

Struik, P.C., Amaducci, S., Bullard, M.J., Stutterheim, N.C., Venturi, G., Cromack, H.T.H., 2000. Agronomy of fibre hemp (*Cannabis sativa* L.) in Europe. Ind. Crops Prod. 11, 107–118. https://doi.org/10.1016/S0926-6690(99)00048-5

Sumner, D.R., 1982. Crop rotation and plant productivity. In: “Handbook of Agricultural Productivity,” (M. Rechcigl, Jr., Ed.), Vol. 1, pp. 273–315. CRC Press, Boca Raton, FL.

Taylor, R., 1990. Interpretation of the correlation coefficient: a basic review. J. Diagnostic Med. Sonogr. 1, 35–39. https://doi.org/10.1177/875647939000600106

Teng, P.S., Penning de Vries, F.W.T. (Eds.), 1992. Systems approaches for agricultural development applied science. Elsevier (ISBN: 1851668918. 309 pp.).

Tilman, D., Cassman, K.G., Matson, P.A., Naylor, R., Polasky, S., 2002. Agricultural sustainability and intensive production practices. Nature 418, 671–677. https://doi.org/10.1038/nature01014

Tripathi, M.K., Chaudhary, B., Sarkar, S.K., Singh, S.R., Bhandari, H.R., Mahapatra, B.S., 2013. Performance of sunnhemp (*Crotalaria juncea* L.) as a summer season (pre-monsoon) crop for fibre. J. Agric. Sci. 5, p236. https://doi.org/10.5539/jas.v5n3p236

Unger, P. W., 1984. Tillage and residue effects on wheat, sorghum, and sunflower grown in rotation. Soil Sci. Soc. Am. J. 48, 885-891. https://doi.org/10.2136/sssaj1984.03615995004800040037x

Valenzuela, H., Smith, J., 2002. ‘Tropic Sun’ sunnhemp. Univ. of Hawaii, College of Tropical Agr. and Human Resources, Sustainable Agr. Green Manure Crops, No. 11. 3 pp.

van Heemst H. D. J., 1988. Plant data values required for simple crop growth simulation models: review and bibliography. (No. 17). CABO.

van Ittersum M.K., Rabbinge R., 1997. Concepts in production ecology for analysis and quantification of agricultural input-output combinations, F. Crop. Res., 52: 197–208. https://doi.org/10.1016/S0378-4290(97)00037-3

van Oijen M., Schapendonk A., Höglind M., 2010. On the relative magnitudes of photosynthesis, respiration, growth and carbon storage in vegetation. Ann. Bot., 105(5): 793-797. https://doi.org/10.1093/aob/mcq039

Vasileiadis, V.P., Sattin, M., Otto, S., Veres, A., Pálinkás, Z., Ban, R., Pons, X., Kudsk, P., van der Weide, R., Czembor, E., Moonen, A.C., Kiss, J., 2011. Crop protection in European maize-based cropping systems: current practices and recommendations for innovative integrated pest management. Agric. Syst. 104, 533–540. https://doi.org/10.1016/j.agsy.2011.04.002

Verheye, W., 2006. Land use, land cover and soil sciences. Encyclopedia of Life Support Systems (EOLSS).

Wang, K.-H., Sipes, B.S., Schmitt, D.P., 2002. Crotalaria as a cover crop for nematode management: a review. Nematropica 32, 35-57.

Webber, C.L., 1996. Response of kenaf to nitrogen fertilization. In: J. Janick, editor, Progress in new crops. John Wiley & Sons, New York. 404–408.

Wickham, H., 2009. Ggplot2: elegant graphics for data analysis. Springer-Verlag, New York.

Willey, R. W., 1979a. Intercropping: its importance and research needs. Part 1. Competition and yield advantages. Field Crop Abstracts 32:1-10.

Zatta, A., Monti, A., Venturi, G., 2012. Eighty years of studies on industrial hemp in the Po Valley (1930-2010). J. Nat. Fibers 9, 180–196. https://doi.org/10.1080/15440478.2012.706439

Zegada-Lizarazu, W., Monti, A., 2011. Energy crops in rotation. A review. Biomass and Bioenergy 35, 12–25. https://doi.org/10.1016/j.biombioe.2010.08.001

Zegada-Lizarazu, W., Monti, A., 2012. Are we ready to cultivate sweet sorghum as a bioenergy feedstock? A review on field management practices. Biomass and Bioenergy 40, 1–12. https://doi.org/10.1016/j.biombioe.2012.01.048

Zeleke, K.T., Luckett, D.J., Cowley, R.B., 2014. The influence of soil water conditions on canola yields and production in Southern Australia. Agric. Water Manag. 144, 20–32. https://doi.org/10.1016/j.agwat.2014.05.016

Zeng, Z.-H., Lu, Z.-Y., Jiang, Y., Zhang, K., Yang, Y.D., Zhao, P.-Y., 2016. Legume-cereal crop rotation systems in China. Crop Rotations Farming Pract. Monit. Environ. Benefits.

Zhang, F., Noe, J. P., 1996. Damage potential and reproduction of *Meloidogyne incognita* race 3 and *M. arenaria* race 1 on kenaf. Suppl J Nematol, 28, 668-675.

Appendices

Appendix A. Pedological conditions of the experimental trials

Table A.1. Main soil physical and chemical properties at Cadriano (Italy) in the period 2016-2018.

ID	Sand	Silt	Clay	pH	Total $CaCO_3$[a]	Active $CaCO_3$[b]	Organic carbon[c]	Organic matter[c]	Total N[d]	P_2O_5[e]	K_2O[f]	C/N
	%	%	%		%	%	g kg^{-1}	%	g kg^{-1}	mg kg^{-1}	mg kg^{-1}	
1-8	35	47	18	7.30	1.20	1.20	NA	1.58	1.10	59	144	8.30
9,11	11	56	33	6.57	1.15	1.13	7.09	1.22	1.40	56	176	5.06
10,12,13	31	45	24	6.73	0.62	0.60	7.19	1.24	0.95	100	146	7.59

Determination method: [a]Dietrich-Fruehling, [b]Drouineau, [c]Walkley-Black, [d]Dumas, [e]Olsen, [f]M.13.5 DM 13-9-99.

Table A.2. Main soil physical and chemical properties at Guadajira (Spain) in 2018.

ID	Sand	Silt	Clay	pH	Total $CaCO_3$[a]	Active $CaCO_3$[b]	Organic carbon[c]	Organic matter[c]	Total N[d]	P_2O_5[e]	K_2O[f]	C/N
	%	%	%		%	%	g kg^{-1}	%	g kg^{-1}	mg kg^{-1}	mg kg^{-1}	
14	44	35	21	6.85	7.16	NA	5.6	0.76	0.60	15	43	9.33
15	44	35	21	6.90	6.95	NA	5.7	0.78	0.61	14	43	9.34

Table A.3. Main soil physical and chemical properties at Aliartos (Greece) in the period 2017-2018.

ID	Sand	Silt	Clay	pH	Total $CaCO_3$[a]	Active $CaCO_3$[b]	Organic carbon[c]	Organic matter[c]	Total N[d]	P_2O_5[e]	K_2O[f]	C/N
	%	%	%		%	%	g kg^{-1}	%	g kg^{-1}	mg kg^{-1}	mg kg^{-1}	
16-20	63	25	12	7.9-8.4	NA	NA	NA	0.5	0.8	NA	NA	NA

Appendix B. Climate variability at the Spanish (Guadajira), Italian (Cadriano), and Greek (Aliartos) experimental sites in the period 2016-2018.

Figure B.1. Maximum air daily temperature (°C) during sunn hemp growing season (May-October).

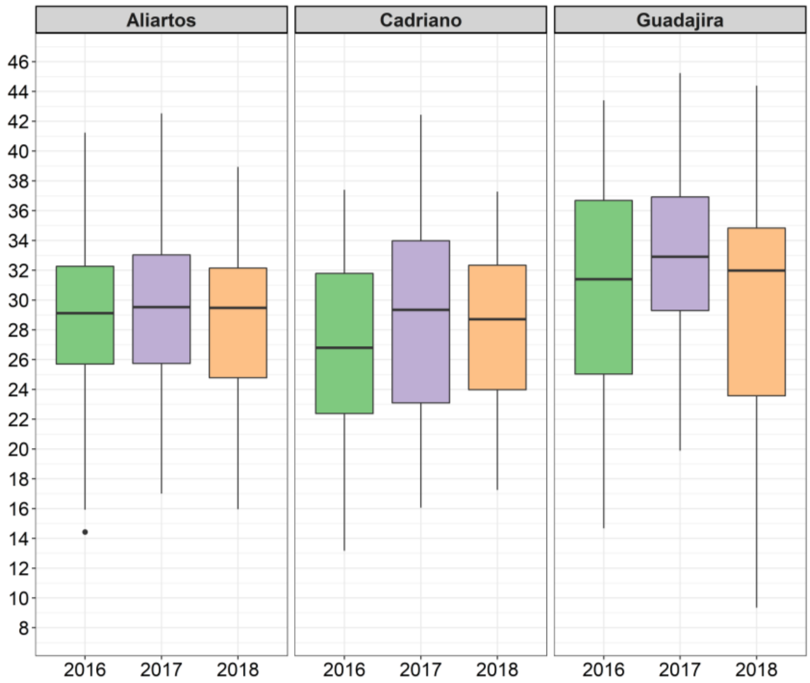

Figure B.2. Minimum air daily temperature (°C) during sunn hemp season (May-October).

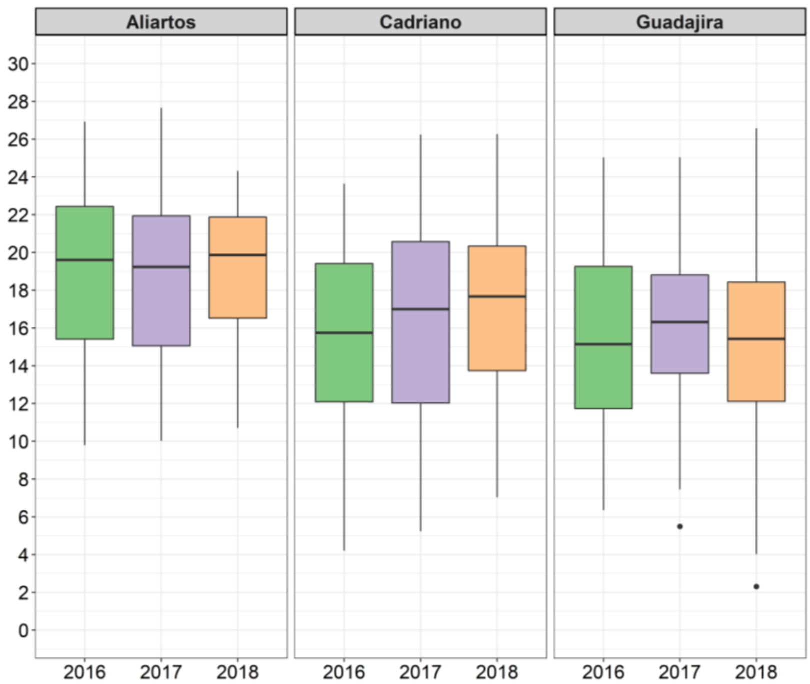

Figure B.3. Daily global radiation (MJ m^{-2} d^{-1}) during sunn hemp growing season (May-October).

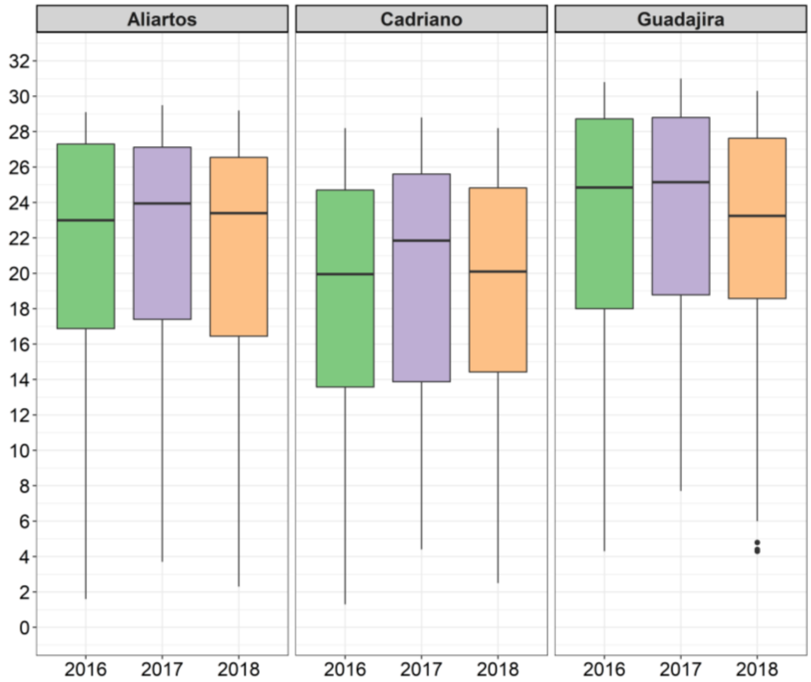

Appendix C. SunnGro model parameters

Table C.1. Parameter values marked with an asterisk were set to defaults reported in literature while the remaining ones were calibrated within ranges defined by literature or experimental results (E).

Parameter name	Description	Min	Max	Value	Unit	Reference
Phenology						
TBaseEmergence	Base temperature for emergence from planting	8(3)	9.2(16)	9.47	°C	a,(b)
TCutOffEmerg	Optimum temperature for emergence from planting	28	43	30	°C	b
TTEmergFlower	Thermal time from emergence to flowering	47.34	63.94	63	°Cd	E[3,16]
TBaseFlower	Base temperature for flowering	8	11	9.41	°C	q
TCutOffFlower	Optimum temperature for flowering	27	29	28	°C	q
DayLenghtIf	Day length threshold above which no accumulation of physiological time occurs			14*	hour	c
DayLenghtIns	Day length threshold below which maximum physiological time accumulation occurs			6*	hour	c
TTEmergPlant	Thermal time to emergence for a plant crop	47	64.29	59.15	°Cd	E[1,3]
Branch emission						
TBaseBranchDevelop	Base temperature for branch population development	5.95	8.05	6.72	°C	d[2]
TCutOffBranchDevelop	Optimum temperature for branch population development	30	45 (even >)	38.35	°C	d
TTEmergPeakBranchPop	Thermal time from emergence to peak branch population	1037	1500	1318.48	°Cd	E[3]
SBNmax	Maximum number of secondary branches per plant	2	36	25.87	unitless	E
kSB	Empirical parameter of the Logistic function for branch emission	-	-	0.007683	unitless	E[4]
bSB	Empirical parameter of the Logistic function for branch emission	-	-	-9.4960	unitless	E[5]
Leaf appearance						
TBaseLeafEmission	Base temperature for leaf emission	8.9	10.9	9.48	°C	a
TCutOffLeafEmission	Optimum temperature for leaf emission	30	35	30.45	°C	e
LNavg	Average number of leaves per branch	2	87.5	25.87	unitless	E
kL	Empirical parameter of the Logistic function for leaf appearance	-	-	0.0651	unitless	E[6]
bL	Empirical parameter of the Logistic function for leaf appearance	-	-	-7.6870	unitless	E[7]
Leaf area extension						
MaxNumGreenLeavesWW	Maximum number of green leaves per branch under well water conditions			30*	unitless	f
MeanLeafLength	Mean leaf length	3.06	11.9	11.65	cm	E[8]
MeanLeafWidth	Mean leaf width	6	32.4	29.86	mm	E[9]
Photosynthesis						
TBasePhotosynthesis	Base temperature for photosynthesis	0	10	5.88	°C	d
FractGrossPhotoGroResp	Fraction of gross photosynthesis lost for growth respiration	0.19	0.31	0.238	unitless	g
TBaseRootExtension	Base temperature for root extension	0	10	6.22	°C	d
TCutOffRootExtension	Optimum temperature for root extension	24	33	30.45	°C	h
RefMaintResp	Maintenance respiration at 10°C	0.01	0.03	0.011	Mg Mg^{-1} d^{-1}	g
MaxPartFractAerialDM	Maximum partition fraction to aerial dry mass	0.5	1	0.987	Mg Mg^{-1}	E
MaxRadConvEfficiency	Maximum radiation conversion efficiency	0.95	8.68	6.55	g MJ^{-1} d^{-1}	i,l[10]
PARExtCoeff	PAR extinction coefficient	0.826	0.91	0.83	unitless	m
PartCoeff	Coefficient of the exponential function for aerial dry mass partitioning	0.51	0.69	0.497	unitless	n[11]
MinPartFractAerialDM	Minimum partition fraction to aerial dry mass	0	0.19	0.0483	Mg Mg^{-1}	E
RootLengthMassRoot	Root length per unit root mass	7650	10350	9014	cm g^{-1}	c[12]
MaxRootLengthDensity	Maximum root length density	1	2.8	1.858	cm cm^{-3}	o[13]
MinRootLengthDensity	Minimum root length density	0.4	0.8	0.724	cm cm^{-3}	o[14]
RootDepthIncreaseGDD	Root depth increase per growing degree day	0	1.2	0.57	cm $°Cd^{-1}$	e[15]
CropCoeff	Crop water use coefficient			1.05*	unitless	p

Q10ForMaintResp	Fractional increase in respiration rate per 10°C rise in temperature	2*	unitless	e

Literature pertaining to *Crotalaria juncea* L.: a) Qi et al., 1999; *Vigna unguiculata* (L.) Walp.: b) Craufurd et al., 1996; g) Van Heemst, 1988; h) Dart and Mercer, 1964; m) Littleton et al., 1979; o) Moroke et al., 2005; p) Allen et al., 1998; q) Craufurd et al., 1997; *Glycine max* (L.) Merrill: d) Van Heemst, 1988; e) Boons-Prins et al., 1993; *Pisum sativum* L.: i) Lecoeur and Ney, 2003; generic defaults: c) Stöckle et al., 2003; f) custom defined; l) Van Oijen et al., 2010; n) Stella et al., 2015.

Notes: [1]range: ±15% around experimental default (55.9); [2]range: ±15% around default value (7); [3]Tbase=10°C, Tcutoff=25°C; [4]autotune calibration (AC) performed starting from experimental default (0.0084); [5]AC performed starting from experimental default (-7.1463); [6]AC performed starting from experimental default (0.0111); [7]AC performed starting from experimental default (-10.3421); [8]boundaries estimated as experimental mean value (7.48) ± 1.5SD; [9]boundaries estimated as experimental mean value (19.2) ± 1.5SD; [10]boundaries of gross photosynthesis (GP) rate were estimated by multiplying net photosynthesis (NP) rate' boundaries (min:0.57, max:4.34 as reported in i) by GP/NP ratio (derived from l, min:1.67, max:2) [11]range: ±15% around default value (0.6); [12]range: ±15% around default value (9000); [13]upper layer; [14]lower layer; [15]upper limit; [16]range: ±15% around experimental default (55.69).

Additional references

Allen, R.G., Pereira, L.S., Raes, D., Smith, M., 1998. FAO Irrigation and drainage paper No. 56. Rome: Food and Agriculture Organization of the United Nations, 56(97), e156.

Boons-Prins, E.R., De Koning, G.H.J., Van Diepen, C.A., 1993. Crop-specific simulation parameters for yield forecasting across the European Community (No. 32). CABO-DLO.

Craufurd, P.Q., Ellis, R.H., Summerfield, R.R.J., Menin, L., 1996. Development in cowpea (Vigna unguiculata). I. The influence of temperature on seed germination and seedling emergence. Exp. Agric. 32(1): 1-12. https://doi.org/10.1017/s0014479700025801

Dart, P.J., Mercer, F.V., 1965. The effect of growth temperature, level of ammonium nitrate, and light intensity on the growth and nodulation of cowpea (*Vigna sinensis* Endl. ex Hassk.). Aust. J. Agric. Res., 16(3): 321-345.

Lecoeur, J., Ney, B., 2003. Change with time in potential radiation-use efficiency in field pea. Eur. J. Agron., 19(1): 91-105.

Littleton, E.J., Dennett, M.D., Monteith, J.L., Elstonff, J., 1979. The growth and development of cowpeas (*Vigna unguiculata*) under tropical field conditions: 2. Accumulation and partition of dry weight. J. Agr. Sci., 93(2): 309-320. https://doi.org/10.1017/S0021859600037977

Moroke, T.S., Schwartz, R.C., Brown, K.W., Juo, A.S.R., 2005. Soil water depletion and root distribution of three dryland crops. Soil Sci. Soc. Am. J., 69(1): 197-205.

Qi, A., Wheeler, T.R., Keatinge, J.D.H., Ellis, R.H., Summerfield, R.J., Craufurd, P.Q., 1999. Modelling the effects of temperature on the rates of seedling emergence and leaf appearance in legume cover crops. Exp. Agric., 35(3): 327-344.

Stöckle, C.O., Donatelli, M., Nelson, R., 2003. CropSyst, a cropping systems simulation model. Eur. J. Agron., 18(3-4): 289-307.

Van Heemst, H.D.J., 1988. Plant data values required for simple crop growth simulation models: review and bibliography. (No. 17). CABO.

Van Oijen, M., Schapendonk, A., Höglind, M., 2010. On the relative magnitudes of photosynthesis, respiration, growth and carbon storage in vegetation. Ann. Bot., 105(5): 793-797. https://doi.org/10.1093/aob/mcq039